UNIVERSITÀ DEGLI STUDI DI PADOVA

Dipartimento di Ingegneria Industriale DII

Corso di Laurea Magistrale in Ingegneria dell'Energia Elettrica

Tesi di laurea magistrale

High voltage covered conductor overhead lines: detection of incipient tree faults

Relatore: Prof. Roberto Turri

Correlatori: Ing. Roberto Spezie (Terna S.p.a.)

Ing. Massimo Petrini (Terna S.p.a.)

Ing. Francesco Palone (Terna S.p.a.)

Laureanda:

Caliari Giulia,

1183846

Anno Accademico 2019/2020

“è solo

un momento buio,

non disperare:

è grazie a lui che poi

tornerai ad apprezzare le albe”

[Gio Evan]

Dedicato alla mia famiglia

e alla mia cara nonna Bice.

Abstract

The aim of this thesis is the study of a new type of high voltage overhead power line, made by means of an insulation layer located around the conductor: these are the covered conductor lines. In particular, the work focuses on the study of the behaviour of these conductors when they get in contact with the vegetation around, which can touch or fall on the line. After the falling of a tree on the covered conductor line, in the point of contact between the tree and the line, there will not be the formation of the arc, but partial discharges are generated. These partial discharges pulses travel along the line as travelling waves and are detected by means of the sensors located at the line end. Thanks to this automatic on-line measurement system, it is possible to control the line and detect the incipient fault caused by the fallen tree, before the outage of the line itself. Moreover, with the study of the time needed by the pulses to travel along the line, it is possible to localize the incipient tree fault and clean the line from the fallen tree. After an exhaustive theoretical part in which these arguments are explained, the study of this type of conductor is simulated using the software, EMTP-RV, modelling the covered conductors line and simulating the incipient tree faults.

Riassunto esteso in lingua italiana

Questo lavoro di tesi si incentra sullo studio di un nuovo tipo di conduttore aereo in alta tensione. Esso è diverso dai tipici conduttori aerei, perché presenta uno stato protettivo isolante attorno al conduttore vero e proprio in metallo: per questo motivo viene definito *covered conductor,* ossia conduttore ricoperto. Grazie a questo strato isolante, esso ha la peculiarità di riuscire a permettere alle fasi di scontrarsi a vicenda in caso di eventi meteorologici avversi o di tollerare il contatto con elementi esterni alla rete. È questo infatti il caso, di un probabile contatto tra questi conduttori e un eventuale albero che cade su di essi. L'interesse di questi conduttori è infatti quello di utilizzarli per quelle linee che attraversano zone boschive, in cui l'interferenza con la vegetazione non è poi un evento così raro. A differenza dei normali conduttori aerei in alta tensione, i quali produrrebbero un guasto che farebbe attivare le protezioni di rete, mettendo momentaneamente fuori uso parte della stessa, i covered conductors, grazie al loro isolamento, permettono la caduta di un albero su di essi, resistendo a questa stressante situazione per qualche ora, prima che si verifichi un guasto che faccia aprire la linea. Tra l'albero e l'isolante, a causa della deformazione del campo elettromagnetico del conduttore, vengono tuttavia prodotte delle scariche parziali, piccoli impulsi di corrente, che si propagano istantaneamente lungo la linea. È proprio tramite lo studio di questi fenomeni che si può risalire alla localizzazione del guasto e alla messa in sicurezza della linea: esse infatti si propagano lungo la linea come se fossero delle onde viaggianti. Gli impulsi delle scariche parziali vengono rilevati da degli appositi sensori, bobine di Rogowski, disposti lungo la linea o al termine di essa: tramite un'analisi automatica e sempre attiva di questi fenomeni, è possibile capire se lungo la linea c'è stato questo tipo di inizio guasto (*incipient fault*). Inoltre, tramite la misurazione del tempo impiegato da questi impulsi per propagarsi lungo la linea, ricostruendo il diagramma reticolare delle onde viaggianti, tenendo presente che esse si riflettono nei punti di discontinuità, è possibile calcolare la distanza alla quale è avvenuto il guasto, nota la velocità di propagazione e la lunghezza totale della linea sorvegliata. Così facendo, è possibile individuare il punto in cui l'albero è caduto sulla linea, mandando una squadra di operai sul posto a ripulire il danno, prima che la situazione si evolva e diventi un guasto fase-terra a tutti gli effetti con le conseguenze note.

Nella parte teorica viene inizialmente presentato lo stato dell'arte dei conduttori ricoperti in alta tensione, presentandone costi e benefici. Viene poi esposto il fenomeno della formazione delle scariche parziali, con un approfondimento su quelle generate dalla caduta di un albero. I risultati esposti vengono dalla bibliografia riguardante studi precedenti: in particolare da studi effettuati

prima in laboratori di alta tensione, e successivamente sul campo. Quest'ultimi fanno riferimento ad una linea finlandese, *SAX trial line*, una linea di prova utilizzata per lo studio di questi fenomeni: è in Finlandia infatti che è stata costruita la prima linea aerea in alta tensione formata da conduttori ricoperti. Grazie a questi lavori sul campo è stata studiata la propagazione delle scariche parziali lungo la linea al variare delle condizioni ambientali. Infine, vengono presentati gli strumenti di misura utilizzati per l'individuazione questo fenomeno fisico e per l'analisi automatica delle scariche parziali.

Nell'ultima parte della tesi, lo studio viene portato in un ambiente di calcolo, per la simulazione tramite un software. Il programma utilizzato è EMTP-RV, un software utilizzato per simulare i transitori elettromagnetici: in questo caso viene utilizzato per la simulazione di un contatto tra albero e linea aerea in alta tensione in covered conductor, con la conseguente formazione di scariche parziali che si propagano lungo l'intera lunghezza della linea, fino a giungere ai sensori. Quest'ultimi sono collegati a degli oscilloscopi sui quali è possibile apprezzare l'ampiezza e la forma degli impulsi di corrente generati dal contatto albero-linea. Dopo una prima parte di modellizzazione di questo nuovo tipo di linea, vengono eseguite una serie di simulazioni in cui cambiano le condizioni in cui si verificano il guasto; inoltre lo studio viene eseguito al variare della frequenza del modello della linea e al variare della gestione del neutro.

Index

Introduction

This work is written during an internship with the Italian network operator, Terna S.p.a., which is the company responsible in Italy for the transmission and dispatching of electricity on the high and very high voltage grid in all the country. There is an interest from this company about a new type of overhead conductors which can be put in the forest area, close to the vegetation present in the territory. Therefore, in this thesis work a study about a new type of high voltage overhead power line is presented. This new type of line is made using the covered conductors, a traditional overhead power line with an insulation layer around the inner metal conductor. This insulation layer permits to the phases to withstand the collapse with each other and the interference with any external object. In particular, this line is able to withstand the stress caused by a tree which is fallen on the line without causing a fault and an outage of the power network. A traditional high voltage overhead line, when it is touched by an external object, like a tree, generates a fault, with the opening of the network protection and the interruption of the power supply.

However, the scientific literature is quite rich about the covered conductor line in middle voltage, due to the large use of this technology at this voltage level in a lot of countries, but it is quite poor about this argument in high voltage. This thesis is based on the Finnish experience on a high voltage covered conductors, in fact, Finland is the first country which took care about this argument and built a covered conductor line between two industrial cities. The results presented in this work are referred to lots of studies done, first in high voltage laboratory, and then in the field using an experimental line called SAX trial line. In particular, the work used as reference for the results of the field experiments is the Ph. D thesis written by Pertti Pakonen in the High Voltage Laboratory of Tampere University of Technology, in Finland.

The aim of the thesis is to study the partial discharges generated as soon as a tree falls on the covered conductor line. Due to the electromagnetic field deformation, the partial discharges, little current pulses, are generated and they propagate immediately along the line as travelling waves. With the study of their propagation using the lattice diagram, it is possible to localize the incipient fault location, in order to clean the damage. These partial discharge pulses are detected using special sensors, Rogowski coil, which are able to collect only the pulses. They are put along the line, or, preferably, at the line end, in the substations. Through an automatically on-line measurement of the discharges presented in the network, it is possible to monitor the line and detect if an abnormal situation has happened. When partial discharges due to an incipient tree fault

are detected by the system monitoring, the time of arrive of the pulses at the sensor are recorded and the fault point is localized.

The thesis consists in six chapters. The first one shows the state of art of the high voltage covered conductors line, explains the several benefits of this new technology, the electrical design of this line, the costs and the motivations that led to the study of it. In the second one, the partial discharges phenomenon is explained and a large technical study about partial discharge generated from the contact between the tree is done. In particular, the wood of the tree is studied to understand the phenomena that led the discharge generation. In the third chapter, the study of the propagation of the pulses along the line is presented, with a review of the travelling wave theory and their behaviour in a discontinuity point. In the fourth one, the measurements instruments are presented, in particular the Rogowski coil, a partial discharges sensor used to remove the voltage frequency signal and carry out only the pulses. With an automatic analysis, the system is able to detect the partial discharges and understand if they are due to an incipient fault caused by a fallen tree on the monitored covered conductors line. Finally, in the last two chapters, the practical work is shown. The study is carried in a computing environment, in order to simulate what is explained in the previous chapters: the software used is EMTP-RV, a program used to simulate the electromagnetic transients. In the fifth chapter a modelling of the covered conductor line is shown and the SAX trial line is built in this computing environment. In the sixth chapter, instead, several simulations are executed, in order to test the several conditions in which the incipient tree fault could be generated: an earth fault with one phase or two phases and a short circuit fault with two phases in contact with each other. The results of the simulations respect the expected forecasts, and confirm the theoretical aspect of the phenomenon.

Chapter 1

Covered conductor lines

In this first chapter the state of art of covered conductor lines is presented, with a particular focus on high voltage overhead power line. First of all, the structure of this kind of conductor is explained, to understand the reasons that make such conductor so special. Then, some of the problems related to normal overhead power line are presented, and it demonstrates why covered conductors may be a concrete solution to these issues. Indeed, the use of these conductors bring a lot of advantages, both from the technical and even environmental point of view; however, like everything, it has some drawbacks. Besides, the costs of a covered conductor line are considered, where higher initial costs than a normal overhead power line, are repaid by lower operational cost. After, a detailed exposition of the design and the accessories of the line is explained, also paying attention to the framework that is used to upgrade a normal bare power line in a covered one with a higher voltage. Finally, one of the firsts high voltage cover conductor power lines, built in Finland two decades ago is presented. It has been used for power transmission in 110 kV, on which a series of different tests are made to study the reliability of such lines, and on which important studies have been executed: they will be presented in this work, about the creation, propagation and localization of partial discharged caused by fallen trees over this covered conductor line.

1.1 The structure of covered conductors

Covered conductors (CC) have two dielectric insulations: the insulation mantel and the air, which are around the internal conductor. The framework of covered conductors consists in the core, the internal metal electrode made by hard and compact aluminium alloy, and the external mantel which is made by a waterproof material, with a great dielectric constant and high breakdown voltage. Usually, the material used for the external mantel is cross-linked polyethylene (XLPE): this type of conductor shows a great reliability in very difficult conditions and also it can withstand the weight of a fallen tree, both mechanically and electrically, for days. This type of covered conductor for the transmission voltage spectrum from 66 kV to 132 kV.

In middle voltage, the conductors are made of aluminium alloy and are covered with 2 mm layer of black and weather resistant XLPE; however, in high voltage, a single cover layer is not sufficient. In the first 110 kV installation, a compacted 355 mm² aluminium alloy conductor, covered by triple extruded XLPE layers, was used: the conductor, so called LMF SAX 355 110 kV, has the structure illustrate in the Figure 1.1.

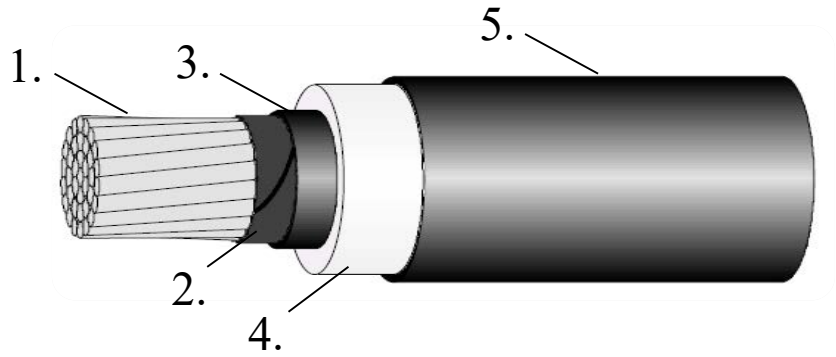

Figure 1.*1.* *The structure of LMF SAX 355 110 kV covered conductor: 1. Core made of compact aluminium alloy, 2. Water-blocking semiconducting tape, 3. Extruded semiconducting screen, 4. First layer of extruded water tree resistant XLPE, 5. Outer layer of weather resistant black XLPE.*

The structure of a LMF (low magnetic field) SAX 355 110 kV covered conductor is the following:

1. Core of the conductor made of stranded and compacted aluminium alloy;
2. Water-blocked semiconducting tape, wrapped around the metal conductor;
3. Extruded semiconducting screen;
4. Inner insulation made of extruded water tree resistant XLPE compound, with a thickness of 5 mm;
5. Outer insulation layer, made of weather resistant black XLPE compound, 1.5 mm thick.

The inner conductor is round and fully compacted to reduce the external diameter, it has a nominal diameter of 18.1 mm and a nominal weight of 635 kg per km; the nominal diameter of the whole covered conductor is 35 mm and the total nominal weight is 1300 kg per km. Electrically, it can withstand the maximum thermal short circuit current of 23 kA for one second, while the nominal current capacities are 340 A at 50°C and 566 A at 80°C. The outer XLPE layer, with thickness of 1.5 mm, is also UV resistant. Moreover, the critical field intensity of the air is not exceeded by the electric field intensity on the insulator.

Another type of covered conductor used in high voltage power lines, is a conductor of 2150 mm^2: the core is made of 490 mm^2 of aluminium and 65 mm^2 of carbon fibbers. The saved weight, due to use of carbon fibbers instead of steel, is used for the insulation made by polyurethane mantel.

In the following table (Table 1.1), parameters of another type of high voltage covered conductor are reported.

Table 1.1 *110 kV SAX covered conductor parameters*

Diameter of compacted conductor	22.5 mm
Water blocking	Powder
Tensile strength	294 N/mm^2
Elongation	4%
Resistivity	$32.8 \cdot 10^{-9}$ Ωm
Screen	Water-swallable tape + extruded XLPE compound
Insulation	5.0 mm thick XLPE compound
Outer insulation	1.5 mm thick track and UV resistant XLPE compound
Cable diameter	39 mm
Weight	1730 kg/km
Breaking load	108 kN
DC resistance (20 °C)	0.0949 Ω/km
Nominal current capacity (at 20 °C, 0.6 m/s wind, 1000 W/m^2)	660 A (70 °C conductor temp)

Table 1.2 *Comparison between parameters of 175 mm^2 LYNX conventional bare conductor and 240 mm^2 covered conductor*

Parameters	**175 mm^2 LYNX**	**240 mm^2 CC**
Unit weight (kg/m)	0.865	1.3
Rated breaking strength (kN)	79.73	73.45
Bare diameter (mm)	19.53	35.0
Cross sectional areas (mm^2)	226.2	240
Young modulus (kg/mm^2)	8200	6373.2
Coeff. of expansion (/°C)	0.0000178	0.000023
Basic span (m)	130	130
Tension limit at -5.6 °C (kN)	23.32	36.73
Wind pressure (N/m^2)	380	380
Radial ice thickness (mm)	9.5	9.5
Tension limit at 5 °C (kN)	15.95	11.99

Basic sag at 50 °C (m) for max span 150 m	2.94	4.24

In order to make a comparison with the existing bare conductor of 175 mm^2, a covered conductor of 240 mm^2 is installed on a known 132 kV pole: the differences are quite small, as reported in Table 1.2. The only big difference is the diameter, that influence the load calculations. However, as will be seen later, the covered conductor has a lot of advantages due to the external isolation, as the toleration of the contacts and clashing without any damages for a long time and in different climate conditions, that make this kind of conductor better than the traditional one, on many point of view.

1.2 Issues with traditional conductors

When power network was created, for economic and supply motivations, power was transmitted at high voltage, but the distribution was left with a great variety of different voltage, so the utilities and equipment formed a complex and uneconomical system. Because keeping is uneconomical keep such a large range of voltage level, it was decided to unify the different levels. Besides, with the increase of power demand, the size of conductor needed to increase as well; this process could not continue forever, because the existing pole network would not stand the strain. A more economic e physically solution is needed to better control the power distribution and meet the present increasing demand. The aim for network owners is the reconstruction of the entire network, eliminating unnecessary voltage levels and increasing where is required a big demand; the problems are expansive price, but above all, the public does not want accept a plethora of new tower lines for overhead lines. Two solutions are possible to reach the goal of eliminate numerous voltage levels and to improve the supply economically:

1. New building, but with low profile, with a single pole construction;
2. Upgrade the existing 33 kV or 66 kV to 132 kV lines, using as much as possible the existing structure.

As it will present after, both solutions are possible with cover conductor power line.

Another issue for the network companies is to follow the increasing demand to supply energy, but without any interruption of service. Network owners have to compensate the consequence from undelivered energy to the customers: this is possible increasing the reliability of the network and minimising the time spent in repair manoeuvres. Covered conductors provide an effective method

to increase the reliability of overhead line, mostly in case of network failure, where the costumer damage can be minimized if the problem can be cut out and quickly solved. In fact, covered conductor lines offer safety features against failure, even with the possibility to detect the fault location with the analysis of partial discharges travelling on the line.

Traditional bare conductors, in fact, cannot withstand the extreme and severe weather conditions causing common power line damage. These extreme weather conditions are usually atmospheric overvoltage, flashover voltage, wind that induce vibration and object fallen on the line, which interference with the normal distribution of power supply. The peculiarity of covered conductors is to withstand the phase clashing, during a strong wind, and the object contact that touch them, as a fallen tree abated after a storm; they can also withstand severe and extreme weather conditions, like a snow storm and freezing conditions, as show in Figure 1.2.

Figure 1.2 *Covered conductor line under freezing condition.*

Another issue for traditional high voltage overhead lines is the electro-magnetic field intensity detected on ground, below the phases, which creates disturbance to human and his devices. LMF SAX, as seen before, is the first covered conductor for high voltage lines installed for transmission

of power energy. Due to its low magnetic field, LMF SAX conductors can be installed close to dense building areas and in proximity to housing developments, where high electromagnetic field could be a considerable issue for people. Covered conductor is also a space saving and environmentally friendly in countryside: it can be installed where ordinary line does not fit, i.e. in narrow path inside the forest, without the need of cutting many trees or their branches, resolving an environmental issue so dear to public opinion.

1.3 Advantages of using covered conductors

The purpose of this section is to show the advantages that make high voltage cover conductor better than traditional bare conductor in overhead lines. Covered conductors offers the following advantages:

- Compact design;
- Excellent tolerance in conductors clashing and tree leaning;
- Good tolerance in withstand extreme weather condition;
- More safety;
- Possibility of upgrading an old bare conductor keeping the old structure;
- Improved supply quality;
- Lower operating cost;
- Friendly to wildlife;
- Lower magnetic field;
- Corrosion resistant.

The main reason why covered conductors are used, is to make the overhead lines more tolerable against conductors clashing with each other during adverse weather conditions (without any supply quality problems or any arcing damage), but above all against tree branches than could touch the conductors. Covered conductors in USA is known as ‘tree cable’, because they can withstand the weight of a fallen tree mechanically and electrically for days: for this reason, covered conductors are preferred in wooden areas, as it will present in this work. Thank to this ability to tolerate the contact, due to their insulating layers, covered conductors are more compact, with a closer distance between phases, compared to conventional bare overhead lines. The clearance in fact between phase would be become one third respect that in conventional bare installation, so the platforms and the structures can therefore be smaller and narrower, and the tower be shorter and less bulky, with a money saving and a low visual impact: an example of smaller and narrower design of a high

voltage line is reported in Figure 1.3. For middle voltage, covered conductors are also a safety choice, because during human activities, in case of accidental contact, it is not so dangerous and fatal as with bare conductors, i.e. when people could accidentally touch lines while fishing with rod.

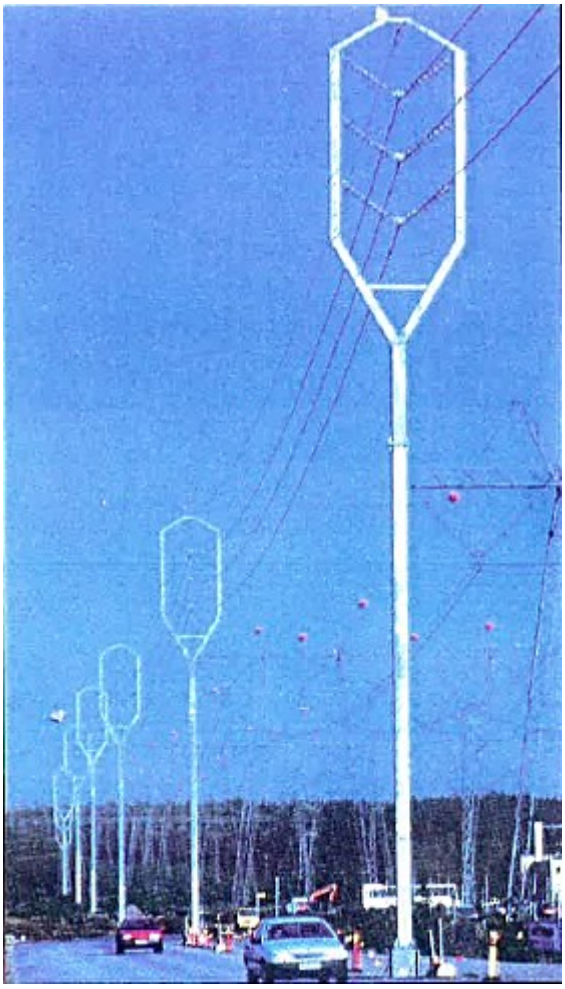

Figure 1.3 *A 110 kV covered conductor line with single leg steel pole construction: the design is slimmer and less bulky. The visual impact is lower respect traditional high voltage tower.*

Thank to more compact space used, covered conductors can be utilized for upgrading an old overhead bare conductor line, increasing power delivery capacity, without the need for new building or a widener right of way. The reconstruction of the high voltage transmission line is possible, replacing existing bare conductors, only with covered conductors, while all other components of the power line remain the same. With the same voltage level, covered conductors

require a narrow line corridor, with save in leave way and in cutting trees, in case of passage through a forest.

As it has already been presented before, thanks to its insulation, covered conductor is a sustainable solution against adverse weather conditions, avoiding damages to the line that disturb the power transmission. The network has a good reliability and improves its quality supply, due to low number of failure, with operational costs saving in not repairing damages. Besides, network companies, with a small number of outages, do not have to compensate the electricity not provided to the consumers. Looking at the experience with covered conductors both in high and in middle voltage, with the use of such lines, reliability has increased by five times: the number of failure/year, on a section long 100 km, is 0.9 for covered conductors and 4.5 for bare conductors. The number of outages is similar to that of underground cables.

Today, environmental issues have grown in importance: more pressure is put to use environmentally acceptable electricity solution for power lines. Covered conductors is ecologic and more environment friendly than traditional bare conductors, for many reasons. First of all, the narrower corridors prevent many trees are cleared or their branches are cut, protecting the forest areas and decreasing the disturbance to natural vegetation. Each kilometre of covered conductor power line could save ca. 34 000 m^2 of forest land, with about 16 600 kg of CO_2 absorbed annually by trees. Moreover, covered conductors reduce problems and disturbances to birds in areas populated by gees or swans, which could easily see the line, allowing risks of unintentional contacts. Environmental impact means not only impact with vegetation, but also visual impact for people looking at the landscape: public opinion prefers smaller structures instead of to the bulky tower used for high voltage power lines. Finally, European Commission has launched a new Integrated Product Policy (IPP) approach, focus on eco-design and on the product life cycle. The assessment based on life cycle indicates that the most harmful to the environment is the underground cable, because after usage it is left under the ground without any recycling operation.

In the end, because the phase conductors are closer to each other, the electro-magnetic field is smaller. The electro-magnetic field (EMF), produced by SAX power line, can be lower than one third, compared with the existing bare lines with horizontal configuration. In Figure 1.4 magnetic field density trend is shown, to comparison magnetic field inducted by conventional bare in horizontal and vertical configuration with one inducted by covered conductor in vertical configuration. The compactness of the line reduces the EMF levels by self-cancelling. Even for this benefit, covered conductors can be called “eco-lines”.

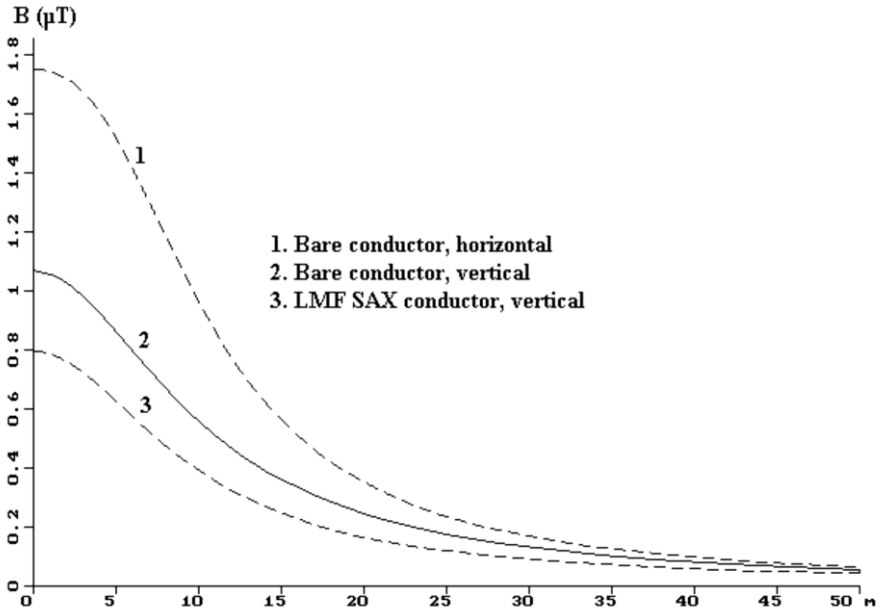

Figure 1.4 *Magnetic field density, 1.8 m above ground, with I = 100 A. Comparison between bare conductors and covered conductors.*

1.4 Cost assessment

The profitability of covered conductor networks was studied, including the investment, maintenance and outage cost. A high voltage transmission line using covered conductors has got higher cost than normal overhead bare line but not than undergrounded one. There is to consider, however, the several benefits this type of line has, as seen before, like environmental friendly, safety and reliability aspects which, after all, may make covered conductors an important investment. A complete cost comparison between a HVCC transmission line with a normal HV line with bare conductors is not an easy task. For example, in urban areas is difficult make a comparison because the costs are high using any type of conductor.

Due to the higher weight, the span tends to be shorter and the structures are more. The costs of foundations and towers are similar in both lines, but the installation work in covered conductor line is about 20% more expansive, mainly caused by the use of AGS clamps. The bigger contribution to increase so much the price is the extra material cost of AGS clamps and of covering itself: insulation cost cloud reach more than double than a bare conductor. All this leads a total line cost per km of about 25% more than normal bare line. However, cover conductor technology

is anyhow less expensive than a cable, so it is a cross between the conventional bare line and the underground cable.

Considering the outage costs, as seen before in the advantages section, covered conductors has fewer damage and fault due to its features. This leads to a saving money in case of energy not supply to the consumers, in fact for network owners, power supply not delivery to consumers means not gains. The compact design lead also to a saving money in building stage: network owners have to buy the right-to-way in the lands where the power line passes through. Narrower is the corridor of land needed to build the line, less is the cost for right-to-way: for cover conductor lines, this would make a considerable savings, in fact line corridors are narrowed (from 46 to 12 m) with the land purchase expenses decrease over 5 000 euro per km.

The benefits leading with such line are certainly more acceptable by public opinion, both in terms of visual appearance and environmental aspect. This type of overhead line is a suitable and innovative alternative, that request an initial investment, but that for a lot of reasons is the ideal solution in areas where different conditions require its usage.

1.5 Drawback

In this section some issues linked to the use of covered conductors are presented. First of all, corrosion is a problem that occurs whenever sheath is penetrated: a several water blocking mechanisms are used, to limit the possibility of corrosion, and a lot of test are done to determine which is the most resistant among the water blocking technique. A solution that could eliminate corrosion is the utilization of copper, instead of aluminium alloy for the core metal conductor. However, copper is a material more expansive, but its high conductivity and corrosion resistant make it an alternative choice only for coastal areas, where saltiness is presented in the air.

Other problem that cause line failure is long term vibration in the connection points. This problem concerns all overhead line, and it can be eliminated with the reduction of the line tension. Vibration occurs when the wind gives uplift energy to the conductor; line can vibrate for long time, even for years, without reduce its lifetime. Novel surface of covered conductor can modify wind flow patterns, reducing the energy transmitted into the line and therefore the vibration. Also the high weigh of the whole conductor is helpful to decrease the vibration; if it is needed, the use of spiral vibration dampers can help to damp vibration levels, but often dampers are not needful for covered conductor line.

Last problem is lightning, particularly relevant for covered conductor line. When flashover strikes the line, the arc does not move, but it stay in the same point, causing an overheating of the conductor with permanent damage. In fact, the difference from conventional bare line is that the latter is self- restoring and the fault can be resolved in few instant, while for a damage in insulated line, it have to wait that workers fix the damage where fault happened. Research is focus on the way to reduce effects of lightning on covered conductor and its lifetime: it is therefore possible to use arc protection device or surge arresters. The development of surge arresters opens up a new way in quality supply and line design. Lighting protection device means that not only the conductors, but all the network equipment is now better protected from lightning.

1.6 Electrical design

In terms of electrical design, covered conductors have different aspects compared to normal overhead lines. In conventional overhead line design, at the tower, the phase-to-phase clearance is calculated by the need to keep an acceptable level in mid-span clearance with specific conditions. This means that on the towers of normal overhead bare lines, the phase-to-phase clearance is significantly over-dimensioned (under the electrical point of view): with covered conductors, the situation is totally different, with the possibility of phase touching under specific conditions. For the insulation coordination, phase-to-phase clearance is calculated traditionally, but using different factors: the equation used are referred to a Cigré publication by Y. Ojala *et al.* (1998). In this publication, phase-to-ground clearance insulation level is chosen considering that arcing horns limit the fast front voltage and that switching overvoltage do not overcome 3.5 p.u.: phase-to-ground clearance results in 1.02 m, while the clearance for switching overvoltage requirement result of 0.78 m. For phase-to-phase clearance, are used the same equations, but some assumptions have been made during calculations: as reducing the gap factor (K_g) at 1.20, using the ratio of phase-to-phase to phase-to-ground switching overvoltage of 1.45, and finally assuming that phase-to-ground power frequency voltage is at opposite polarity when fast transient pulse occurs. It results clearance of 1.23 for fast-front pulse and 1.28 m for slow front pulse: the clearance result definitely small considering the accessories used, that are mainly the same. Figure 1.5 shows a typical covered conductors clearance for high voltage levels, with V-set insulation in vertical configuration.

Another different between traditional bare line is in arcing behaviour: when flashover occurs in bare conductors between phase, the arc immediately starts to move, instead when flashover occurs

in covered conductors, the arc remains in the extinction point, causing very likely melting of the conductor itself. Conductors must be provided with an effective shielding against lightning faults. Lightning produces overvoltage to the line, either striking directly the line or the neighbourhood. Arc damage must be avoided with appropriate protection method. Protection systems can be valued on economical bases: the costs for repair a permanent damage and for decreasing quality

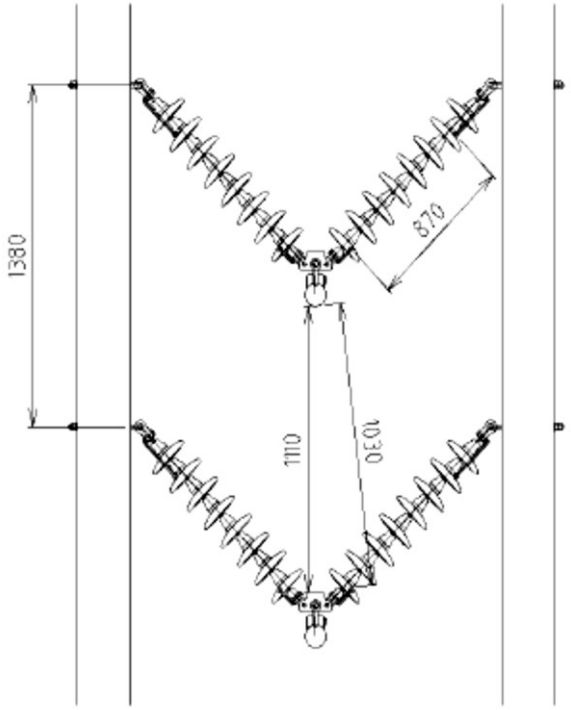

Figure 1.5 *High voltage covered conductor clearance in vertical configuration with V-insulation set.*

are compared with the costs of installing arc protection systems.

Factors to be taken into account are:

- the lightning density;
- the height of the trees closes to the line;
- the specific resistance of the ground;
- the relative number of stayed poles;
- the presence of other lines near the CC lines.

Arcing horns would be necessary, due to flashover could happen at the tower: live end arcing horns, however, must have a galvanic contact with the conductor. Avoiding corrosion issues, despite covered conductors hold better corrosion, insulation is pierced as little as possible. Arc Protection Devices (APD) do not prove effective at HV system: for the current design is preferred

not to use arcing horns, but instead the gapless metal oxide surge arrester is preferred. Arc gaps, in fact, at high voltage (132 kV), have a long operational delays, caused to their process of initial discharge at these voltage levels: as arc gap to operate could take up to 2 μs, surge arresters could operate in ns. It is possible the use of surge arresters in the covered conductor line construction as an integral part of the line, in the form of tension insulator surge arrester (TISA) and line insulator surge arrester (LISA). These surge arresters have dual role: a mechanical ability able to replace the tension insulator, and an electrical reliability in terms of performance of the circuit and security. Moreover, these surge arresters make possible to upgrade the actual system, increasing power transmitted on overhead network line, using the existing steel tower structure and wood poles. As said previously, for the public opinion, the appearance of overhead lines and their supporting structures take more and more importance; the height and the profile of overall structure is a dominant feature to be considered. The operation of a LISA in lightning condition does not cause a circuit breaker, this surge arrester is needed to be installed only every two or three spans.

In covered conductor lines, it is recommended using insulation piercing accessories. It is better do not use normal bare accessories, peeling off the covering, because this could create cuts to the conductor strands, that could be consider an initial crack. In fact, under cycling loads of vibration, these cracks grow more and more, until wire is broken: initial cracks decrease considerably lifetime of the conductor stand. It is important that covered conductor accessories do not require peeling off the insulation covering, and it is possible using a new type of tension clamp that can be useful both with covered conductors and bare conductors. Insulation piercing connectors (IPC) make the installation easier improving also the water tightness of the total system and the electrical performance. This connector, called armour grip suspension (AGS) clamps, in fact, contains aluminium teeth that can penetrate through the insulation layer into the aluminium core. Since it is not considered reasonable to let the clamp float at the same potential between the conductor and earth, a galvanic path is established from the AGS-clamp rods to the conductor, by the short-circuiting clamp at the ends of the armour rods. Short-circuit requirement for the armour rods is 31.5 kA/0.5 s. In Figure 1.6 design of AGS-clamp and suspension set is presented.

Usually vibration is a problem with overhead power lines, but with covered conductors a lot of studies indicate that conductors with large dimension can vibrate less that the smaller ones. Normal tension limit indicates no vibration problems for 50 mm^2 covered conductors at 28 N/mm^2, but tests indicate much higher tension for larger conductors without any vibration problems. Conductors seen in previous section, with 355 or 240 mm^2 diameter can be installed at 50 N/mm^2.

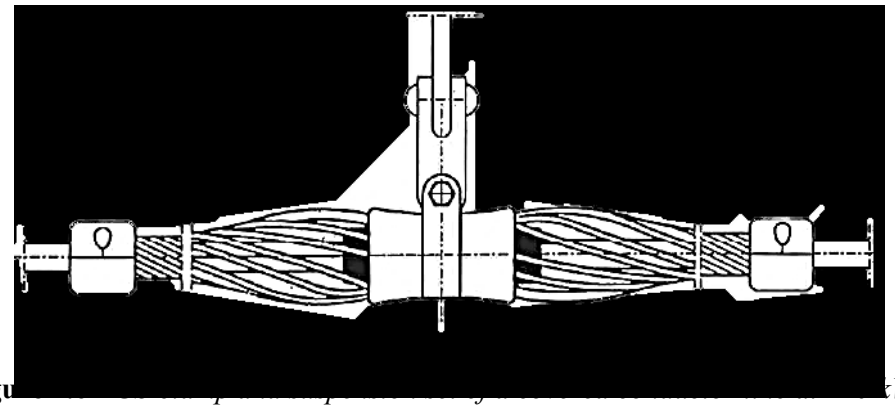

Figu *kV*

Usually some parts of the line need to be disconnected during repairing works, e.g. while removing fallen trees on the line or transformer maintenance. In order to make maintenance and fault recovery time as short as possible, it needs to have different sections in the line, with several disconnection points. A simple disconnector can be used for cover conductor line and can easy operate with live line sticks in each phase. So this solution is ideal for maintenance where full breaking capacity is not needed.

As already explained, covered conductors are able to reduce phase distance, until one third respect a bare line: it means also more compact supporting structures. Most economical solution has proven to be the wooden pole, not only for MV, but even for HVCC lines. Normally wooden pole is directly embedded into the ground, without any specific foundation. Lifetime of a treated wooden pole is about 40-50 years; moreover, to minimise negative environmental impact, it is possible recycling the material used for the pole. It tried to make a new design, to avoid the use of cross arms, with the insulators directly mounted on the pole, but fabrication cost must be compared with using of just a single cross arm. Some novel tower design for 132 kV covered conductors used in Poland are illustrated in Figure 1.7.

For refurbishment or new building, three options are proposed:

1. single pole, horizontal configuration;
2. single pole, triangular configuration;
3. single pole, double circuit.

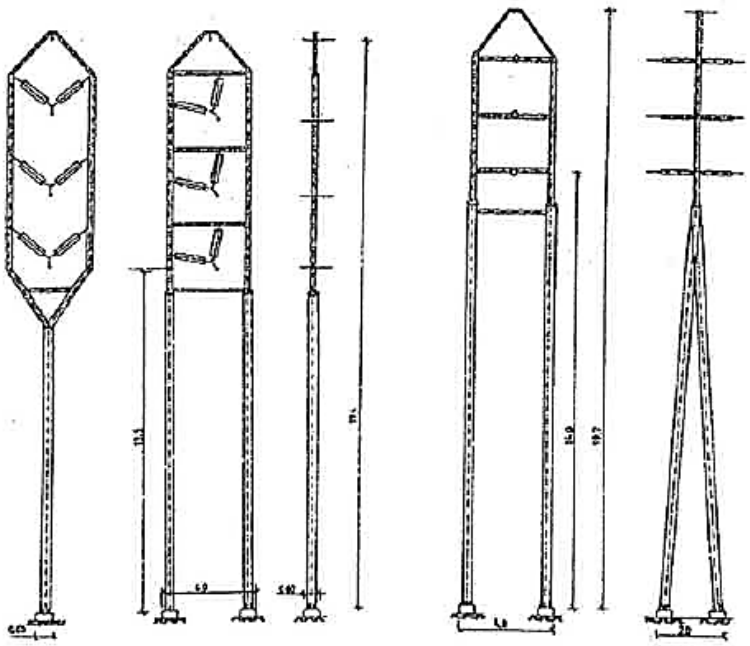

Figure 1.7 *New design of 132 kV covered conductor towers installed in Poland*

1.7 Programme of test

Covered conductors during their development have been subjected to a thorough and long programme of test, conduced both in laboratory and in the field. Several type of test has been achieved, with the aim of testing their behaviour during some situations that may arise during the exercise: in this section the various test will be presented.

Due to the compact space between phases, there is a possibility conductors clash together during a storm or with strong wind. First test was to study the behaviour of the conductors when they are clashing together. During the field test, with a voltage of 120 kV and with the ambient temperature that varied between +10 and +30 °C (the weather varied from sunshine to rain), conductors were subjected to clashes with a rate of 20 times per minute. Test was stopped after about 540 000 clashes, without reporting any visible damage to the covering layer of the conductor. The arrangement for clashing test is presented in Figure 1.8.

In the second test, conductors did not clash together, but they were in continuous contact with each other. In this field test, the voltage stayed the same (120 kV) and the ambient temperature varied between +2 and +22 °C, the contact was stopped after 17 days with no puncture on the covering

layer. Only the outer layer of the covering present minor damage due to electrical discharges. The long-time contact test arrangement is illustrated in Figure 1.9 a) and b).

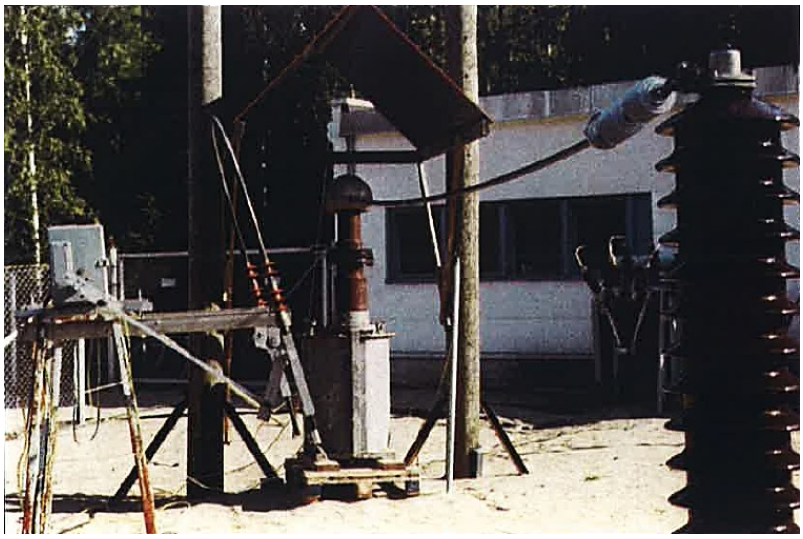

Figure 1.8 *Clashing test arrangement.*

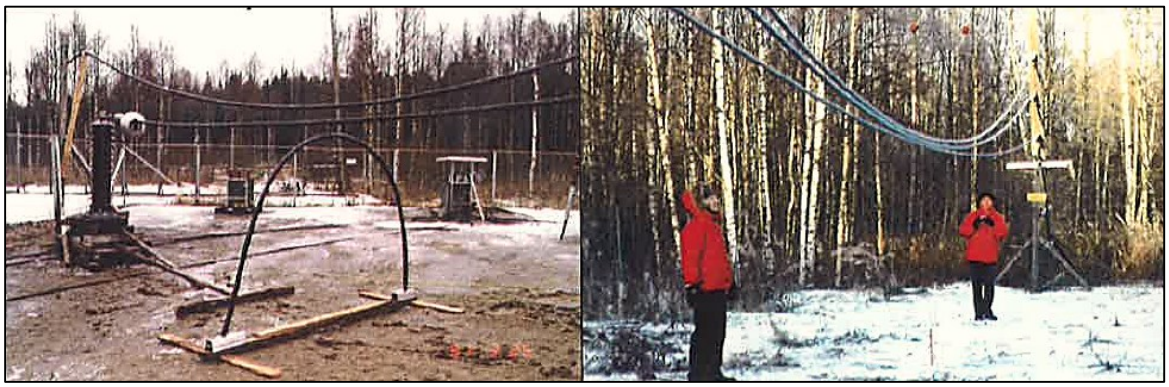

Figure 1.9 a) and b) *Long-time test for contact between HV covered conductors in field.*

The following test was conducted to study the effects of trees leaning on the conductors. Test was carry out inside an electrical laboratory, where a lot of different kind of tree from forest were planted in the laboratory, and the trial conductors were touched by trunk or branches of these planted tree. Voltage was 71 kV and contact between conductors and trees caused corona and high radio interferences noise. Besides, some trees started to dry and sometimes with visible burning.

Other kind of test concerns the formation of electrical water tree in cover material. Electrical water trees are channels with tree shaped, which can grow slowly inside the XLPE insulation if moisture enter into the conductor: this phenomenon can ruin the electrical integrity of the insulation. Different materials and alternative structure were subjected to a long time test, to carry out the best

material to avoid water tree formation and its progression inside the HVCC. As seen in the first section, cover conductor's structure is provided with a water blocking layer and special water tree retardant material in XLPE layers.

The following test was carry out to demonstrate long term operation with various climatic conditions. The outer layer is made of black UV XLPE compound that is also weather resistant: this layer contains 2-3% of carbon black. UV radiation test and other ageing test was conducted to demonstrate covered conductor behaviour in different climatic areas.

The most critical test was phase-to-phase switching impulse test conducted on the pole top structure. Test for voltage withstand were made with linearly rising voltage of 6 kV/s until flashover was reached. Test conditions was:

1. dry and clean;
2. wet and artificially polluted;
3. clean and rain.

The phase-to-phase switching impulse could be estimated to withstand about 390 kV, and the ratio between phase-to-phase and phase-to-ground was assumed 1.45. The second (wet and artificially polluted) and the third (clean and rain) test conditions gave the minimum level of phase to phase withstand of 360 kV, but no flashover occurred from phase to ground: the ratio between phase to phase and phase to ground withstand voltage was 1.73. Other tests were carried out increasing (+19%) phase-to-phase clearance, to achieve adequate withstand levels between phase-to-phase and phase-to-ground. However, even in these conditions all flashovers occurred between phases. It is preferred to have phase-to-ground flashover probability greater than phase-to-phase, from the operational point of view: therefore, it was decided to increase again the space between the conductor attachment points until 1.9 m. Besides, corona at the voltage of 123 kV did not provide any practical limitations to the phase-to-phase clearances. Pole test arrangement is illustrated in Figure 1.10 a), inside a high voltage laboratory; while Figure 1.10 b) show a flashover occurred during the wet condition (number 2.) between phases.

A further test was based on measurement of pre-discharged currents between phases caused by directly lightning on the span. An example of flashover between conductors and formation of pre-discharged channels is shown in Figure 1.11. From the results critical span length was definite, i.e. the maximum span length used to avoid flashover on the span with a certain probability.

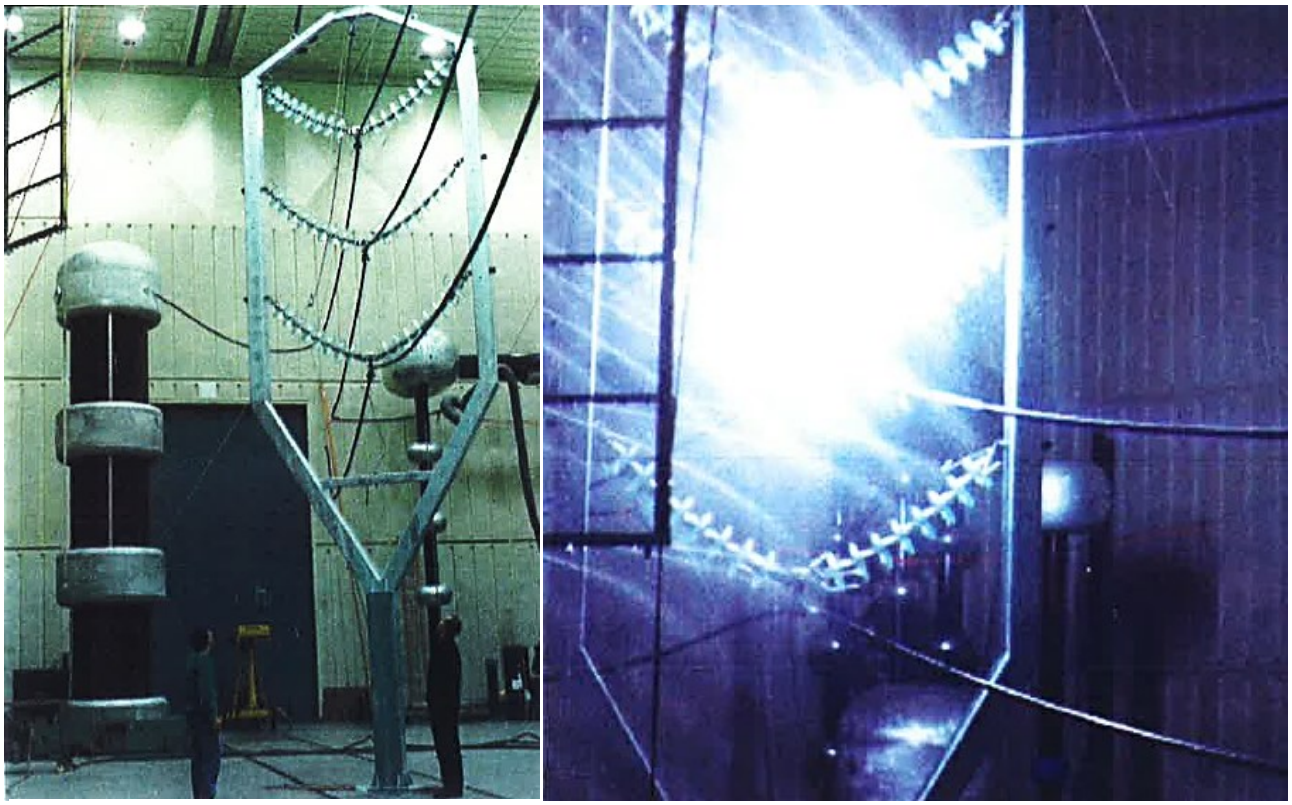

Figure 1.11 a) *Pole top test in High Voltage Laboratory of Helsinki Technical University* **b)** *A flashover during wet tests*

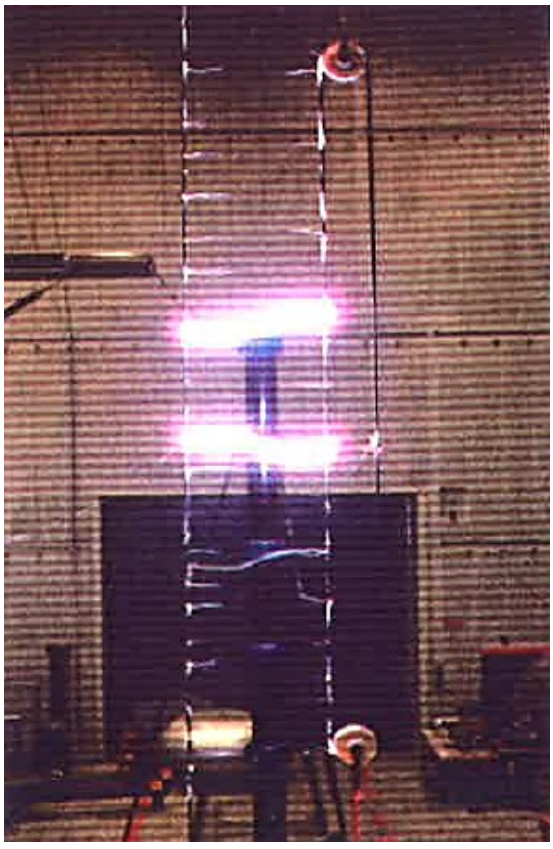

Figure 1.10 *Pre-discharged channels and a flashover between covered conductors installed in laboratory.*

Finally, short time withstand current tests were conductor on suspension clamps used on the tower. Connection of clamp to the aluminium alloy conductor, without peeling the covering, is made using short-circuit connection by piercing the covering and clamp is also connected to two of the rods. This arrangement was test to withstand the shot-circuit requisite of 31.5 kA/0.5 s.

1.8 Upgrading

The total dimension of a high voltage line supporting tower or pole is determined mainly by two factors: the system rate voltage and the design of basic insulation levels. Between the insulation level, needed for the operating voltage of the system, and the impulse withstand, to maintain insulation below transient overvoltage conditions, a considerable margin is required. If a system has 145 kV as maximum operating voltage, three lightning impulse withstand voltage are suggested: 450, 550 and 650 kV peak. In a 145 kV system that can withstand a lighting impulse voltage of 550 kV peak, the minimum phase-to-ground clearance is the minimum air clearance of 1100 mm. Therefore, the overall line dimension and tower geometry is set by air flashover characteristics. The way to upgrade a transmission line, avoiding to increase the structure height or conductor space, is to control and limit the lightning impulse voltage, and ensure that propagating impulse wave is reduced at the mid span position to less than the phase-to-phase flashover level. Upgrading is possible using an efficient surge arrester in the line suspension point, that can reduce the peak of the incident lighting surge.

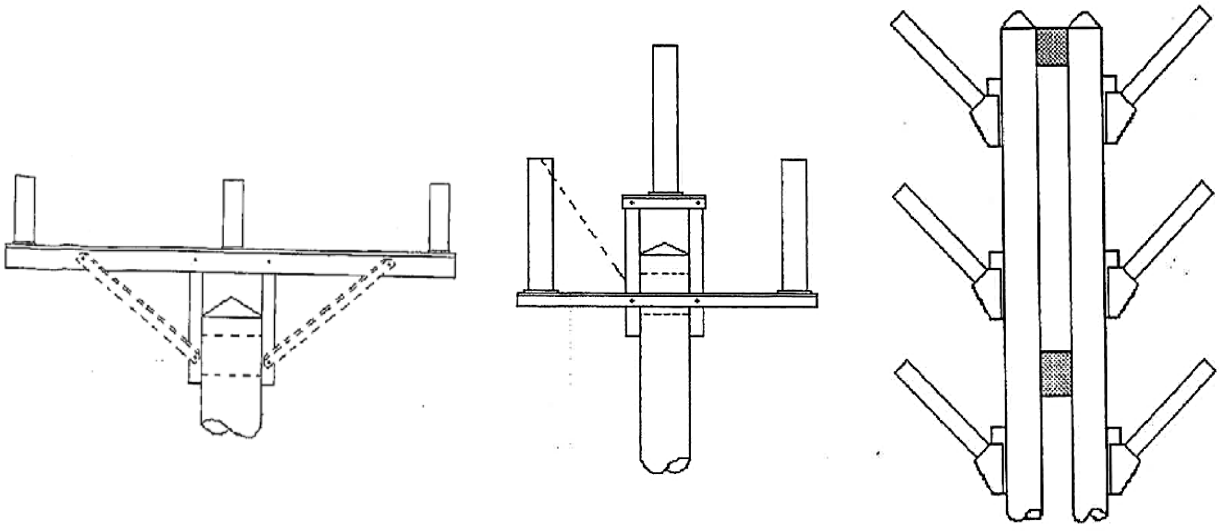

Figure 1.12 *HVCC in **a)** horizontal arrangement, **b)** triangular configuration and **c)** dual circuit on single pole.*

Covered conductors are a low cost and low profile alternative that can reuse existing 33 kV pole positions of existing circuits, to upgrade power line to 132 k V. Upgrading 33 kV bare lines to 132 kV high voltage covered conductor lines is possible using different configurations and existing structures. The configuration for HVCC are the following: single pole in horizontal configuration, single pole in triangular configuration, single pole with dual vertical circuit and existing Trident line. The use of single pole in triangle configuration reduces the costs of the lines, thanks to the use of only a single LISA on alternate poles as lightning protection. The new design of a dual circuit on a single structure with covered conductors has been calculated to be feasible. This novel types of covered line can replace existing Trident lines. Existing Trident line has been designed and set using the basis and regulation of traditional factor of safety. The direct replacement of existing old bare conductors with HV SAX covered conductors do not involve any other change, in fact poles, foundations, insulators and stays are sized also for larger and heavier covered conductors. In these following figures horizontal configuration, triangle arrangement and single pole dual circuit are shown respectively in Figure 1.12 a), b) and c).

1.9 The Finnish experience

In this section the first high voltage covered conductor line is presented, both because it was the first to be built at this voltage level, and therefore it was a reference for the next installations, and because in this work, next chapters will be reported to this specific covered conductor line.

Scandinavian countries were the first to develop overhead lines that use covered conductors since the mid-eighties. The first country to introduce in high voltage transmission line covered conductor was Finland. In 1995 a Finnish utility located near Helsinki wanted to build a novel 110 kV transmission line in order to feed the industrial area of Sula from Mätäkivi. There was already an existing line and the new piece of line would be about 6 km long. The line would pass through a growing urban area, and most of it would be visible to everyone. Therefore, environmental issues were from the beginning a primary aspect of the project, both for the aesthetic impact and for the narrow wayleave. It was presented the opportunity to insert covered conductors on the line: at the end, it was decided to use conventional bare conductors and LMF SAX covered conductors on half art of the line each. The line started to work in April 1996 and from the beginner it has performed very well, with good quality supply and without any disturbance in energy delivery. In this way new high voltage line is an experiment to determine new criteria for building new compact structure in small corridors, both in forest and in densely populated areas, Figure 1.13.

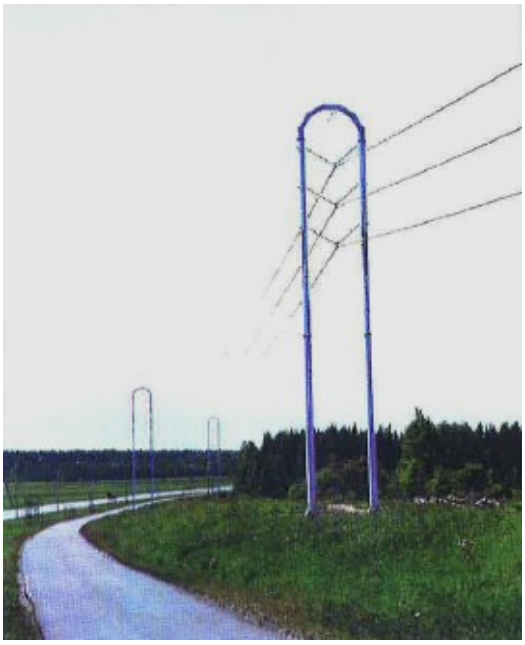

Figure 1.12 *Towers of Mätäkivi-Sula 110 kV SAX line in Finland.*

Cables were made by means of a stranded and compacted aluminium alloy conductor of 355 mm^2 water-blocking with swell powder. They are wrapped with semiconductor swell tape around the conductor, and finally they are insulated by triple extruded XLPE layers, water tree resistant and weather track resistant. Thanks to this special insulation, the feedback from this first installation was positive, in fact the covered conductor lines had less fault than normal bare line, during thunder storm and strong wind.

Because the Finnish high voltage covered conductor was unique, its performance in field was constantly monitored with vibration recorders that had registered vibration frequency and amplitude every 15 minutes. After that results were analysed, minimum lifetime was calculated on the measurements and it was estimated to be about 455 years, but on the results it was also estimated a decreasing in lifetime raising by about 25% the conductor tension. In order to minimize extra costs, the idea was to use conventional material for the line design whenever possible. Conventional V-insulator set were used for HV SAX line, that is normal U 70 BL of toughened glass. Besides, armour grip suspension (AGS) clamps, used usually in optical fibre cable installation, were used as suspension clamps, avoiding conductor coating to be peeled off. Using connectors that pierce the conductor coating in armour rod ends, it was possible to make a metallic contact between the external insulator and the inner conductors, minimizing the stress on the conductors. AGS clamp were one of major deviation to traditional design. The configuration

including AGS-clamp and V-insulated set is illustrated in Figure 1.13. Initial estimations suggested no vibration dampers were needed, therefore no extra dampers were installed; if dampers would be necessary, they could be installed without any problems at the end of AGS clamp. Other deviation from conventional design was the tower type, that in this Finnish HV SAX application was an inverted U-shape tubular tower, with vertical phase configuration. The overall height of the covered conductor tower was shorter than conventional ones, but the height of lowest conductor was 1 m higher, Figure 1.14.

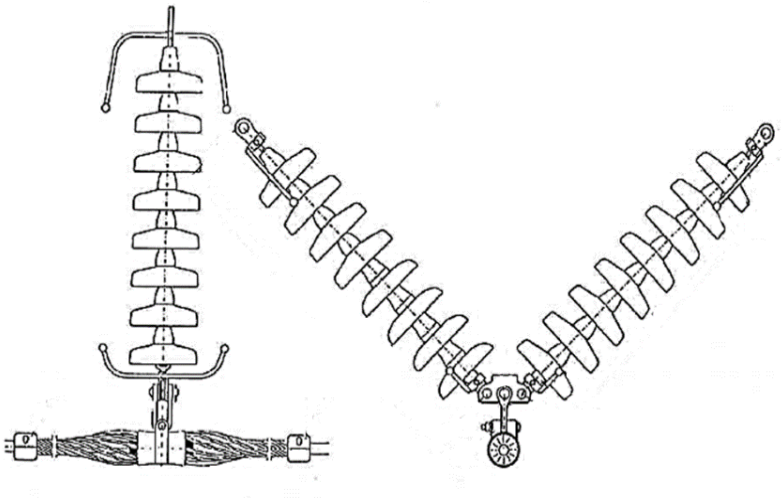

Figure 1.13 *V-insulator set and AGS suspension clamp.*

Installation procedure of covered conductors in Finland was not different from the stringing of traditional bare conductors. Stringing equipment used was typically used for optical cable stringing. The allowed bending radius of 60 cm and installation temperature of -20 °C rarely were a restriction to stringing work. Special attention was also paid to the grounding of the conductors, both before and during stringing, especially in the vicinity of another energised lines. During installation work the conductor end always was in contact to ground, because induced voltage could be present on the conductor and the covering prevented to induced voltage to ground.

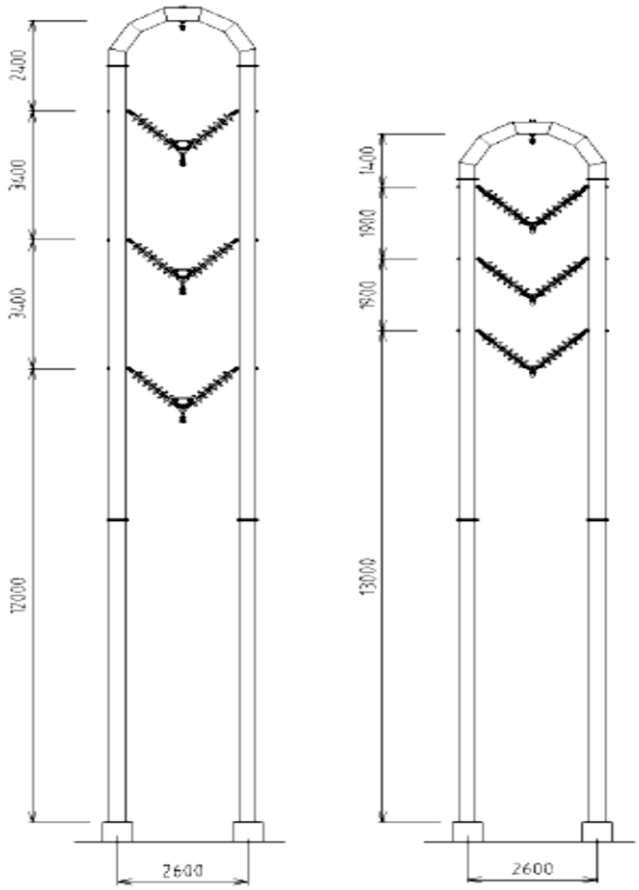

Figure 1.14 *Comparison of towers height for 110 kV transmission line U-shaped. On the left conventional bare conductors; on the right covered conductors.*

Cost comparison was possible to evaluate how much covered conductor line was more expansive than traditional and which were factors that contribute to rise up the cost. The comparison was not an easy task because different type of line (CC and bare line) were been thought for different areas and climatic conditions; Mätäkivi-Sula line were exploited for pass through a forest area. In this new covered power line spans were shorter, increasing the number of tower; nevertheless, tower and foundations cost were no different. Installation work was about 20% more expansive mainly due to AGS-clamps, aside from covering conductors itself, that had led the cost to be more than double respect to bare conductor: the overall cost of the line was in total increased to 25% per km. On the other hand, the benefits brought by this new technology, made the line more acceptable to the people thanks to lower appearance impact and eco-friendly aspect (magnetic field decreased to 30%), but also more acceptable to the network owner for low number of fault and outage of the line.

Finnish experience with high voltage covered conductors had demonstrated to be very positive and it encouraged other countries to follow this example, thanks to the fact that every results and data collected were cheering. Since it was the first line of this kind, several studies were carried out, as it will see in this work, the automatic monitoring and detection of partial discharges on the line caused by a fallen tree dropped on the line.

Chapter 2

Partial discharge caused by a tree falling

In this second chapter, partial discharge phenomenon is presented, in particularly partial discharges which are made by a tree that fall on the covered conductor line. First of all, the creation of partial discharges during an incipient tree fault is explained and then various types of them are presented, especially surface discharges which are usually made by the contact between the tree and the covered conductor. After most of the chapter is used to explain the features of trees, the wood composition and how the amount of moisture can modify the electrical characteristics of trees; tree resistance and earth resistance (in addition to the environmental characteristics) affect the magnitude of a partial discharge formed. Several test both in laboratory and in field are carry out to study this phenomenon and how much these characteristics influence the results. In the last part, equivalent circuits of incipient fault caused by a tree on a high voltage covered conductor line, based on the number of phases involved, are presented.

2.1 Incipient tree fault and partial discharges

With the term incipient tree fault (ITF), it is indicated the operational state of the line where a tree has fallen above the line, but it has not yet caused a fault thanks to the mechanical and electrical capacity of the covered conductor to withstand trees, as it can be seen in the Figure 2.1. A fallen tree on the line is not a normal operational condition, but it not lead to an immediate interruption of the energy supply; only an electrical breakdown of the covering cause a fault, with an immediate outage of the line. The fallen tree distorts the electric field of the conductor and causes the formation of partial discharges (PD) in the air around the conductor, between the tree surface and that of the covered conductor. This could lead to a breakdown of the covering and therefore cause an earth fault with the outage of the line.

Conventional fault detection methods cannot detect a fallen tree on the covered conductor line, due to the low tree impedance (tens or hundreds of kΩ), compared to covering conductor one (tens of MΩ at 50 Hz). There are two different types of incipient tree fault:

- The incipient earth fault (IEF), which is all the cases where the tree gets in contact with one or more phases (and possibly with the ground wire), but phase conductors are not in contact with each other;
- The incipient short circuit fault (ISF), which is all the cases where, unlike before, two or more phases are in contact with each other.

Figure 2.1 *A tree fallen on a covered conductor line.*

In power cables, there is the grounded shield on the outer layer that avoids any outside objects to disturb the electric field in the insulation. In covered conductors this grounded shield is not presented, and therefore any dielectric, semiconducting or conducting objects in the vicinity of the covered conductors could distorts the electric field in the surrounding air. A field distortion sufficiently strong leads the formation of partial discharges in the air: PD manifest themselves with small current pulses both in the tree and in the conductors that touch directly the tree. As it is presented after in the next sections, the magnitude and pulse shape of partial discharge in covered conductor can be affected by several factors, as the number of phases (and ground wire) in contact with the tree, the electrical features of the tree, the climatic and seasonal variations.

When an electrical breakdown occurs in only one phase, it leads to a permanent earth fault, which usually actives the conventional protective relays, if the relays are set for this fault impedance. Due to the fault, supply interruption to the costumers may be relatively long: the tree has to be

removed and the conductor has to be repaired before the supply can restart. If the electrical breakdown occurs in two or more phases, it leads to a short circuit fault, with the phases in contact directly to each other, and even when they are close enough. A short circuit is more harmful than the earth fault, causing a voltage drop in all the feeders connected to the same busbar. Moreover, the short circuit causes forces than further stress the network components, particularly the windings of the transformers: if there is a high short circuit risk, the line is de-energized immediately avoiding any additional damage to the network and its components.

Medium voltage covered conductor lines usually can withstand the stress due to a fallen tree for weeks or even mouths, so a visual inspection after a strong storm is enough adequate to avoid supply interruptions. High voltage covered conductor lines can withstand the stress due to a fallen tree for one or more hours before the electrical breakdown. A response time of 10-20 minutes is adequate for the incipient fault detection system in case of incipient earth fault (5-10 for incipient short-circuit fault), to leave enough time to network operators for rearrange an alternative power supply before de-energize the line and permit the repair operations. As it will see in the next chapters, automatically detection system is needed with continuous on-line PD measurements.

2.2 Classification of partial discharges

Partial discharges are small current discharges and they could be of different type: however, all are united by the fact that they bridge the insulation between conductors, due to the non-uniformly distributed electric field. Local electrical stress results in partial discharges, in form of various current impulses and voltage impulses, with less than 1 second duration; PD in high voltage equipment causes a movement of charges. In the case of a falling tree, the discharge region is confined on one side by a semi conductive material, formed by a natural tree, and on the other side by a part of the dielectric, which in this case is cross-linked polyethylene (XLPE). Usually a partial discharge happens when an insulator does not work as it should, due to internal structural damage or surface pollution: insulators have some impurities and void which cause weak regions in the insulator, and when dielectric constant of void is low compared to that of insulator itself, it causes therefore the formation of partial discharges. In the case of a contact between tree and covered conductor, partial discharge happens due to electric field distortion through thermal, chemical and electrical mechanisms. As time passes by, PD causes significant degradation in the insulators, though the following discharges are smaller in magnitude, due to previous damage, failure occurs in the insulator, with an irreparable damage in insulator system. Appearance of partial discharges

is the main reason for the degradation (both mechanically and chemically) and electrical breakdown of the insulator. Dielectric materials are divided into inorganic and organic dielectrics: inorganic dielectrics, such as glass, mica and porcelain are more immune to partial discharge effects, while polymers are part of the group of organic dielectrics and are more susceptible. The main reason that causes degradation is the heat energy: thermal effects on insulting materials, due to partial discharges, cause the deterioration of the insulating material.

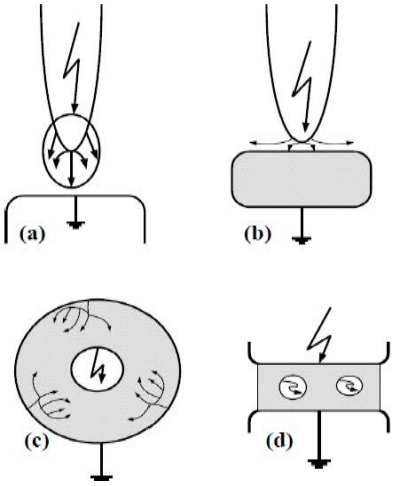

Figure 2.2 *Classification of partial discharges*: **a)** *Corona discharges,* **b)** *Surface discharges,* **c)** *Treeing channel and* **d)** *Cavity. discharges.*

Partial discharges can be classified in various way. The most used way separates the discharges in three types:

1. *Corona discharge*: it results by non-uniformity of electric field on the conductor with sharp edge. The insulator around the conductor could be gas, air or liquid, and corona discharge affects directly this surrounding insulator, as in Figure 2.2 a);
2. *Surface discharge*: it takes place on the interface of dielectric material, outside from power equipment, as in Figure 2.2 b). Factors which affect such discharge are the permittivity of the dielectric material and the voltage distribution between the conductors. Partial discharges made by a leaning tree on a covered conductor lines are surface discharges;
3. *Internal discharge*: it occurs inside the insulation system, due to the void in the material. Usually, the proprieties of an insulating material used in high voltage equipment are tested by a PD measurements. Included in internal discharges, there are two types of phenomena discharges:

- *Treeing channel*: due to high intensity fields, the insulating material is deteriorated, and therefore continuous PD occur, called treeing channels, as in Figure 2.2 c);
- *Cavity discharge*: it happens in liquid or solid insulating materials which present some cavities inside the material, as in Figure 2.2 d). The cavities are filled generally with air or gas: discharges occur when the gas in these cavities is overstressed.

Partial discharges can also be classified using another way, based on the visual characteristics of the breakdown channels and the waveform of the discharge current. Discharges cavities or in short gap spaces can be divided into: spark, pseudo glow and pulseless glow discharges. Spark discharges are characterised by high luminosity, rapid raise times and narrow breakdown channels, while pulseless discharges emit only a diffuse glow: pulseless and pseudo glow cannot be detected with conventional PD pulse detectors.

2.2.1 Characteristics of surface discharges

Discharges on the surface of dielectric produce two typical PD patterns, presented in Figure 2.3. The representation of partial discharges on an ellipse is an old method to visualize the discharges on the screen of an oscilloscope: partial discharges are superimposed on an ellipse representing the sinewave of the voltage. The position of the voltage peak is indicated by the signs "+" and "-", the zeros by "0", while the rotation of the time base by the arrow. In Figure 2.3 a), there are two half cycles, with the same amplitude in both half cycles, in Figure 2.3 b), instead there is a great amplitude difference between the half cycles. The discharges on a half cycle are greater in number and smaller in magnitude than the other half cycle.

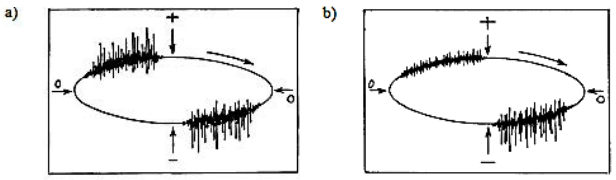

Figure 2.3 *Partial discharge pulse patterns on elliptical time base:* **a)** *two half cycle and* **b)** *one half cycle.*

When it is applied an increasing AC voltage, both number and magnitude of surface discharges increase rapidly. When the voltage is sufficiently high, very large discharges occur in negative half cycle, caused by the formation of stable ions deposited on the surface of the dielectric material. The shape of applied voltage affects the recurrence of surface discharges, in addition to the

dimension and permittivity of the dielectric material. Whit a positive electrode, electrons leave positive ion space on the solid, while when the electrode is negative, negative ions and electrons are deposited on the solid. This charge deposition and accumulation on the dielectric surface affects the recurrence of the discharges and the PD patterns. In fact, the total electric field during a discharge is the sum of the applied field and the field due to charge deposition on the surface of insulator during the preceding half cycle. The surface resistivity of a polyethylene sample affected by partial discharges ranges from 10^6 Ω (whit wet surface) to 10^{11} Ω (with dry surface) per square, compared to 10^{15} Ω per square for not exposed to partial discharges area.

2.3 Electrical proprieties of trees

In order to understand the next sections a prior knowledge about electrical proprieties of trees is needed. In fact, there is a correlation between the electrical proprieties of trees and partial discharges: the resistance and earthing resistance of tree are the main parameters to keep in consideration when a discharge takes place, in addition to the environmental conditions which also influence the discharges. In a covered conductor, the electric field around the phase is not bounded by a grounded shield as in cable, therefore any tree branch in contact whit the conductor or in vicinity distort the electric field. If the tree distorts sufficiently the electric field partial discharges are generated in or on the covering; electric field geometry in covering layer and around it is affected by several factors, as the geometry and radius of the conductor, the proprieties of semiconductor layer, thickness and permittivity of the covering layer, but mostly by the proprieties (size, shape, dielectric and conductivity proprieties) of the field distorting tree. So it is very important the study about the electrical characteristics of a natural tree when it is in contact whit a covered conductor lines.

2.3.1 Characteristics of trees and wood

The covered conductor lines presented in this work are designed to their use in a forest area, where the right of way is narrow, avoiding to cut out a lot of vegetation. Globally, forest areas cover about 30% of the land area (Figure 2.4), but a large part of it is far away from populated areas. In Finnish environment, the tree species most common are pine, spruce, birch and aspen; these are among the seven most widespread tree species in the world forest. Therefore, these four species are studied in this chapter. As said before, the most important characteristics of a tree, in order to study the incipient fault and generation of partial discharges, are its electrical proprieties. In fact, mechanical problems are not a relevant issue for the conductor, so a mechanical analysis is not

considered in this work from the point of view of incipient tree fault. The trees of all these species, completely grown, are tall enough to reach the line conductors, if the conductor suspension height is approximately 12-15 m.

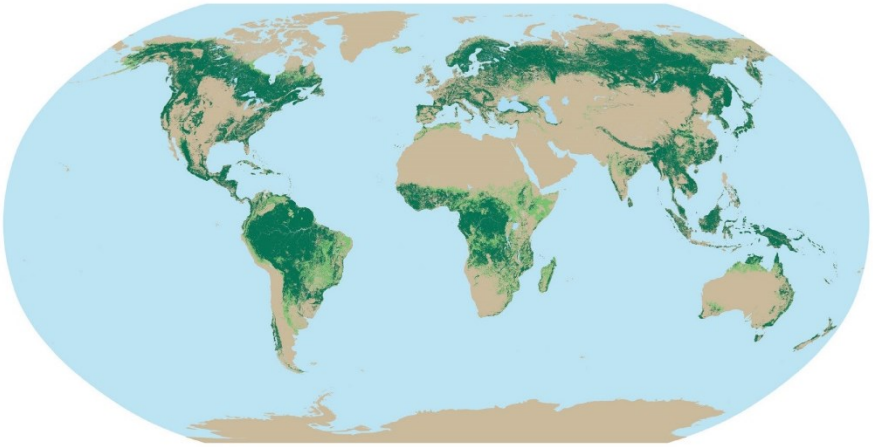

Figure 2.4 *Distribution of forest in the world, marked by green colour.*

To understand the characteristics of trees, electrical proprieties of wood need to be studied. In particular, the moisture content in the wood has a considerable effect in the electrical proprieties of the tree. Therefore, it is important to divide the wood in so called green wood, present in living tree, and timber, which instead is more dry. Besides, it is important make another distinction between electrical proprieties of wood in AC and DC: in DC the effect of moisture content in wood is more pronounced in resistivity than in AC. Other significant factors affecting the electrical proprieties are the frequency and the electric field applied to the wood.

All trees have three main parts: the roots, the trunk and the branches. The trunk can be divided radially by growing rings, like in Figure 2.5. The outer part, called sapwood, is produced by the rapid growth in spring and summer: it is a softer and lighter coloured wood, it is the food storage and sap conduction takes place. The thickness of this layer is in the order of 10 cm. The inner part, the so called heartwood, is produced by slow growth in autumn and winter: the central part of the tree, provides mainly the mechanical and structural rigidity for the trunk.

Considering the species named before, the most common in Finland, pines have strong and thick roots, which provide a strong anchoring system into the ground; spruces and birches instead have a weaker root system, which makes the trees more susceptible to the storm damages. Often young

birches are very thin with slim stem and branches, which easily lead them to clash against power lines, during a storm or under snow load.

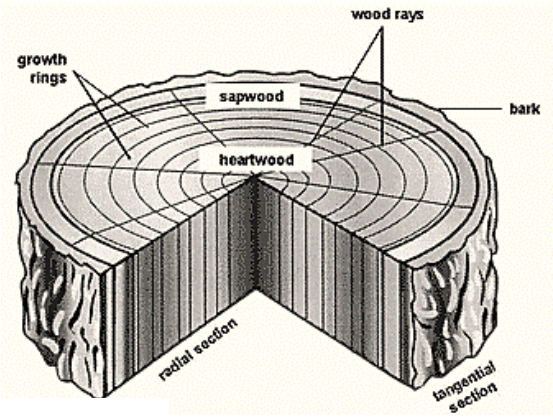

Figure 2.5 *Horizontal and radial section of a tree trunk. Radial section can be divided in sapwood and heartwood.*

2.3.2 Moisture content of wood

The resistivity of wood is a function of the moisture content, the temperature and the frequency and magnitude of power voltage. The moisture content (u_w) of the wood is definite as:

$$u_w = \frac{m_w}{m_0}, \tag{2.1}$$

where m_w (kg) is the mass of water in a wooden object, while m_0 (kg) is the dry mass of the same object. To evaluate the moister content of a wooden object, its mass must be measured when it is moist and when it is dry. In various part of the tree, the moisture content is different: the root, which never can come in contact whit the line, are the moistest part of the tree, while the branches, which can easily come in contact whit the power line, are the driest part of a tree. Moisture content variation is explained by the amount of fluid that flows in the various part of the tree. From the point of view of the trunk, sapwood have a higher moisture content respect to heartwood. Considering for example a pine, the moisture content in heartwood is about 26-54%, while the moisture content in sapwood is in the range of 96-177%. In Figure 2.6 there are two examples of trend of moisture content (%) in a spruce (a) and in a pine (b), along the horizontal section, as the ray of the trunk grows.

Increasing the moisture content in the wood, the resistivity decrease. Therefore, a high moisture content in sapwood is favourable for the incipient tree fault, because it increases the generation of partial discharges, respect to hardwood, which cannot come in contact directly with the covered

conductor line. Considering the anatomical structured of a tree is, it is very probable covered line comes in contact with the external tree layer, closer to sapwood layer, promoting the partial discharges generation.

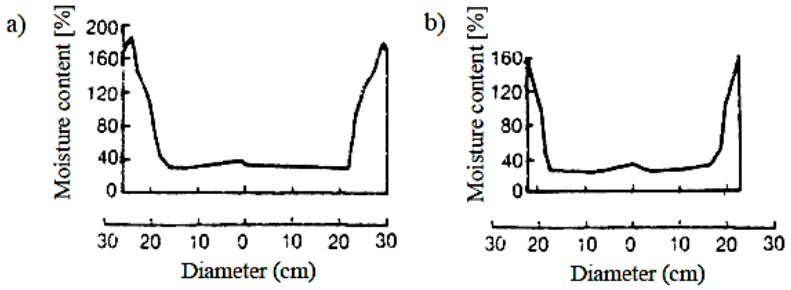

Figure 2.6 *Horizontal moisture content variation at a height of 55 cm from the ground in* **a)** *spruce and in* **b)** *pine.*

Moisture content variation is present also in vertical, along the stem. Vertical variation in moisture content is greater in that trees containing more sapwood, where an increase of moisture content is visible from the base of the trunk to the top of it. Considering the same tree, a variation in moisture contain is considerable great whit the seasonal changes: this variation during the seasons can be seen both in sapwood and in heartwood part of the tree. Other factors that can influence the moisture contain are the quality of the site and the age of the tree. The bark contains different quantities of moisture: considering pines and poplar, the outer part of the bark contains 25-35% of moisture content, with small variation during seasons, in contrast with the inner part of the bark with moisture content of 200-250% with high variation in seasons.

2.3.3 Electrical characteristics of wood

As it seen before, the behaviour of a tree or its branch, in the proximity of a covered conductor line, depends on it shape and dimension, in addition to its electrical proprieties (resistivity and permittivity). The latter are affected by the moisture content of wood and by the composition and structure of the wood cell wall. The chemical composition of the wood cell, in particular the amount of lignin in the cells affects the resistivity of wood. The conductivity of the wood increases as the lignin content increases: the conductivity in the wood is a non-linear function of the moisture content, the magnitude and the frequency of applied voltage. In DC, the logarithm of the electrical conductivity of the wood, in function of the moisture content u_w, has a linear relationship, until the fibre saturation point at about 30%, as shown in Figure 2.7.

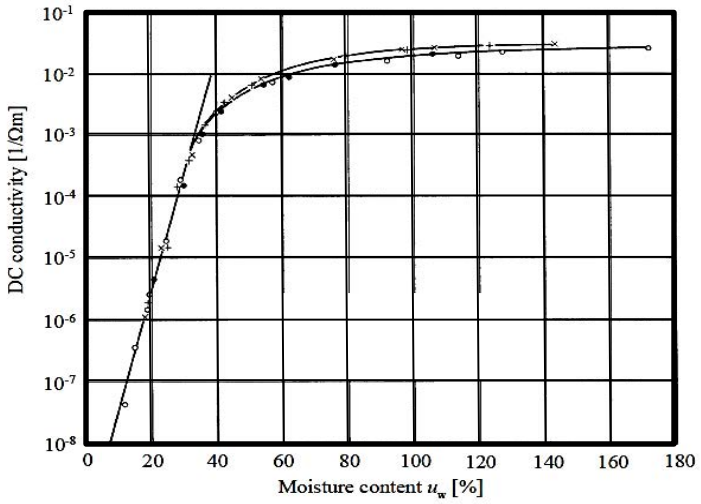

Figure 2.7 *Dependence of the DC electrical conductivity of wood on the moisture content.*

Instead, in AC the conductivity of the wood is strongly influenced by the frequency applied, in fact, increasing the frequency, the conductivity of the wood increases, as shown in Figure 2.8. In AC the moisture content influence less the conductivity of the wood respect to the DC. However, the effect of frequency on the conductivity decreases if the moisture content increases: beyond a certain frequency, the AC conductivity increases, but the moisture content of the wood is less influential.

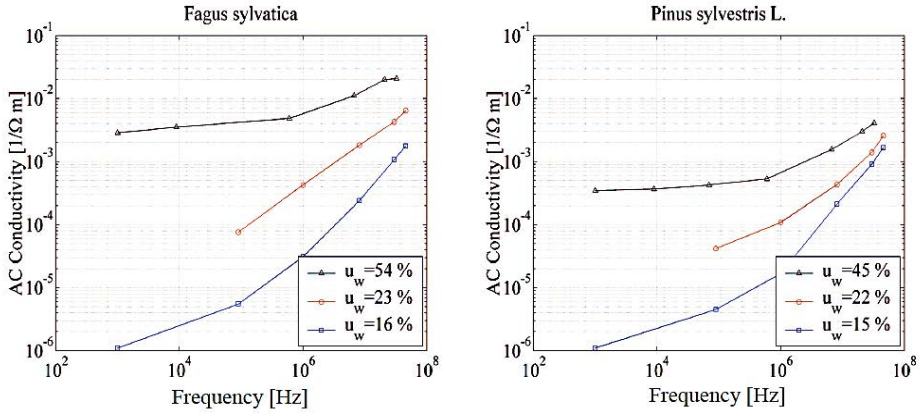

Figure 2.8 *AC conductivity of the wood in function of frequency applied, with 18 °C of temperature, in a beech and a pine, at different moisture contains of wood.*

Finally, the resistivity of the wood decrease whenever the temperature increase, as show in Figure 2.9. With low moisture content of wood (between 0.1% and 9.8%), the dependence between resistivity and temperature is linear, but for high moisture contain (between 15.5% and 29.9%),

the dependence is no longer linear, showing some nonlinearity among the 0 °C: this phenomenon would be due to the freezing of the water into ice crystals.

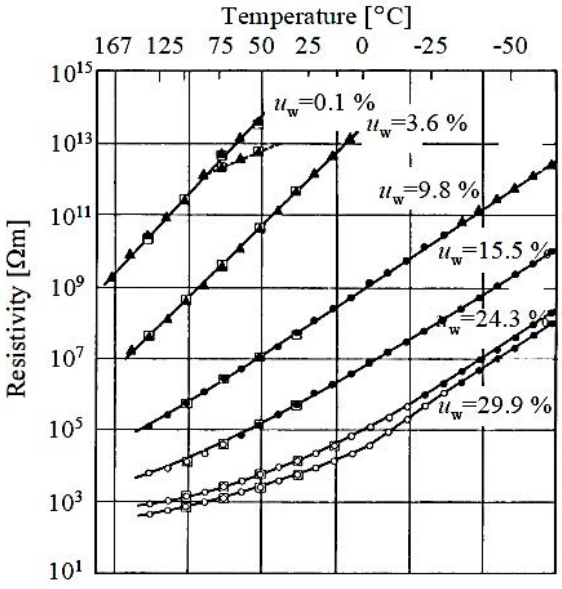

Figure 2.9 *Resistivity of wood on temperature in case of different moisture contents of wood* u_w.

2.4 Electrical characterisation of trees felled on the trial line

In the previous section a general presentation about the characteristics of trees has been presented. In this section the focus goes to the trees that are present in the Finnish forest area, which can go in contact with Mätäkivi-Sula covered conductor line (Forest-SAX line). Several test, both in field and in high voltage laboratory, have been carry out, to study the characterisation of these trees that can be found along the line pattern: to do that, a covered conductor trial line has been made and the various test have been done using this trial line. Natural trees were felled on the trial line during the field test, in order to study the phenomenon of partial discharges creation, related to an incipient tree fault, considering different environmental conditions. The characteristics, the patterns, the temporal variations and the magnitude of partial discharges have been studied in order to understand how these can affect the detectability of incipient tree faults. The resistance and earthing resistance of trees are relevant factors to consider during conventional operations of fault relay, and during the detection of an incipient tree fault: therefore, the resistances and earthing resistances of trees were studied during these tests.

Considering the trees studied in the various test, the majority of the trees utilised were spruces and birches. Although the pine is the most diffuse tree in Finnish forest, spruce (56%) and birch (29%)

are more susceptible to bend or fall on a power line, as shown in the pie chart in Figure 2.10, considering their structural characteristics (as seen in § 2.3.1) and the experience of the line owners. The statistical considerations on pines (10%) and aspens (5%) are less meaningful, cause the small number of samples used in tests, which tried to follow the real conditions of fallen tree on the line.

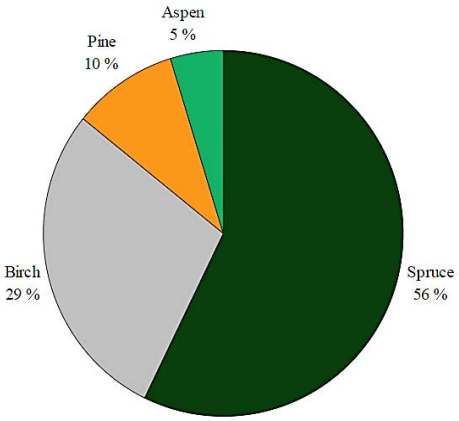

Figure 2.10 *Species of trees felled on the test line.*

The aim of these test was to understand if the detection of trees that fall on a high voltage covered conductor line is possible with an economical and feasible PD measuring system, and if this measuring system works well in different season conditions. During the test, to simulate a natural tree falling, part of the roots of the tree were broken and then an excavator pushed the tree in contact with a de-energized CC trial line, as shown in the Figure 2.11, which illustrate the steps for set the test. After the falling of the tree on the line, the earthing resistance of the tree was measured, and only after the measurements the line was energized. Probably in this test arrangement, covered conductors experiences a different electrical stress, compared to a natural fall, because in the test the tree falls on a de-energized line. Besides, no load was connected to the line during the test, and therefore the temperature rises caused by losses in conductors was minimal. Finally, it was to consider that at the PD frequency range, a power transformer represents a capacitive load.

Figure 2.11 *Steps of test arrangement:* **a)** *the roots of a tree felled on trial line,* **b)** *the contact point between the tree and the 110 kV covered conductor and* **c)** *an example of a tree lying on the 110 kV Forest-SAX trial line.*

2.4.1 Resistivity of trees felled on the trial line in different seasons

The resistance, resistivity and earth resistance of the trees were measured using the two configurations in Figure 2.12. The tree resistances R_{tx} were measured in the trunk from a point, that is 20 cm above the ground, to the contact point between the phase and the conductor, at a height of about 10-12 m (Figure 2.12 a)). The earthing resistances R_{te} were measured before the test, from a point in the trunk 20 cm above the ground, and a ground electrode distant 30-50 m from the tree (Figure 2.12 b)). The foot end resistivity ρ_f was measured on a portion of trunk between 0.2 m from the ground and 1.5-2.0 m, whit d_v= 1.3-1.8 m, before the tree was felled against the line (Figure 1.12 a)); while the top end resistivity ρ_t was measured after the tree had

been removed from the test line, on a portion of trunk starting at the contact point between tree and phase conductor, and ending after a distance of d_v= 0.3-0.5 m under that point (Figure 1.12 b)).

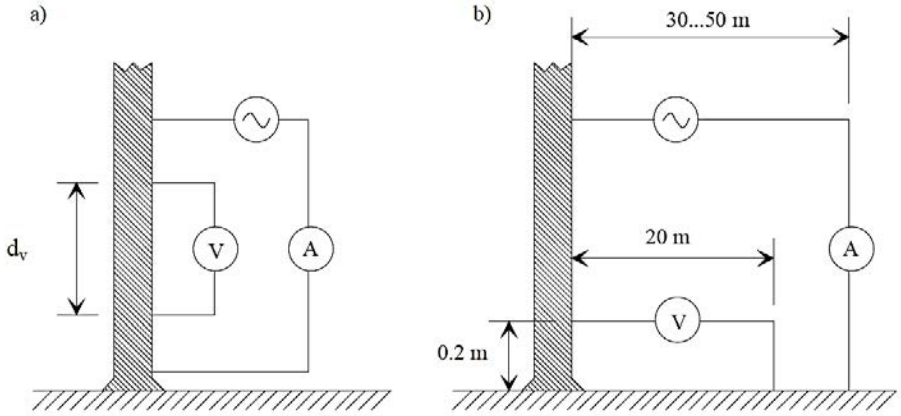

Figure 2.12 *Configuration used in measurement of* **a)** *tree resistance, foot end and top end resistivity and* **b)** *earthing resistance of tree.*

The results of the measurements of various resistances are summarized in Table 2.1. In the table, in addition of values of tree resistance R_{tx} (Ω), earthing tree resistance R_{te} (Ω), foot end resistivity ρ_f (Ωm) and top end resistivity ρ_t (Ωm), there are also the type of tree whit its identification number, its height (m), its perimeter (m), the ratio between resistance and earth resistance of the tree R_{tx}/R_{te}, the ratio between the resistivity ρ_f/ρ_t and the seasonal conditions as the ambience temperature T (°C), the relative humidity in the atmosphere RH (%) and the month of the year.

Considering spruces and birches, the average value of relative humidity RH, in case of spruces, is 79%, while in case of birches is 83%; the average temperature is 9 °C for the spruces and 7.6 °C for the birches. Considering the same month of the year, the resistances and earth resistances of birches are higher than those of spruces: the average resistance of the birch is over twice than the average resistance of spruce, and also the average earth resistance of birch is twice than that of spruce.

Table 2.1 *Results of measurements on the trees.*

Tree ID	*Tree species*	*Height of tree* (m)	*Perimeter of tree* (m)	R_{tx} (Ω)	R_{te} (Ω)	R_{tx}/R_{te}	ρ_f(Ωm)	ρ_t(Ωm)	ρ_f/ρ_t	*T* (°C)	*RH* (%)	*Date*
10	spruce	19	103	112 280	20 995	5.3	4287	209	20.5	2	84	06/03
54	spruce	14	53	244 740	19 281	12.7	1916	145	13.2	0	57	07/03

56	birch	14	40	601 727	54 947	11.0	2422	289	8.4	-7	74	07/03
50	spruce	18	53	188 236	32 867	5.7	1538	159	9.7	0	55	08/03
51	spruce	19	80	612 647	38 171	16.1	11601	797	14.6	-10	80	08/03
40	spruce	17	62	30 382	2 855	10.6	102	-	-	16	63	11/09
41	spruce	18	59	25 099	3 533	7.1	124	-	-	8	93	12/09
45	aspen	18	51	33 456	2 348	14.2	65	-	-	15	61	12/09
49	birch	18	51	53 260	4 106	13.0	204	-	-	14	61	12/09
76	spruce	17	57	23 997	1 255	19.1	46	-	-	14	63	13/09
80	birch	17	51	42 910	3 226	13.3	287	-	-	3	91	13/09
91	pine	20	68	47 283	3 066	15.4	260	-	-	15	65	13/09
66	pine	17	85	18 171	5 363	3.4	228	43	5.3	13	55	19/09
73	spruce	17	50	55 265	4 917	11.2	149	44	3.4	14	53	19/09
3	spruce	21	114	12 994	1 699	7.6	234	59	4.0	6	87	06/11
84	spruce	18	70	28 099	2 106	13.3	193	72	2.7	4	92	07/11
85	spruce	16	64	31 978	2 898	11.0	185	77	2.4	5	90	07/11
86	spruce	19	65	29 609	422	70.2	59	58	1.0	5	89	07/11
26	birch	18	52	69 373	4 277	16.2	327	145	2.2	7	98	08/11
36	birch	17	43	150 524	6 838	22.0	471	164	2.9	7	82	08/11
37	birch	18	42	202 110	6 153	32.8	327	136	2.4	7	82	08/11

This difference may be explained by the different in moisture content and in lignin content of wood. The resistivity of wood decreases as the lignin content increases: the top end and the foot end resistivity of birches are on average twice respect those of spruces, however the average of relative values R_{tx}/R_{te} and ρ_f/ρ_t are almost the same both for birches and for spruces.

Climatic conditions and seasonal variation are important factors to keep in mind in the results interpretations. In Figure 2.13 the variations of the tree parameters are represented: each parameter is divided in the month in which the measurement has been taken, September, March or November. In fact, in the different seasons, variations in characteristics of tree, air and earth are present, due to different temperatures and climatic conditions. In March, the average value of resistance of trees and earth resistance is about 10 times respect the same value in September. In March, the two highest resistance (R_{tx} above 600 kΩ) were measured with an atmospheric temperature below the zero degrees centigrade (-7 and -10 °C), the other one (R_{tx} below 250 kΩ) were instead measured with an atmospheric temperature at or above the zero degrees centigrade (0 and 2 °C). The resistivity of wood increases as the temperature decreases. As shown in the follow figure, the standard deviation in March is higher than other month, it is probably due mainly to the low number of samples and also to the fluctuating of the atmospheric temperatures below and above

the zero degrees centigrade. Temperature above zero, during daytime, causes defrosting of the tree surface and therefore an increase in conductivity: the atmospheric temperature, in fact, have a greater effect on the resistance of the tree than on the earth resistance, because in March the ground remains frozen for several hours of daytime, unlike the tree surface, even if the atmospheric temperatures are above 0 °C.

The resistivity at the foot end changes more than at the top end of the tree. The tree top end resistivity has a great effect on the deformation of the electric filed when a tree comes in contact with the conductors and thus when partial discharges is generated. This smaller variation of top end resistivity respect to foot end resistivity is a preferable characteristic in PD detection. However, top end resistivity was measured after the test, while foot end resistivity was measured before the test, and this could be affected the results. Anyhow, the values measured after the test correspond better to the real conditions of an incipient tree fault, when a tree lies on an energized covered conductor lines.

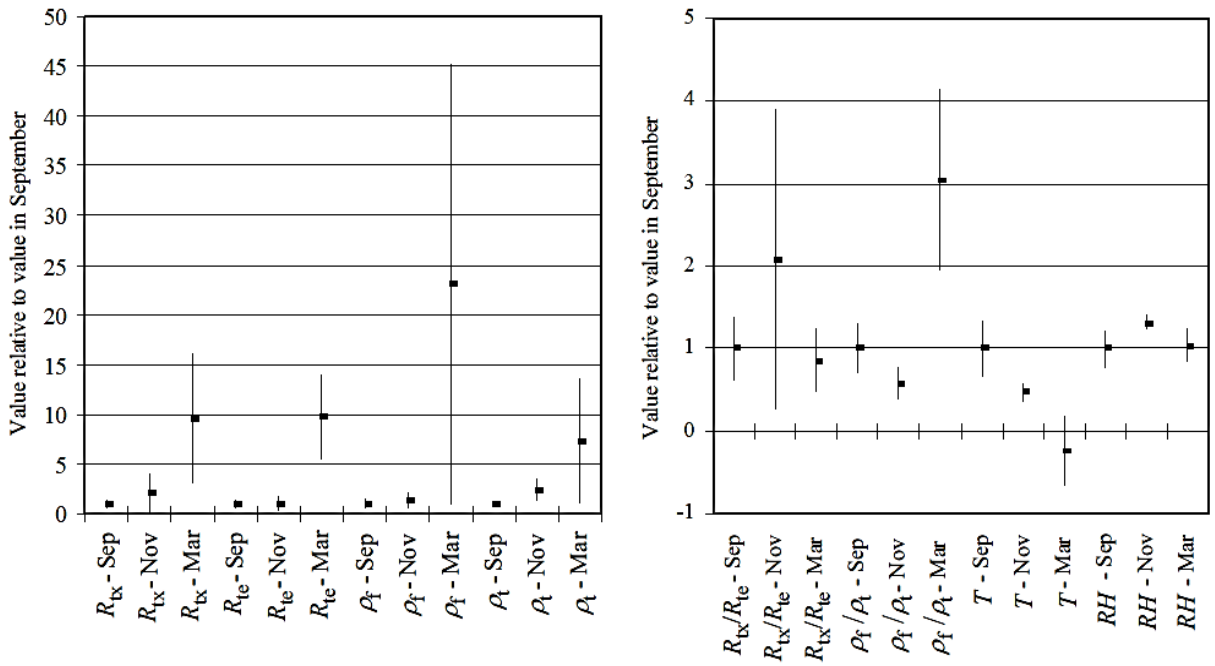

Figure 2.13 a) *Resistance (R_{tx}) and earth resistance (R_{te}) of tree and resistivity at foot end (ρ_f) and top end (ρ_t) of tree, in March and November relative to the corresponding values in September.* **b)** *The ratio between resistance and earth resistance of tree (R_{tx}/R_{te}), the ratio between foot end resistivity and top end resistivity (ρ_f/ρ_t), the temperatures and relative humidity of air in March and November, relative to the corresponding values in September. The average values are marked with black square and the standard deviation of each relative value with a line: each average value is relative to the corresponding average value measured in September.*

Tree resistance and earthing resistance have an important role in the partial discharges magnitude and in the detection of incipient tree fault. These resistances play a big role in the operations of conventional protective relays when an electrical breakdown occurs in covered conductors: a wide variation in resistance and earth resistance of tree is not desirable. Of course, wintertime is the most difficult season for detect tree fault with conventional relays.

2.4.2 Power frequency current flowing in the trunk

Conventional protective relays based only on resistance and earthing resistance of the tree are not sufficiently, due to the capacitance between the covered conductors and the tree that have a considerable effect on the fault impedance seen by protective relays.

In order to evaluate the capacitance resulted by the tree fault, the first thing to consider is the power frequency current which flows in the tree trunk during the incipient tree fault. In the field test, it was measured used the configuration reported in Figure 2.14, whit steel nails embedded in the trunk to a deep of 5 cm used as measuring electrodes, which had a distance d_c of 0.1-0.2 m. In Table 2.2 is presented a summary of the power frequency current measured in field test.

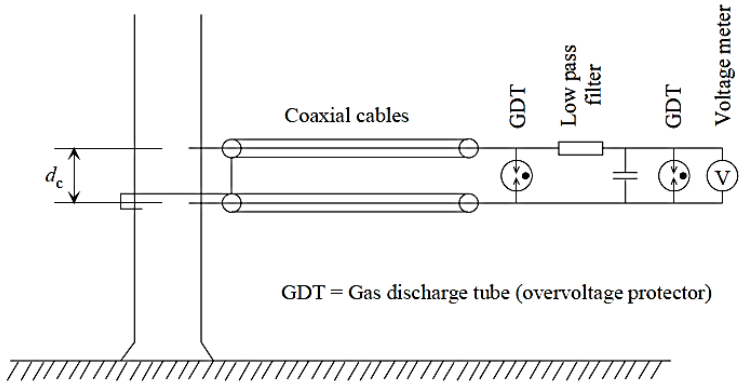

Figure 2.14 *Measurement of the RMS current flowing in the tree trunk during the field test.*

The average RMS current, measured during the test at the bottom of the tree trunk, were generally higher (3.5-10.7 mA) in case of tree in contact with only one or two phases, respect to the cases where tree was in contact whit phase conductors and also the ground wire (0.9-4.9 mA). The resistance and the earthing resistance of the tree were measured using the method descripted in §2.4.1, and their sum is presented in Table 2.2.

As concern the incipient tree fault impedance, in case of covered conductors, it is dominated by the capacitive reactance of the covering more than that of tree trunk which is nearly at ground

potential. In case of an incipient tree fault, with the tree in contact with only one phase conductor, all the incipient tree fault current flows in the trunk between the phase and the earth: the incipient tree fault impedance Z_{if} is calculated as:

$$Z_{if} = \frac{U_L}{I_{if}}, \tag{2.2}$$

where U_L is the RMS voltage of that phase in contact whit the tree and I_{if} is the RMS incipient tree current which flows in the trunk. Assuming that U_L= 110 000/$\sqrt{3}$ V ≈ 63.5 kV and using the mean value of the current I_{if} of the Table 2.2, the incipient tree fault impedance Z_{if} can be calculated using the Equation 2.2. The incipient tree fault impedances are in the order of few megaohms, which is too high to be detected by a conventional earth fault relay.

Table 2.2 *Power frequency currents measured with normal operational voltage (≈ 63.5 kV) from the tree trunk during field tests.*

Tree ID	***Tree species***	***Contact***	***Date***	***T* (°C)**	***RH* (%)**	R_{tx}+R_{te} (kΩ)	***Mean* I_{rms} (mA)**	Z_{if} (MΩ)	C_{tc} (pF)
91	Pine	L3, gw	13/09	15	65	50.3	0.9	-	-
49	Birch	L1, L2, gw	12/09	14	61	57.4	1	-	-
37	Birch	L3, gw	08/11	7	82	208.3	1	-	-
84	Spruce	L3, gw	07/11	4	92	30.2	1.4	-	-
73	Spruce	L1, gw	19/09	14	53	60.2	1.5	-	-
66	Pine	L1, L2, gw	19/09	13	55	23.5	2.2	-	-
3	Spruce		06/11	6	87	14.7	2.4	-	-
50	Spruce	L1, L2, gw	08/03	0	55	221.1	2.4	-	-
10	Spruce	L1, L3, gw	06/03	2	84	133.3	2.5	-	-
51	Spruce	L1, L2, gw	08/03	-10	80	650.8	2.6	-	-
76	Spruce	L1, gw	13/09	14	63	25.3	3.2	-	-
45	Aspen	L1, L2, gw	12/09	15	61	35.8	3.2	-	-
36	Birch	L3	08/11	7	82	157.4	3.5	18.1	176
40	Spruce	L1, L2, gw	11/09	16	63	33.2	3.8	-	-
56	Birch	L3	07/09	-7	74	656.7	3.9	16.3	196
54	Spruce	L3, gw	07/03	0	57	264.0	4.5	-	-
80	Birch	L3, gw	13/09	3	91	46.1	4.9	-	-
85	Spruce	L3	07/11	5	90	34.9	7.4	8.6	371
86	Spruce	L3	07/11	5	89	30.0	8.3	7.7	416
26	Birch	L2	08/11	7	82	73.7	9.8	6.5	491
41	Spruce	L1	12/09	8	93	28.6	10.7	5.9	537

The capacitive reactance X_{ctc}, between the conductor and the tree, can be calculated as

$$X_{ctc} = \sqrt{Z_{if}^2 - (R_{tx} + R_{te})^2} \tag{2.3}$$

where R_{tx} is the tree resistance between the ground and the contact point between the tree and the phase conductor, while R_{te} is the earth resistance of the tree. The capacitance C_{tc} yielding the reactance X_{ctc} at 50 Hz can be calculated as

$$C_{tc} = \frac{1}{j2\pi 50 \cdot X_{ctc}}. \tag{2.4}$$

All the results, obtained by Equation 2.4, are reported in Table 2.2.

2.5 PD phenomena related to incipient tree faults

All the characteristics of an incipient tree fault explained before have been studied using data acquired in extensive tests conducted both in field and in high voltage laboratory. A tree that lies on a covered conductor is considerate a complicate electrode configuration, in which the covered conductor forms a high voltage AC electrode and where the semiconductive tree (roots, trunk, branches and leaves or needles) forms the grounded electrode. Besides, different parts of the tree might not be at the same potential with each other, causing numerous partial discharges, each one with different characteristics and mechanisms. If a point has a sufficiently electric field distortion, both corona and surface discharges can occur. Moreover, branches and needles far from covering conductors are seen as an electrode configuration that lead to a corona discharges generation, while if parts of tree are close to the covered conductors are seen as an electrode configuration that lead to surface discharges generation. The aim of these test is to have the possibility to study the partial discharge waveforms, understanding their characteristics as the magnitude, the time rise and their time evolution.

2.5.1 PD phenomena in laboratory tests

First test that is explained is the laboratory test: partial discharges waveforms caused by a tree falling on a high voltage covered conductor line were studied in a high voltage laboratory. The measurement configuration is presented in Figure 2.15: the PD current was measured by a shunt resistance connected between the ground and the trunk, and the PD waveforms were measured and made visible on an oscilloscope. The PD pulse were instead measured by a PD sensor, based on the Rogowski coil, on the high voltage side, integrated in a current transformer.

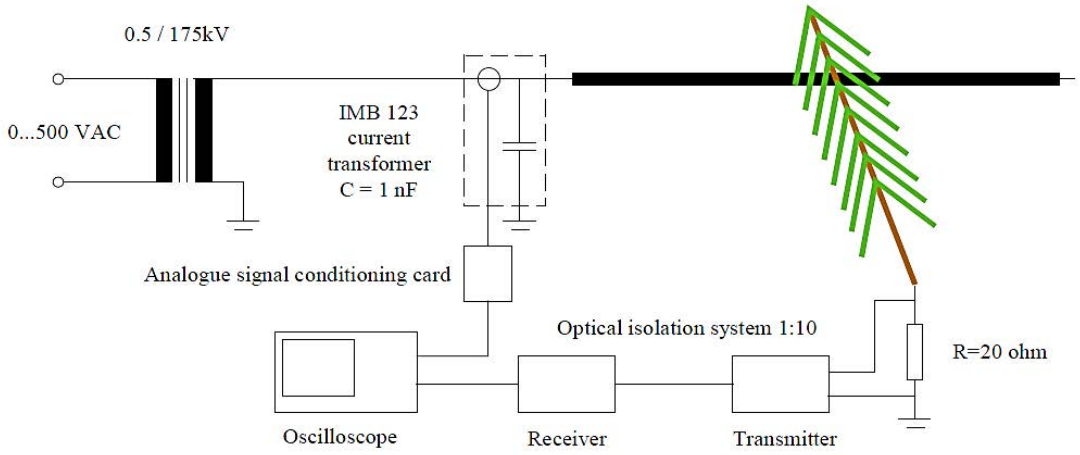

Figure 2.15 *Test configuration used for measured current pulse waveforms in the trunk during and incipient tree fault.*

Some pulse waveforms and amplitudes, collected during the tests, are present in Figure 2.16. The propose of the tests was to understand the order magnitude of pulse (approximately hundreds of mV), variation of rise time and the frequency content of the partial discharge signals due to a tree in contact with a high voltage covered conductor lines. In Figure 2.16 are shown on the left the current pulse waveform, where it is possible to see the rise time in different partial discharges, and on the right the power spectral density (PSD) of partial discharge signals. All these pulses were measured on the high voltage side, caused by a spruce fallen on a 110 kV covered trial line, with a RMS voltage of 68 kV and a diameter conductor of 185 mm^2.

The variations in peak amplitudes, waveforms and rise times were very wide. For example, for the rise time, the variation is in the range of 60-80 ns and 0.5-0.8 µs. The reason for this variation can be related to the several mechanisms of partial discharges formation, as the distance between the conductor and the tree, which is different in each partial discharge generation point. Sometimes, the pulses occur at very short time intervals causing two or three pulses that are superimposed: it could be attributed to discharges formation in different points almost simultaneously. From visually point of view, discharges are a bluish diffuse but steady glow with some occasional luminous arcs around those parts of tree that are in contact with the conductor: arcs are typically few centimetres long, from the origin point in the tree and the conductor surface.

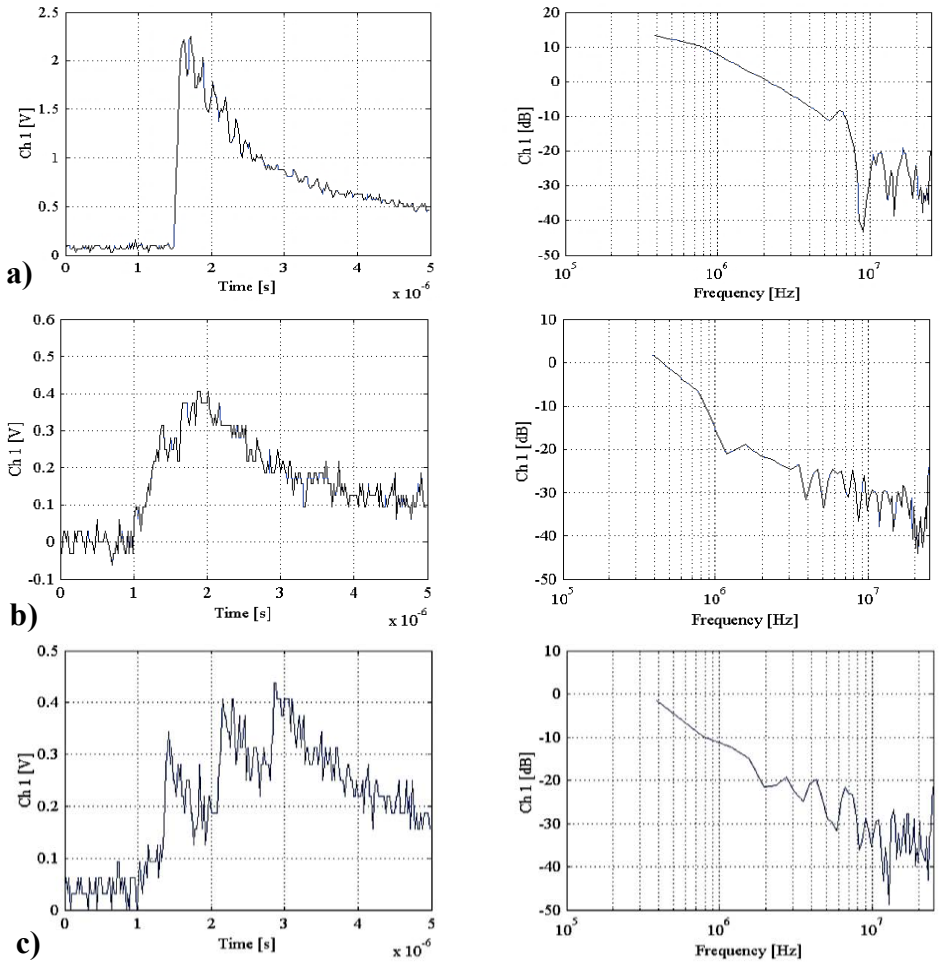

Figure 2.16 *Current pulse waveform (left) and power spectral density (right) of three PD pulse, whit* **a)** *short rise time (70 ns),* **b)** *long rise time (0.7 μs) and* **c)** *superimposing of three pulses.*

2.5.2 PD magnitude in Forest-SAX trial line

One of the main parameters, that affect the distance on the line at which an incipient tree fault can still be detected, is the magnitude of the partial discharges impulses made by a tree falling on the line. Therefore, in the field test, the propose of the measures was to carry out a complete result of several incipient tree faults, that includes amplitude of partial discharges, in addition to usual parameters like resistance and earth resistance of the trees. A summary of the PD magnitudes collected during the field test is presented in Table 2.3: the magnitudes are representing in terms of voltage at the output of the PD sensor, but it should take in account that the PD sensor would measure the current flowing in the conductor.

Table 2.3 *Incipient tree fault parameters.*

Tree ID	*Tree species*	*Contact*	*Date*	*T (°C)*	*RH (%)*	R_{tx} (Ω)	R_{te} (Ω)	ρ_t (Ωm)	U_{pp} (V)
56	Birch	L3	07/03	-7	74	601 727	54 947	69.5	0.04
51	Spruce	L1, L2, gw	08/03	-10	80	612 647	38 171	223.2	0.05
3	Spruce	L1, L3, gw	06/11	6	87	12 994	1 699	21.3	0.05
26	Birch	L2	08/11	7	82	69 373	4 277	45.1	0.10
80	Birch	L3, gw	13/09	3	91	42 910	3 226	-	0.11
54	Spruce	L3, gw	07/03	0	57	244 740	19 281	36.3	0.11
41	Spruce	L1	12/09	8	93	25 099	3 533	-	0.13
10	Spruce	L1, L3, gw	06/03	2	84	112 280	20 995	56.5	0.16
50	Spruce	L1, L2, gw	08/03	0	55	188 236	32 867	44.6	0.23
76	Spruce	L1, gw	13/09	14	63	23 997	1 255	-	0.26
66	Pine	L1, L2, gw	19/09	13	55	18 171	5 363	38.1	0.39
36	Birch	L3	08/11	7	82	150 524	6 838	49.3	0.43
37	Birch	L3, gw	08/11	7	82	202 110	6 153	40.7	0.54
49	Birch	L1, L2, gw	12/09	14	61	53 260	4 106	-	0.54
85	Spruce	L3	07/11	5	90	31 978	2 898	21.5	0.57
91	Pine	L3, gw	13/09	15	65	47 283	3 066	-	0.70
85	Spruce	L3	07/11	5	89	29 609	422	17.8	0.90
45	Aspen	L1, L2, gw	12/09	15	61	33 456	2 348	-	1.08
84	Spruce	L3, gw	07/11	4	92	28 099	2 106	20.1	1.25

The magnitudes of partial discharges are in terms of peak-to-peak voltage U_{pp} and they are taken as the 97.5% percentile of a series of 500-1000 pulses which are measured per each tree in the phase that have the highest magnitude. The measured presented in Table 2.3 were taken after 10-5 minutes the energization of the line with an incipient tree fault. The ambient temperature and the relative humidity of the air are reported. The trees, used for the test, are located at different distance from the measuring point location: however, no corrections have been done to the PD magnitude, to correct the propagation attenuation along the line between the incipient fault and the measuring location. Such correction is difficult to make since the large variation in pulse rise and fall time and the propagation modes: in fact, pulses related to different ITF may have different frequency content and different attenuation, as will be shown in Chapter 3. It was seen the smallest PD magnitudes measured in the site closest to the measuring location are almost similar as the smallest PD magnitudes of the sites 2 km far from mesurement location. It is probably caused by the background noise in measuremnts which limit the smallest detectable pulses. Large number of

factors could affect the measurements of the PD magnitude, so no definitive conclusion can be taken on the basis of the measurements: ambient temperature seems to have conseguences on the PD magnitude, therefore the environmental factors must be evalueted studying the PD magnitude due to an incipient tree fault. The PD magnitude, instead, seems to not have a correlation with the humidity of the air; sure, the PD magnitude has a strong correlation with the tree resistance, the earthing resistance of the tree and the tree top resistivity.

2.5.3 Intensity of partial discharges as a function of time

In order to implement the incipient tree fault detection algorithm, the temporal variation of PD magnitude is relevant as much as the magnitude variation in different tree species and different seasons.

Two examples of the PD magnitude are presented in Figure 2.17 and 2.18, in the first imagine, there is an incipient earth fault, while in the second one, there is an incipient short circuit fault. The PD magnitude is considered as peak-to-peak voltage of the pulse measurement, the phases plotted are L1 and L3: in incipient earth fault the phase interested by the fault is L3, instead of in incipient short circuit fault the phases are both.

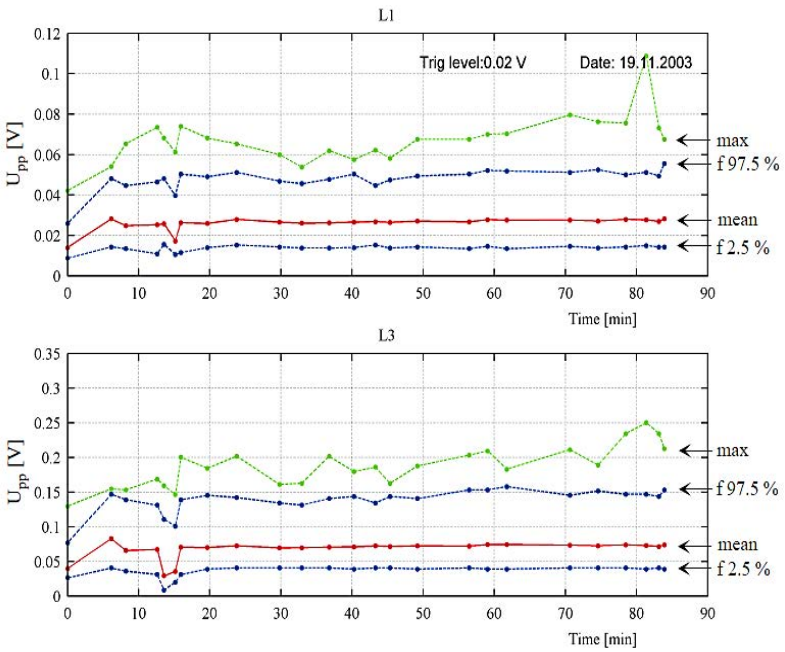

Figure 2.17 *PD magnitude in phases L1 and L3 in an incipient earth fault: most of the discharge activity was at phase L3. The measurement was conducted 1 minute after the energization of the line with the incipient fault.*

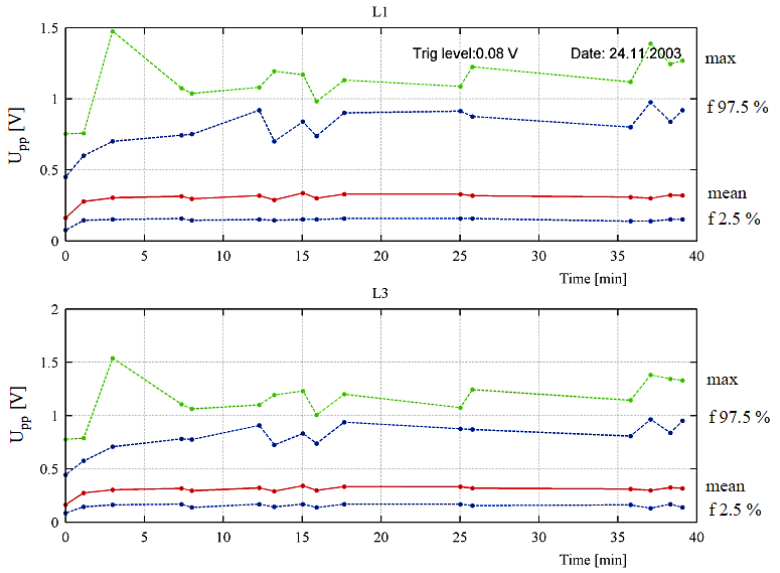

Figure 2.18 *PD magnitude in phases L1 and L3 in an incipient short circuit fault whit a direct contact between the phase L1 and the phase L3. The measurement was conducted 6 minutes after the energization of the line with the incipient fault.*

The red line represents the mean and each dot of that is the mean value from a group of 800 pulses measured in one sequence triggering shot. The blue dot in two lines 'f 2.5%' and 'f 97.5%' are the 2.5% and 97.5% percentile of a distribution of 800 pulses, while green dots represents the maximum value of that group of 800 pulses.

2.6 Equivalent circuits of incipient fault caused by a tree on a HVCC line

In this section the equivalent circuits, which could represent different kind of incipient tree faults, are present. An incipient fault due to a tree lying on a covered conductor line can be characterised by the earthing resistance of the tree and by the impedance of the tree and covered conductor, which impedance are both frequency dependent. The three basic fault configurations that will present are:

1. One phase in contact whit the tree;
2. Two or three phases with the tree;
3. Two or three phases in contact whit each other and with the tree.

First two fault configurations are incipient earth faults, while the third is an incipient short circuit fault. Each of three basic fault configuration can be divided in two based on if the tree is in direct

contact whit the ground wire. The last fault configuration, with direct contact between phases, is considered the most harmful, due to the risk of a short circuit between phase conductors and a damage of the covering. Moreover, such fault causes a voltage drop in feeders connected in the same busbar in which the fault occurs and furthermore network components, particularly the winding of the transformer, are subjected to additional stress caused by short circuit forces. As it will be seen in the next chapter, the propagation of a partial discharge pulse is affected by the capacitive coupling between the phases. The capacitive coupling between the phases increases with the increasing frequency, since both the capacitive susceptance of the covered conductor and the AC conductivity of the tree increases. The characteristics of fault configuration depend on the location of the tree respect to the nearest tower and the line, the high of the tree, the weight and geometry of the branch, the tower top configuration and the length of the span.

2.6.1 A tree in contact with one phase conductor

In Figure 2.19 is represented the equivalent circuit in case of a tree in contact with a) only one phase conductor and b) with one phase conductor and the ground wire. The incipient fault impedance due to a tree falling on a covered conductor can be divided in three parts:

1. Impedance of covered conductor dominated by the capacitive reactance (C_{tc});
2. Impedance of the tree, from the contact point (between phase conductor and tree) to the ground, dominated by resistance of a portion of tree R_{t1} and the earthing resistance of the tree R_{te}.
3. Impedance of the tree, from the contact point of conductor to the contact point of the ground wire, dominated by resistance R_{t0}, the resistance due to the contact between ground wire and the tree R_{tg}, and finally the earthing resistance of the ground wire R_{ge}.

An example of an incipient earth tree fault measured simultaneously in three phase conductors is presented in Figure 2.20. The power spectral densities (PSD) are also represent on the right of the Figure. The tree is in contact with the ground wire and with the phase L3: the magnitude of PD pulse is largest in phase L3, while the pulses in L1 and L2 are in opposite polarity and the magnitude of peak-to-peak voltage is 30-40% less than in phase L3.

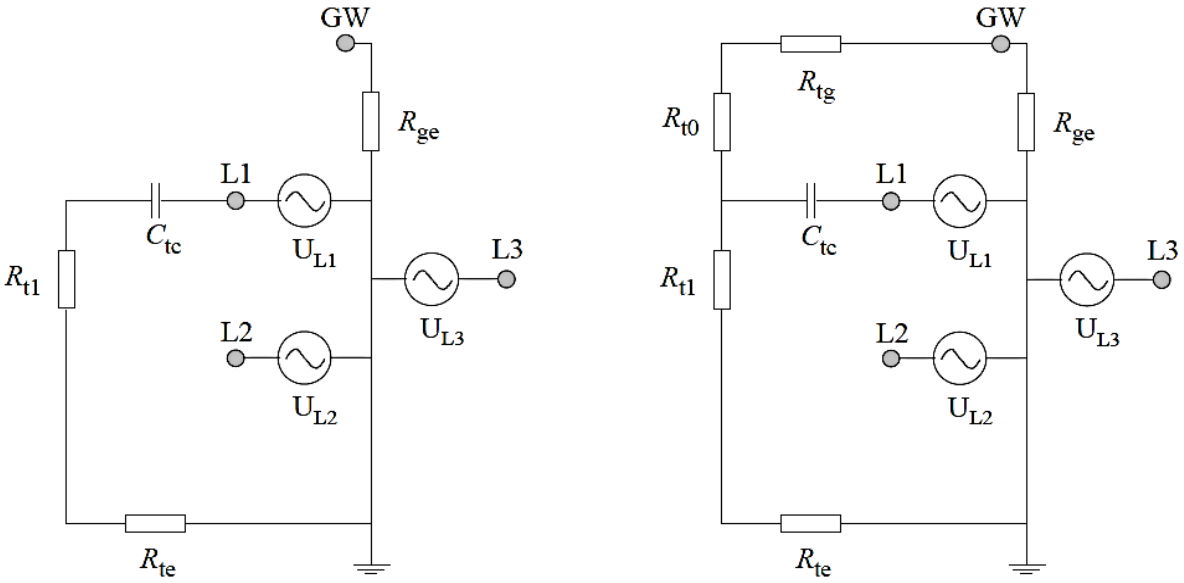

Figure 2.19 *Equivalent circuit of a tree in contact with* **a)** *only one phase conductor and* **b)** *phase conductor and also the ground wire of a covered conductor line.*

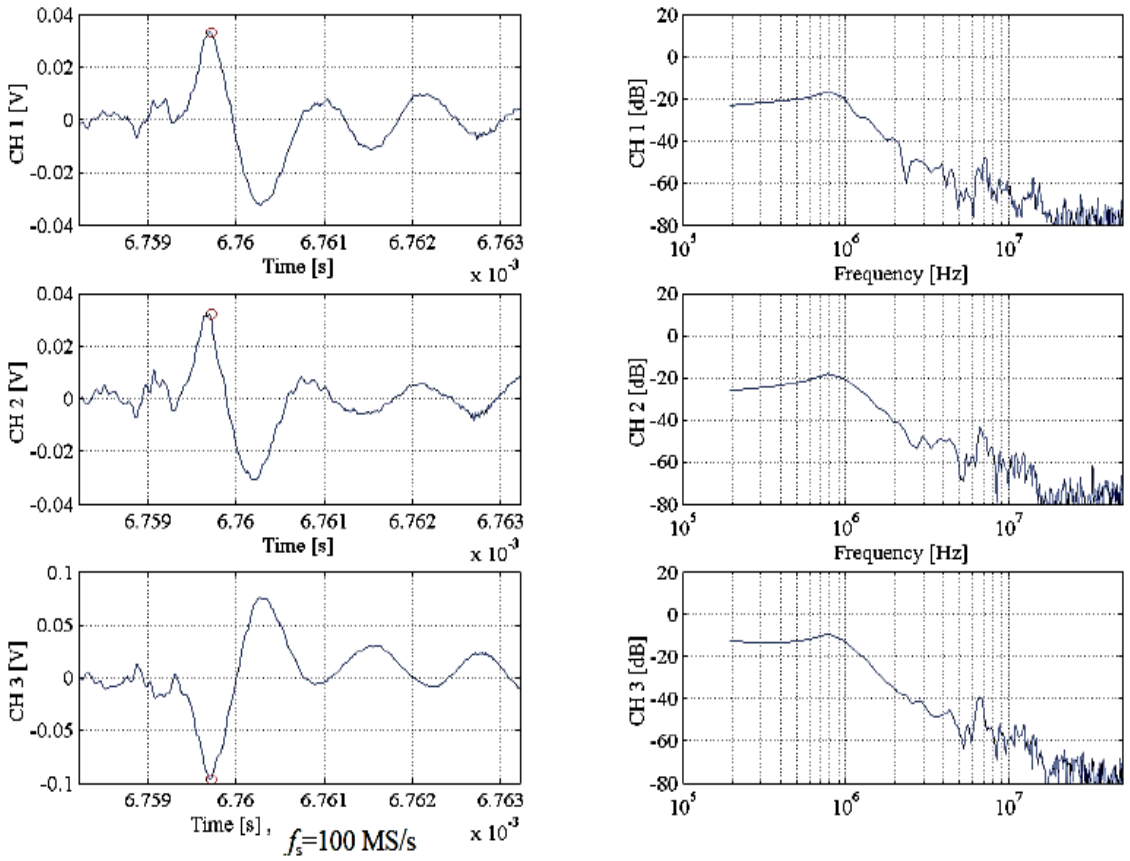

Figure 2.20 *PD pulse waveforms in phase L1, L2 and L3 during an incipient earth fault and relative PSD.*

2.6.2 A tree in contact with two of three phase conductors

In Figure 2.21 are presented two equivalent circuits regarding two incipient earth fault, one between the tree and two phase conductors and the ground wire, and the other between the tree and three phase conductors and the ground wire. The equivalent circuits are more complicates if the number of phase conductor in contact with the tree increases. The impedances in these equivalent circuits are the same of the circuit seen in the previous section.

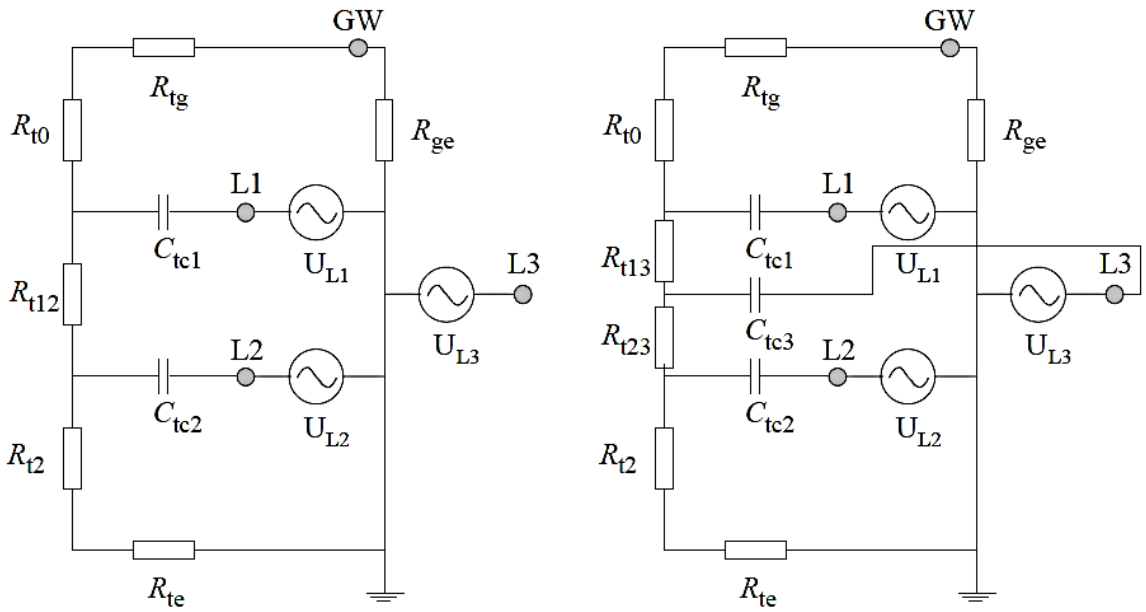

Figure 2.21 *Equivalent circuit of a tree in contact with two or three phase conductors and the ground wire in a covered conductor line.*

As in the previous case, the phases in which discharges occur have the largest PD magnitude, while the others have a small magnitude and a pulse polarity opposite.

2.6.3 Two or three phase conductors in contact with each other and the tree

Sometimes, a falling tree on the line forces two or three phase conductors in direct contact with each other, causing an incipient short circuit fault. Such incipient fault occurs less time, in fact, based on tree test conducted on Forest-SAX trial line, only 1 on 37 trees involves in an incipient short circuit fault. A large spruce fell on the covered conductor trial line and forced phase conductors L3 and L1 in direct contact with each other.

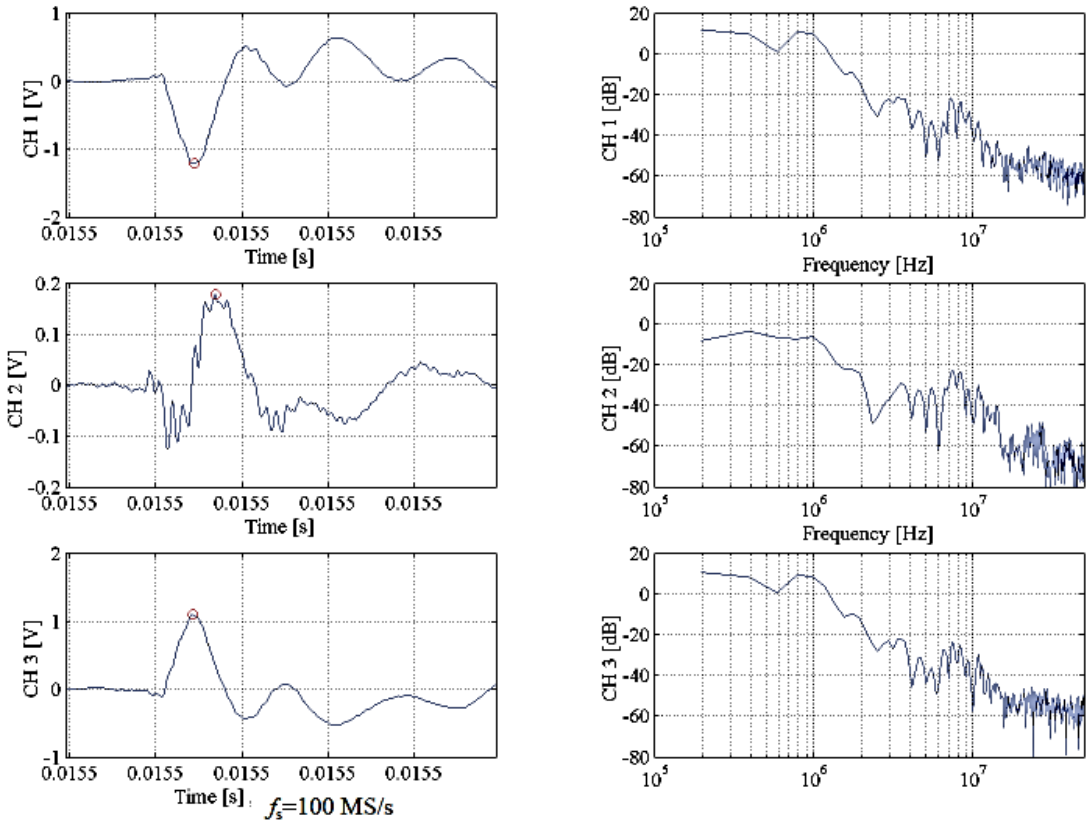

Figure 2.22 *PD pulse waveforms in phase L1, L2 and L3 during an incipient earth fault between L1 and L3 and relative PSD.*

The PD pulse waveforms in phases L1, L2 and L3 during an incipient short circuit fault between L1 and L3 is presented in Figure 2.22: in the Figure is also presented the PSD of relative phases. The phases L3 and L1, which were in contact with each other, are almost the same but inverse polarity. Such characteristic is common to all the incipient short circuit faults that were studied, and therefore can be used as criterion to discriminate automatically between an incipient short circuit fault and incipient earth fault. Moreover, the magnitude of pulse in phase L2 is smaller than one fifth respect to the magnitude of pulses in phases L1 and L3.

Chapter 3

Propagation of a PD signal on a HVCC line

In this chapter the propagation phenomena related to a partial discharge signal travelling on a high voltage covered conductor line are presented. First of all, the travelling waves studies are introduced in order to explain the PD signal behaviour when it travel on the transmission line: it will be presented the parameters of the transmission line and the aspect of wave propagation on such lines, including the reflection and refraction phenomena, and finally the lattice diagram will be introduced. Such a diagram is used to study the propagation of these partial discharges on the 110 kV covered conductor line and moreover some methods used to study the pulse voltage and frequency content of the signal are presented. Then, the focus goes to the effect of surge impedance discontinuity on the propagation, to the attenuation of the pulses during the travel and to the coupling of pulses between the phase conductors. Finally, it will be estimated the maximum length of the line that a single incipient tree fault unit is able to detect.

3.1 Propagation of PD signal on power lines as a travelling wave

The order of magnitude to detect an incipient tree fault on covered conductor lines is typically variable from some hundreds of meters to several kilometres, and therefore the distance between the incipient tree fault and the PD sensor could be very large. Furthermore, the duration of single PD pulse is very short, from nanoseconds to microseconds. For these reasons the partial discharge pulses, as a short current pulses, propagate on the line to the sensor can be seen as travelling waves. Every time that a partial discharge caused by falling tree on the line occurs, a pair of waves are generated, one travelling in one sense, the other travelling in the opposite sense. The resistance, inductance, conductance and capacitance are considered as distributed along the line: there could be any points of surge impedance change, as bifurcation points, changes of line geometry, transposition points and changes in power apparatus connected to the line. At each point of surge impedance change, one part of the travelling wave is reflected back and the other part of the wave continues forward, as illustrated in Figure 3.1. This energy wave separation causes additional distortion and attenuation in signal propagation, beside to that caused travelling normally along the line. As it will be seen in next section, the reflections of the wave are used to locate the partial

discharge sources, keeping in mind that the amount of distortion and attenuation is an important parameter to consider in PD detection.

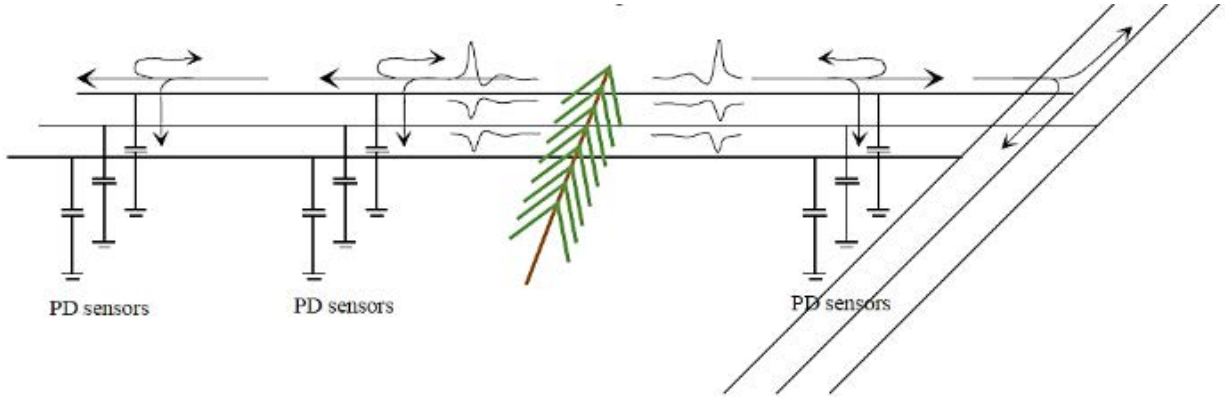

Figure 3.1 *Propagation of partial discharge pulses on a transmission power line as a travelling waves.*

The propagation of partial discharge pulses is analogous to the propagation of atmospheric overvoltage transient, with the difference that in overvoltage transient corona causes additional attenuations. The propagation of partial discharge pulses studied in this chapter, caused by a fallen tree on a 110 kV covered conductor line is studied on the basis of several data acquired during field test on the Forest-SAX trial line. Since wave propagation on a high voltage covered conductor line is an important and relevant part of this chapter, in the following section a theoretical brief background of travelling wave is presented.

3.1.1 Characteristic parameters of a transmission line

A transmission line can be considered as a network characterized by distributed-parameter with these parameters distributed along its length. A differential length of a transmission line Δx is considered in Figure 3.2, where the equivalent circuit can be descripted by the following parameters:

- *r*, resistance per unit length;
- *l*, inductance per unit length;
- *g*, conductance per unit length;
- *c*, capacitance per unit length.

The propagation constant γ of the line is expressed as

$$\gamma = \alpha + j\beta = \sqrt{(r + j\omega l)(g + j\omega c)}. \quad (3.1)$$

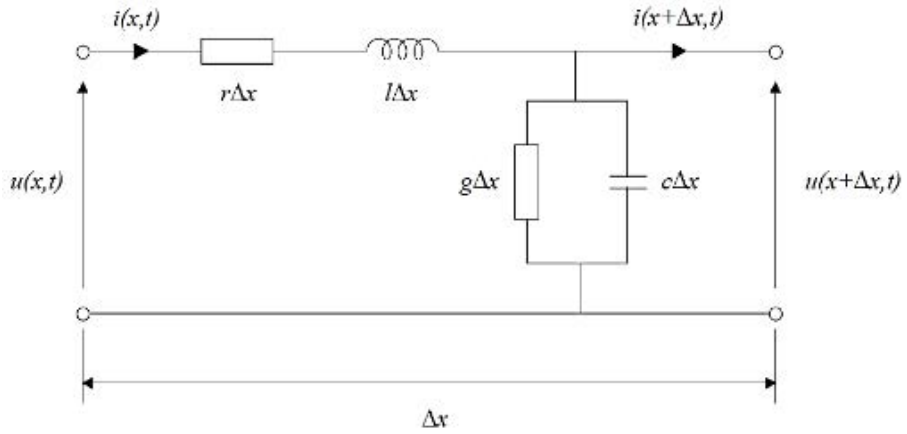

Figure 3.2 *Equivalent circuit of a differential length Δx of a transmission line.*

In the propagation constant, α and β are the real and the imaginary parts, and they represent respectively the attenuation constant (dB/m) and the phase constant (rad/m). Both the constant depend on frequency.

For a travelling wave, the ratio between the voltage and the current in a point *x*, *U(x)/ I(x)* is called characteristic impedance of the line Z_0:

$$Z_0 = \sqrt{\frac{r+j\omega l}{g+j\omega c}} \tag{3.2}$$

Both the propagation constant (γ) and the characteristic impedance (Z_0) are characteristic parameter of a transmission line, depending on *r*, *l*, *g*, *c* and ω, but not on the length of the line.

On the ideal case in which the line is lossless ($r = 0$ and $g = 0$) and distortionless ($r/l = g/c$), the velocity at which waves travel on the line is constant and independent from the frequency, without any dispersion of the signal; if the line is lossless the wave velocity corresponds to the speed of light, and the voltage and the current have the same shape. In this case the characteristic impedance can be written as $Z_0 = \sqrt{l/c}$, and the velocity of propagation as $v = 1/\sqrt{l \cdot c}$, using only the inductance and the capacitance. With a distortionless line, the voltage and the current waves can be determined by the characteristic impedance of the line and they maintain the same shape travelling undistorted along the line, although they could be attenuated. Theoretically, it is possible a line has attenuation without distortion, but the opposite is not possible.

3.1.2 Aspects of wave propagation on real power lines

Of course real power lines are neither lossless nor distortionless. Both attenuation and distortion are caused by variation in inductance and capacitance and by energy losses: the latter are caused by the modification of conductor resistance due to the skin and proximity effects. A wave that travel along the power line is subjected to an attenuation, with the crest of the wave that decrease in amplitude, and to a distortion, with the wave that became more elongated. With partial discharge pulses, that are broadband signals, both attenuation and phase constant are frequency dependent causing distortion of the pulse shape. Moreover, in multiconductor line, as in the three-phase power line, travelling wave have several modes to propagate, each one with own specific attenuation and velocity: this causes they arrive in different instant at the measuring sensor location.

The frequency of interest in partial discharge caused by a falling tree on high voltage covered conductor lines are between few tens and few hundreds of kHz. Usually, the propagation attenuation in overhead power lines is affected by several factors, as the spacing between the conductors, their height above the ground and the existence of the ground wire. Additionally, climatic factors can increase the attenuation, as the frost and the rain. In Figure 3.3 are presented the effect of ratio between conductors spacing, considering also their height above the ground, and the effect of rain and frost on the propagation attenuation on high voltage overhead lines.

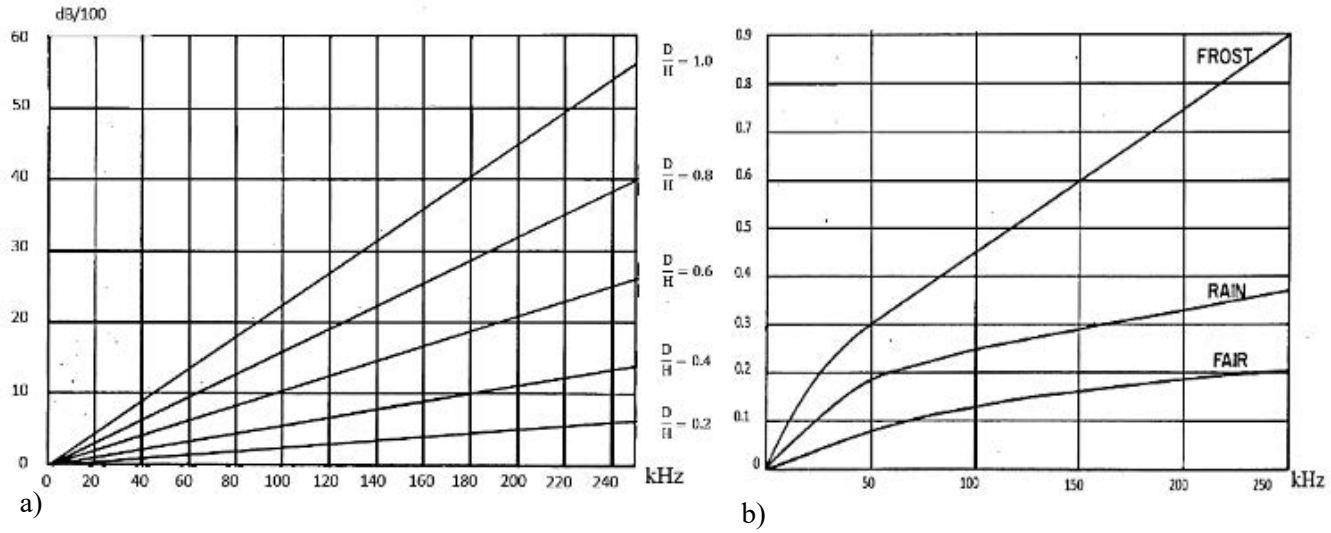

Figure 3.3 *Effect of* **a)** *the ratio between the conductors spacing and their height and* **b)** *rain and frost on the propagation attenuation of a high voltage overhead line.*

As shown in Figure 3.3 a), decreasing the space between conductors and increasing the height of them above the ground, decreases the propagation attenuation. Considering d as the distance between the conductor, the parameter D is obtained as:

$$D = \sqrt[3]{d \cdot d \cdot 2d} = 1.26\, d \tag{3.3}$$

while H is the height above the ground of the conductors. In covered conductors lines an advantage is the reduced phase clearance that leads to a reduced propagation attenuation, compared to a conventional bare line with usual phase clearance, assuming the same height of conductors above the ground. As shown instead in Figure 3.3 b), rain and frost increase the attenuation, caused by the loss in water and ice layers around each conductor: while the rain increases the attenuation by a factor of 2, the ice could increase the attenuation by a factor of 3,5 at 100 kHz (typical PD frequency). Moreover, if the line has the ground wire, the propagation attenuation is reduced respect to without ground wire, and the sag line instead increase attenuation, due to the less height of conductor line above the ground.

3.1.3 Reflection and refraction of waves

Real power line has an impedance different to the characteristic impedance of the line Z_0 and are finite in length. Besides, the line could also be made of a several of pieces with different characteristic impedances, or there could be some local discontinuity. When a travelling voltage and current wave arrives in a discontinuity point, where the characteristic impedance of the line changes, each wave is split in two new waves, in which the proportionality between the current and the voltage is preserved in both side of the discontinuity: one of the waves is reflected back toward its origin, while the other one continues straight head. The separation of the original wave in two and therefore the quantity that is reflected and that refracted depends on the reflection and the refraction coefficients.

It is considered Z_1 as the surge impedance of the line in which the travelling wave is arriving and Z_2 as the surge impedance seen by the travelling wave that reaches the discontinuity point A: they could be resistive, inductive, capacitive, or a combination of these. The original waves are denoted with e and i, the voltage and current waves reflected from the discontinuity are called e' and i', and finally the resultant voltage on the impedance Z_2 and the current through it, are called e'' and i'', as shown in Figure 3.4.

Considering general impedance equation:

$$e = i\, Z_1, \tag{3.4}$$

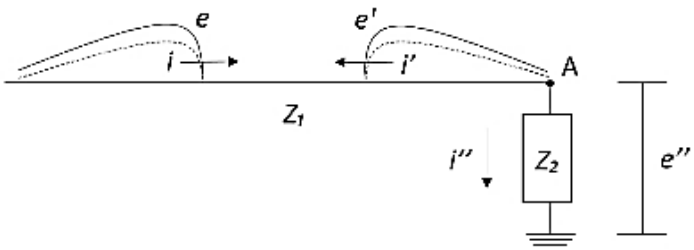

Figure 3.4 *The general circuit considered in travelling wave studies.*

$$e' = i' Z_1, \tag{3.5}$$

$$e'' = i'' Z_2, \tag{3.6}$$

and boundary equations:

$$i'' = i - i', \tag{3.7}$$

$$e'' = e + e'. \tag{3.8}$$

Therefore, if *e''* is written in terms of *e*, using the previous equations:

$$e'' = e + e' = e + i' Z_1 = e + (i - i'') Z_1 =$$

$$2e - i'' Z_1 = 2e - \frac{Z_1}{Z_2} e'' = \frac{2Z_2}{Z_1 + Z_2} e; \tag{3.9}$$

and for the other,

$$i'' = \frac{e''}{Z_2} = \frac{2e}{Z_1 + Z_2} = \frac{2Z_1}{Z_1 + Z_2} i, \tag{3.10}$$

$$e' = e'' - e = \frac{Z_2 - Z_1}{Z_1 + Z_2} e, \tag{3.11}$$

$$i' = \frac{e'}{Z_1} = \frac{Z_2 - Z_1}{Z_1 + Z_2} i, \tag{3.12}$$

Therefore, the voltage reflection coefficient ρ_v is given by

$$\rho_v = \frac{e'}{e} = \frac{Z_2 - Z_1}{Z_2 + Z_1}, \tag{3.13}$$

while the voltage refraction or transmission coefficient τ_v

$$\tau_v = \frac{e''}{e} = \frac{2Z_2}{Z_2+Z_1}, \tag{3.14}$$

As for the current, the current reflection coefficient ρ_i and transmission coefficient τ_i are respectively:

$$\rho_i = \frac{i'}{i} = \frac{Z_2-Z_1}{Z_2+Z_1}, \tag{3.15}$$

$$\tau_i = \frac{i''}{i} = \frac{2Z_1}{Z_2+Z_1}. \tag{3.16}$$

If Z_2 is a short circuit, the transmitted wave is $e'' = 0$ and $i'' = 2i$, while the reflected wave is equal to the arriving wave but opposite, with $e' = -e$ and $i' = -i$. Instead, if Z_2 is an open circuit, the refracted wave is $e'' = 2e$ and $i'' = 0$, and the reflected wave is the same of arriving, with $e' = e$ and $i' = i$.

There is very little information about the impedance behaviour of line and substation equipment in the frequency range of partial discharges, on the range from few kHz to few MHz.

3.1.4 The lattice diagram

The lattice diagram is a useful tool used in travelling wave studies when the system is composed by several line portions, to permit keeping track of the reflection. The diagram is a space-time diagram, with the time on the vertical axis, and the line length on the horizontal axis. If the velocity of the travelling waves is the same in each line portion, the portions of the line are plotted directly proportional to their length; otherwise, the line length are scaled according to the specific velocity of the travelling wave on the different portions of the line. In this way, the diagonals have the same slope and the scale on the vertical axis (time) is the same in every line portion. The lattice diagram is used to calculate the voltage in the discontinuities of the line in different instants: in this work, the diagram is used to determine the instant in which a wave after reflections in different discontinuity points will arrive in the measurement location. In Figure 3.5 an example of a lattice diagram is presented: the line has a finite length with two portions (with two line impedances Z_1 and Z_2), and one point of discontinuity between them; the line end in a resistor R.

In order to understand better the Figure 3.5, the various reflection and refraction coefficients are expressed in the follow equations, using the Equations 3.13-3.14:

$$\beta = \frac{2Z_2}{Z_1+Z_2}, \qquad \gamma = \frac{Z_2-Z_1}{Z_1+Z_2},$$

$$\omega = \frac{2R}{R+Z_2}, \qquad \alpha = \frac{R-Z_2}{R+Z_2},$$

$$\delta = \frac{2Z_1}{Z_1+Z_2}, \quad \phi = \frac{Z_1-Z_2}{Z_1+Z_2}.$$

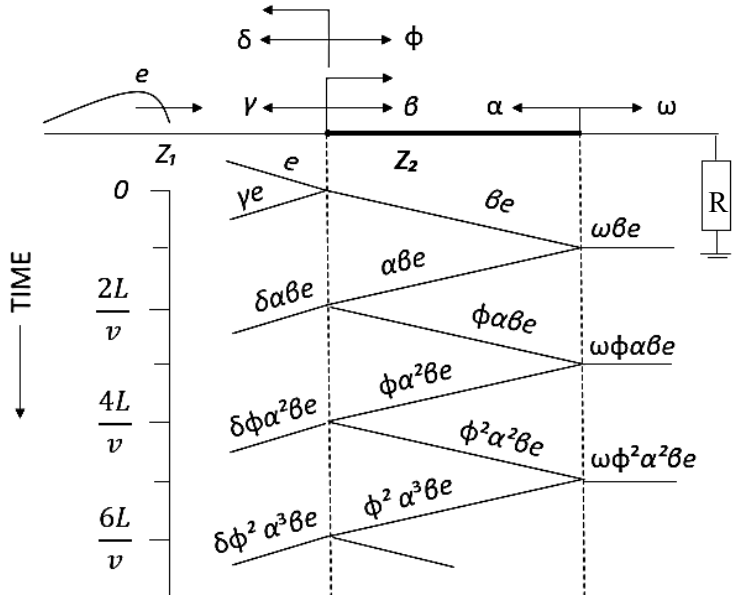

Figure 3.5 *Lattice diagram of two different line portions with a discontinuity point.*

The diagram has the time scale on horizontal axis, with time increasing downward. The starting time t= 0 is defined as the time in which the wave reaches the first discontinuity point, between the two line portions. The lines are plotted diagonally downward, all with a constant slope, and the value of the voltage is a combination of these coefficients in each part of the line. The voltage e arrives to the discontinuity point and transmits a surge βe and reflects a surge γe; the transmitted wave travels to the end and reflects a surge $\alpha\beta e$, while the refracted voltage produced at the resistor is $\omega\beta e$. Now, the reflected surge $\alpha\beta e$ travels back and then transmit a voltage $\delta\alpha\beta e$ and reflects a voltage $\phi\alpha\beta e$, and so on.

The voltage at the discontinuity point e_T is:

$$e_T = e[\beta + \delta\alpha\beta(t-2T) + \delta\phi\alpha^2\beta(t-4T) + \delta\phi^2\alpha^3\beta(t-6T)\ldots], \tag{3.17}$$

where T is the time spent to the surge to travel along one length of the line part with surge impedance Z_2, $T= L/v$. The term $(t-2T)$ indicates that the surge is one whole travel time delay from the zero time.

The Equation 3.17 could be written, factoring out β, as:

$$e_T = \beta e[1 + \delta\alpha(t - 2T) + \delta\phi\alpha^2(t - 4T) + \delta\phi^2\alpha^3(t - 6T) \dots], \quad (3.18)$$

The voltage at time infinity is:

$$E_T(t = \infty) = \beta e[1 + \delta\alpha(1 + \phi\alpha + \phi^2\alpha^2 + \phi^3\alpha^3 + \cdots)] =$$

$$= \beta e\left[1 + \frac{\delta\alpha}{1-\phi\alpha}\right] = \frac{2R}{R+Z_1}e, \quad (3.19)$$

therefore, at time equal to infinity, the continues reflections have eliminated the line piece in the middle (line with impedance Z_2), since the final equation is equivalent to a surge wave travelling on a line with impedance Z_1 and ending on a resistor R.

3.2 Research methods used in wave propagation studies

The wave propagation studies for PD pulses on the 110 kV Forest-SAX trial line are made in terms of attenuation of the peak-to-peak pulse and coupling between the three phase conductors, as a function of the distance from the PD source. The attenuation of a system in function of the frequency, also called frequency response of a system, is determined in various ways: the most appropriate method is one that depends on the system characteristics.

Considering the Forest-SAX trial line, some factors have to be taken in account in the propagation attenuation studies:

- the PD sensor, that are permanently installed on the line, may affect the propagation of high frequency signals;
- since the permanently PD sensor installation, the longest line portion without surge impedance discontinuities is about 4.7 km;
- only the Pyntösjärvenaukee measuring location is free from surge impedance discontinuities that could influence the pulse magnitude observed;
- the PD magnitude and pulse shape of the incipient earth fault and short circuit fault are not constant, and this complicates the comparison of the measurements collected at different time instant;
- the attenuation is used to determine the distance from the ITF.

Generally, a common method used to characterise the frequency response of a system is applying a known sinusoidal extraction in the input of the system, and measuring the output signal at all the desired frequencies. Another way is to use impulse extraction to determine the frequency response

at specific frequencies, on the basis of frequency spectrum in input and output signals. In power lines the examination is more complicate due to the line is not at its characteristic impedance and due to the impedance mismatching between line and power apparatus connected: this impedance mismatching causes errors when propagation attenuation is determined.

Actually, the propagation attenuation is determined using incipient tree fault as signal sources and observing how the peak-to-peak voltage in PD pulses decreases as a function of the distance. The attenuation is estimated measuring the PD pulse magnitude in different locations along the line, from the incipient fault location to the PD sensor, and measuring the reflected pulses in surge impedance discontinuity points at different distances on the line. The sensor locations should be selected in order to avoid surge impedance changes inside the length to be measured: on the Forest-SAX trial line, only the PD sensor in Pyntösjärvenaukee is along the line but free from surge impedance changes close to it. The other two PD measuring locations are close to the end of the trial line, in Tuulikylä and Noormarkku, where the surge impedance changes. Due to the superposition of these pulses which come from the reflections in line end or in impedance change, the pulse magnitudes are distorted at each measuring location, and thus this method is not suitable for this line.

Another method only one sensor is used, in order to measure the pulse and its reflection, with a distortion that tis the same for each pulse measured. In this thesis the propagation attenuation of the line is valued in this way, on the basis of the measurements made in Pyntösjärvenaukee and Tuulikylä measuring location: in Pyntösjärvenaukee the pulses are not influenced by reflections in adjacent points of impedance change, while in Tuulikylä the line junction, 10 meters distant from the sensor, causes distortion in measured waveform. This method provides a convenient method for a roughly estimation of the distance for an incipient fault detection.

3.2.1 Determination of peak-to-peak voltage and frequency characteristic of pulse

Partial discharges originated by an incipient fault are used to study both the attenuation of the amplitude of the pulse, as a function of the distance and the effect of surge impedance discontinuity on the pulse propagation. Additionally, a source of discharges is used as a source of reference signal, with a considerable wide frequency content, more than normal incipient tree fault. This gap device works using the potential difference between the covered conductor and the floating plate electrode: the potential difference increases until the discharge occurs in the gap, reducing the potential difference. This process is continuously repeated.

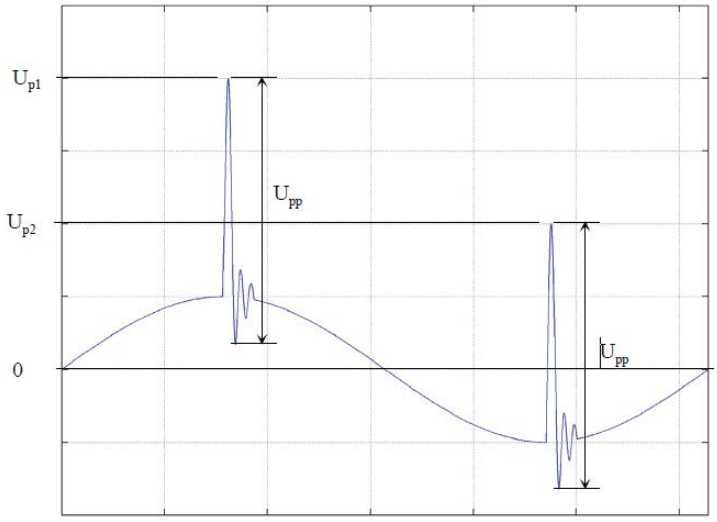

Figure 3.6 *Superimposition of PD pulses on an oscillatory signal, which has a lower frequency of oscillation than PD pulses. The error in pulse peak value U_{p1} and U_{p2} due to the signal superimposition is much larger than the error in peak-to-peak value U_{pp}.*

Both the propagation attenuation and the coupling between phases are studied in terms of peak-to-peak voltage of the pulse measured on the output of the PD sensor used in the incipient fault detection system on the Forest-SAX line. At the output of Rogowski coil, PD sensor used in this work, the voltage is proportional to the derivative of the current that flows in the conductor phase of the line. The PD pulses measured on Forest-SAX trial line are superimposed on an oscillatory signal, whose oscillation frequency is lower than that of PD pulses, as shown in Figure 3.6. Although the magnitude of this signal is usually less than 10 mV, it can cause an error in the peak value of the PD pulse: in order to reduce error in pulse, peak-to-peak value is used to representing PD magnitude, instead of peak value of the pulse. Moreover, power spectral density (PSD) is used to study the frequency dependent characteristic both of the line and the PD sensor connected to it.

For the calculation of peak-to-peak voltage of the pulse and power spectral density (PSD), every pulse of interest is picked up from the data stream of 20 ms or 2 ms, and put in a shorter window of 5 μs: with a sampling rate of 100 MS/s or 1 GS/s, a window of 5 μs correspond to 500 and 5000 samples respectively. The pulse peak-to-peak values are determined in Matlab using a simple min-max method, as the voltage difference between pulse samples with the largest and smallest voltage in this 5 μs time window; also the power spectral density of the sampled pulses is determined using a Matlab function.

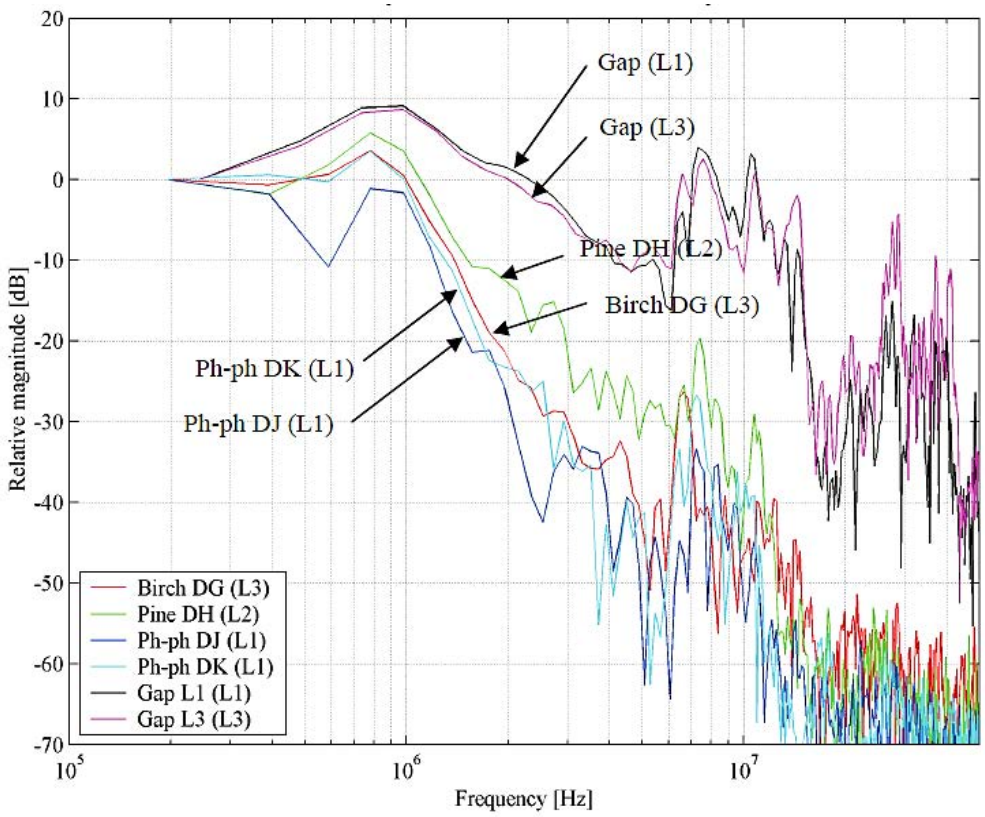

Figure 3.7 *Power spectral densities of the direct pulses of two incipient earth faults, two incipient short circuit faults (with a direct contact between the phase conductors L1 and L3) and two gap discharges, measured at Tuulikylä.*

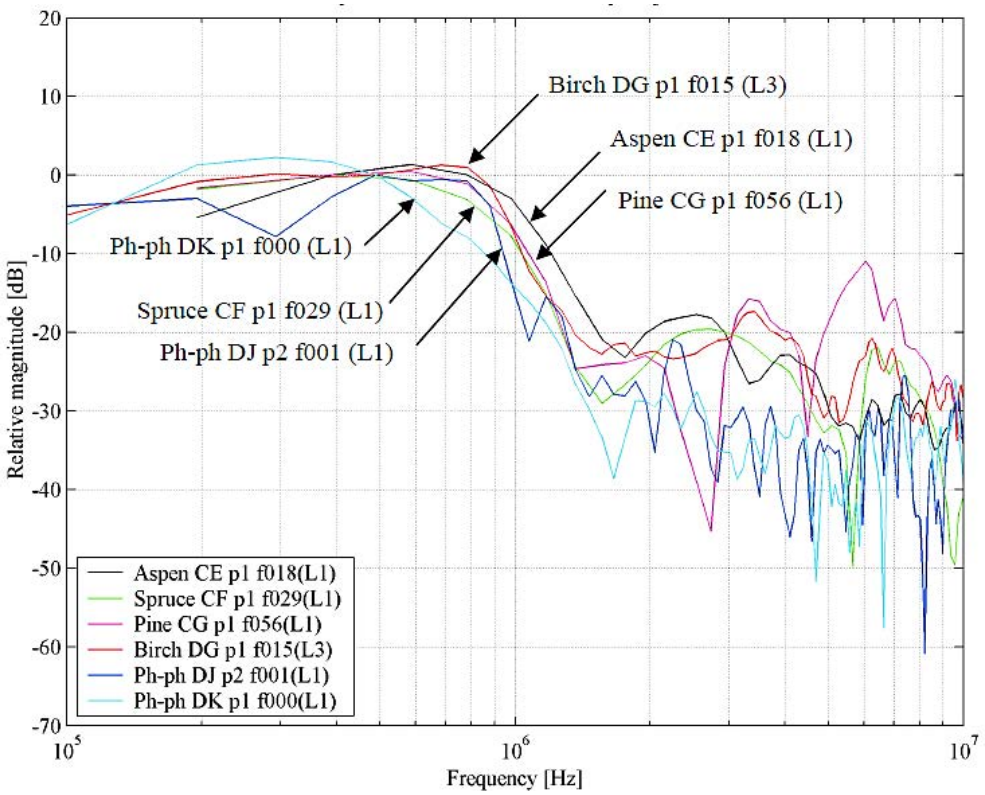

Figure 3.8 *Power spectral densities of the direct pulses of four incipient earth faults and two incipient short circuit faults (with a direct contact between the phase conductors L1 and L3), measured at Pyntösjärvenaukee.*

Figure 3.7 and 3.8 present two examples of power spectral densities (PSD's), considering only the pulses due to the incipient tree faults (ITF's), propagated directly from the locations of discharge source to the locations of measurements in Tuulikylä and Pyntösjärvenaukee. The distance between the incipient tree fault and the measurement location at Tuulikylä is in the range approximately of 3.0-3.5 km, while for Pyntösjärvenaukee location is approximately 0.9-1.3 km. Although some of the PSD's in Figure 3.7 and 3.8 represent the same incipient tree faults (Birch DG L3, Ph-Ph DJ L1, Ph-Ph DK L1), the PSD's content are different, since the pulses that arrive in measurement location are different due to attenuation and distortion phenomena. The PSD, in fact, does not reflect the behaviour of pulses as a function of the propagation distance, but in their frequency content.

The curves are normalized at a frequency of 200-250 kHz to 0 dB. At 1-7 MHz, the difference between incipient earth fault and short circuit fault in power spectral density is visible: for an incipient earth fault the PSD is higher than for an incipient short circuit fault. In general, above the 1 MHz, the pulses caused by an incipient short circuit fault has less power than those caused by an incipient short circuit fault.

Table 3.1 *PD magnitude in each phase and the relation of the phases respect to the phase in which the ITF occurs. In the table every ITF is named with an identification code (Measurement ID), the distance from the measurement point in Pyntösjärvenaukee (MP2), and the status of the transformer connected to the line is expressed. The phase in which the discharge originated is underline with a grey colour.*

Measurement ID	***Distance of ITF from MP2* (m)**	***Pulse peak-to-peak voltage* (V)**			***Relative pulse magnitude* (%)**			***Connection of the transformer to the line***
		L1	***L2***	***L3***	***L1***	***L2***	***L3***	
AK p1 f285	2104	0.033	-	0.113	29	-	100	disconnected
CA p1 f026	894	0.035	-	0.164	22	-	100	disconnected
CE p1 f018	980	0.059	-	0.012	100	-	20	disconnected
CF p1 f029	1033	0.195	-	0.075	100	-	38	disconnected
CG p1 f056	978	0.054	-	0.013	100	-	24	disconnected
CE p2 f018	980	0.035	-	0.092	38	-	100	disconnected
CF p2 f029	1033	0.042	-	0.142	30	-	100	disconnected
DC p1 f021	1149	0.092	0.098	0.275	34	36	100	connected
DF p2 f007	1301	0.034	0.061	0.147	23	42	100	connected
DG p1 f015	1324	0.062	0.070	0.184	34	38	100	disconnected
DG p2 f046	1324	0.053	0.063	0.148	36	42	100	disconnected
DH p1 f021	1335	0.378	0.638	0.220	59	100	35	connected
DJ p1 f000	1205	0.231	0.045	0.231	100	20	100	disconnected
DJ p2 f001	1205	1.019	0.203	1.063	100	20	104	disconnected

DK p1 f000	1228	0.338	0.053	0.369	100	16	109	disconnected
DK p2 f001	1228	0.750	0.117	0.769	100	16	103	disconnected

In Table 3.1 are reported the pulse magnitudes in terms of peak-to-peak voltage of a single pulse for each phase, and then as a percentage relative to the phase in which the discharge occurs; in the case of some incipient tree faults only phases L1 and L3 are measured. The significant variation in the relative pulse magnitudes indicate that the signals of incipient tree faults can propagate in several combinations of modes.

The connection of the transformer has no effect on the PSD of the direct pulse, but it affects the magnitude and the PSD of the reflected pulses. In order to determine the propagation attenuation on the line, based on the magnitude of the direct pulses and reflected pulses from the line end, only when the transformer is disconnected from the line, the measurements should be considered.

3.2.3 Sources of error and notations used

As seen in subparagraph §3.1.4, the lattice diagram can be used to illustrate the propagation of the partial discharges pulses on a power line. An example of the propagation of the pulses caused by a discharge source, is shown in Figure 3.9. The line is divided in two portions, the first portion goes from Tuulikylä (measurement point 1, MP1) to Pyntösjärvenaukee (MP2), the second portion goes from Pyntösjärvenaukee to Noormarkku (MP3); both the propagation velocity and the surge impedance are assumed equal. At the frequency of interest, the impedance of the PD sensors in MP1, MP2 and MP3 are not matched to the impedance of the line, therefore they are considered as surge impedance discontinuities on the line.

As the lattice diagram in Figure 3.9 shows, the number of travelling waves increases as a discontinuity point is reached: from a single wave, after multiple reflection, a great number of waves are created. At the measurement location consecutive waves arrives with short time intervals, and therefore a superposition of waves inevitably occurs. Thus, only few pulse magnitude, obtained from first reflections, are regarded in order to estimate the propagation attenuation; in Figure 3.9, in fact, only first five PD pulse that arrive in measurement point 1, in Tuulikylä, are reported.

As seen in figure, every propagation path of a single PD pulse is named with three number: each number indicates how many reflections a single pulse has experienced in three different measurement points, that for a travelling wave are seen as discontinuity points. For example, in “010”, the first number says the pulse has not experienced any reflections from Tuulikylä PD

sensor at line junction; the second number indicates the pulse has been reflected from Pyntösjärvenaukee PD sensor; the third number indicates the pulse has not experienced any reflections from Noormarkku PD sensors at the end of the line (or with the 110/20 kV transformer, if is connected to the line).

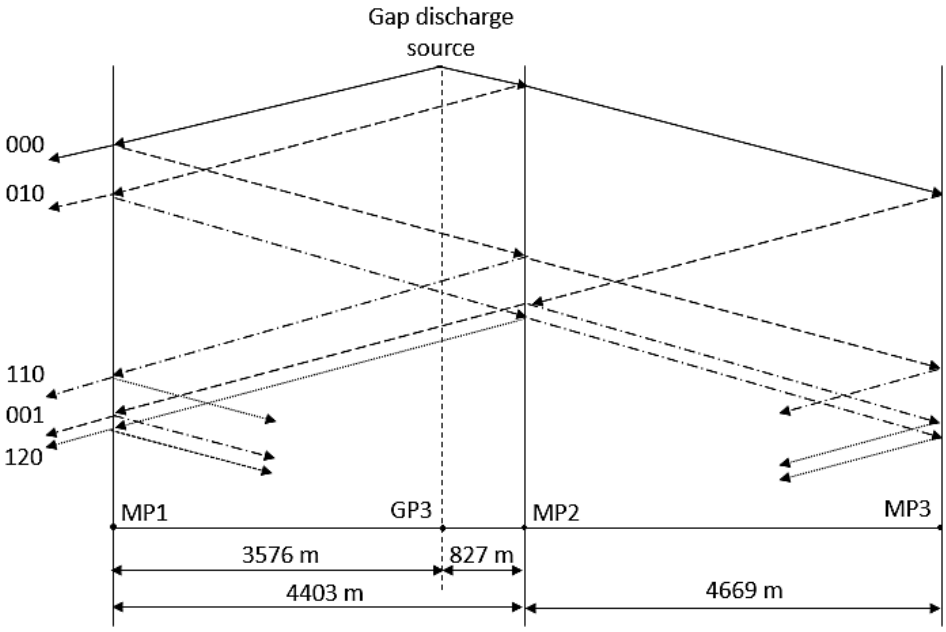

Figure 3.9 *Lattice diagram of the 110 kV covered conductor trial line, with a discharge source located in the middle between MP1 and MP2, at a distance of 3576 m from MP1.*

In table 3.2 there is a list of pulses that arrive in measurement point at Tuulikylä, in order of arrival, with relative delay in μs from the direct pulse, which is considered the zero time. The direct pulse travels directly from the PD source to the PD sensor, while the other pulses before arriving in measurement location have experimented reflections and refractions in other surge impedance discontinuity points, as shown in Figure 3.9 if the representation of the lattice diagram had continued for the other PD pulses. The propagation velocity is assumed of 288 m/μs, because it has been calculated making a difference between the time of arrival of the direct pulse peaks "000" and the time of arrival of the reflected pulse peak "110", which has experimented a reflection from Pyntösjärvenaukee PD sensor; moreover, the distance between the measurement locations are calculated basing on the line map.

Table 3.2 *Time intervals of pulses in PD sensor at MP1, between the direct pulse "000", arriving from the discharge source (GP3), and the other reflected pulses, as in Figure 3.9.*

Pulse	***Propagation path***	***Time stamp* (µs)**	***Pulse***	***Propagation path***	***Time stamp* (µs)**	***Pulse***	***Propagation path***	***Time stamp* (µs)**
Direct	000	0	5 refl.	220	61.2	10 refl.	330	91.7
1 refl.	010	5.7	6 refl.	101	63	11 refl.	211	93.6
2 refl.	110	30.6	7 refl.	230	66.9	12 refl.	112	95.4
3 refl.	120	36.3	8 refl.	111	68.7	13 refl.	340	97.5
4 refl.	001	38.2	9 refl.	012	70.6			

The time intervals in each group of pulses, that arrive almost together, are in the order of 2 µs, and therefore the pulses can be partially superimposed if the duration of a single pulse is longer than 2 µs. The power spectral density of these superimposed pulses, calculated with the 5 µs time window, can has some errors; for the determination of peak-to-peak voltage, in case of the first group of pulses, the values can be determined correctly using the simple min-max method.

Figure 3.10 presents the partial discharge waveforms of two pulses induced by an incipient earth fault and an incipient short circuit fault. The instants at which the reflected pulses in the incipient earth fault have their peak, are marked with broken vertical lines, assuming a pulse propagation velocity of 288 m/µs. The magnitude of the peak is high enough to be visible and pick-up the pulses; the position of the pulse peak "001", however, is slightly different from the calculated position.

This error can be attributed to the following factors (one or more):

1. error in the line length from the measurement in the line map;
2. a lower propagation velocity in the line portion MP2-MP3 respect to in the portion MP1-MP2;
3. distortion of the waveform, due to:
    a. frequency dependant attenuation and phase shift;
    b. superposition with other pulses or signals;
4. the fact that the line ends to an open switch at a distance of approximately 10 m after the PD sensor.

Of course there may be a superimposition of smaller PD and interferences, as those circled in Figure 3.10, and their reflection could cause errors in magnitude and position of the peak pulses

of interest. Moreover, it can be calculated a change in the propagation velocity, from 288 m/µs to 283 m/µs, that corresponds to an increase of 0.57 µs in the propagation time between MP2 and MP3.

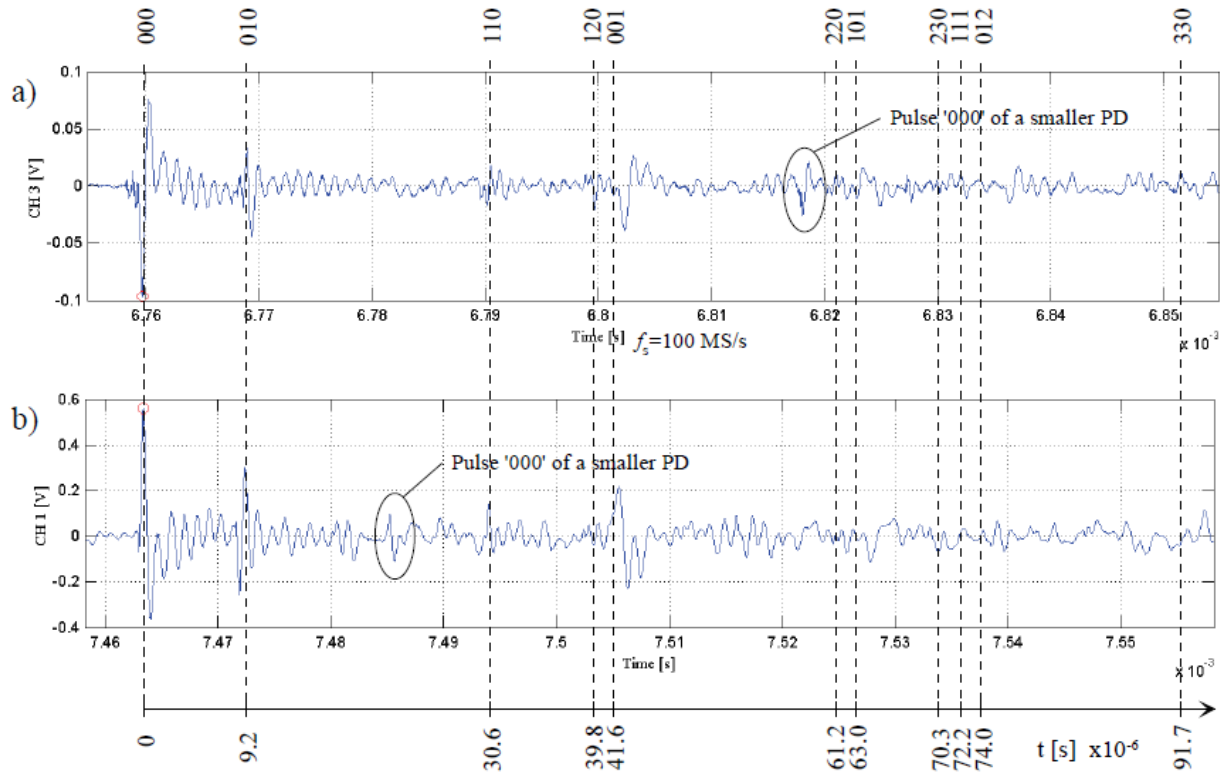

Figure 3.10 *Partial discharge pulse waveforms of an* **a)** *incipient earth fault, and a* **b)** *incipient short circuit fault, both measured at Tuulikylä. The vertical broken lines show the pulse positions calculated for the incipient earth fault, assuming a pulse propagation velocity of 288 m/µs.*

The propagation velocity of the travelling wave on an overhead power line is affected by the earth resistivity: the propagation velocity decreases when the ground resistivity increases. In Figure 3.11 ground resistivity, measured in every poles of the Forest-SAX trial line, is presented. To be precise, the measuring locations are between the pole 1 and the pole 2 (MP1), at the pole 34 (MP2) and at the pole 69 in Noormarkku substation (MP3). The earth resistivity is in general higher between MP and MP3, respect that between M1 and MP2: the earth resistivity was measured for every pole before the ground conductor was buried in the ground. The measurements were taken with the four-point method, with an electrode spacing of 1 m, 2 m, 4 m and 16 m; in Figure 3.11 only the measurements of an electrode spacing of 1 m and 16 m are presented.

On the open field (between the pole 1 and 16, and between the pole 29 and 33) the resistivity is generally higher with 1 m of electrode spacing, respect with 16 m; in the forest area (between the poles 19-27, 34-39 and 60-65) instead, the behaviour is the opposite. On the open space, the surface

layers of the earth are less conductive compared to those in the deeper; for the forest areas it is the opposite.

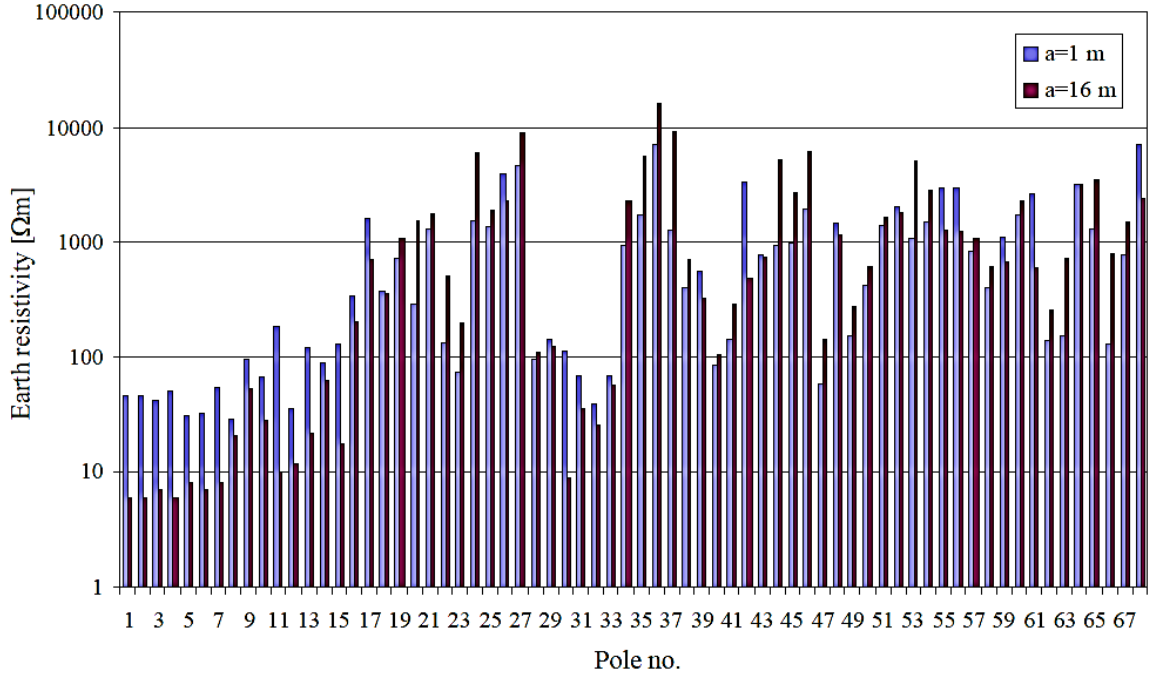

Figure 3.11 *Earth resistivity measured with electrode spacing of 1 m and 16 m, at the poles of the Forest-SAX line, before the installation of the ground conductors. The pole number increases from Tuulikylä (pole 1) and Noormarkku substation (pole 69).*

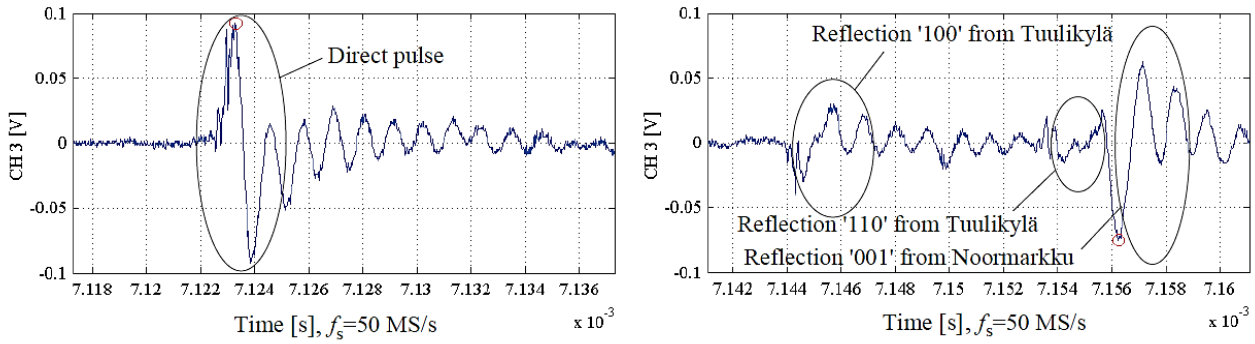

Figure 3.12 *PD pulse waveforms of an incipient earth fault, direct and reflected ("100", "110" and "001"), measured at Pyntösjärvenaukee.*

In Figure 3.12 are presented the waveforms associated to an incipient earth fault measured in Pyntösjärvenaukee. As it can be seen, the reflection "001", relative to the reflection in Noormarkku, is larger in magnitude respect to the other, and moreover it lacks the higher frequency oscillations presented both in direct and in the other reflected pulses: it is due to the reflection coefficient in that PD sensor, which is higher than that in Tuulikylä.

3.3 Effect of surge impedance discontinuity on the propagation

On a long line it may be necessary to install more than one PD monitoring units, for example at both ends of the line or along the line. The PD sensor installed along the line can affect the propagation of the signal: this behaviour has to be considered when the measurement results are interpreted. As seen in the previous chapter, the studies about the propagation of partial discharge pulses are conducted measuring in one location a single PD pulses, which propagates directly from the discharge source unto the PD sensor (direct pulse), and then its counterpart that has travelled in the opposite direction and it has experienced one or more reflections and refractions along the line or at the end of the line before arriving at measurement location. In this section the effect of a surge impedance discontinuity of the line on the propagation of the pulses is studied: all the measurements considered in this section were conducted whit the 110/20 kV transformer, located in Noormarkku, disconnected from the line.

In Figure 3.14-3.16 are presented the PSD's of the three different incipient tree fault (a gap discharge, an earth fault and a short circuit fault), each one with the direct pulse and the reflected ones. All the pulses were measured at the same measurement location, in Tuulikylä. In the figures, the PSD of the direct pulse "000" is marked by a red line; the PSD of the pulses reflected from the PD sensor in Pyntösjärvenaukee "010" is marked by a green line; the PSD of the pulses reflected from both the PD sensors in Pyntösjärvenaukee and at the end junction in Tuulikylä "110" is shown by a blue line; finally, the PSD of the pulses refracted at the PD sensor in Pyntösjärvenaukee and reflected at the line end and at PD sensor in Noormarkku "001" is marked by a black broken line.

All the PSD's are normalized at a frequency of 400 kHz to 0 dB, except for the gap discharges in which the frequency of normalization is 500 kHz. In the Figures 3.14-3.16, the PSD's related to only the phase in which the discharge has originated are presented. In all the cases, low frequencies tend to attenuate in the pulses that have experienced reflection respect to the direct pulse, while the high frequencies tend to accentuate. Only in case of pulse "001" the situation seems to be opposite: the pulse has experienced two refractions and a reflection at the end of the line. In case of this pulse high frequencies are attenuated respect to the pulse that travels directly from the discharge source to the PD sensor in measurement location.

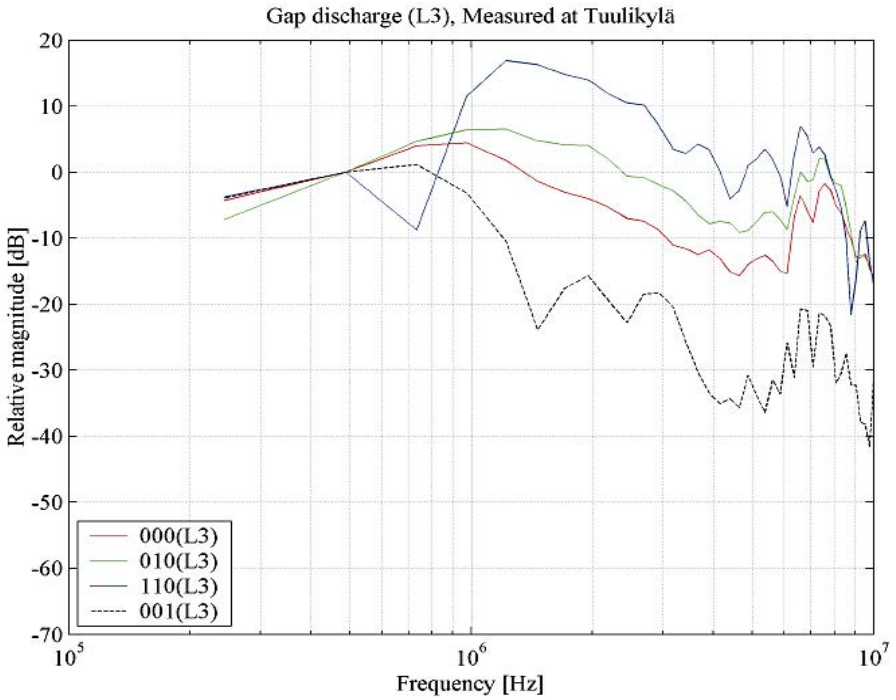

Figure 3.14 *Power spectral densities of a gap discharge pulse, related to the phase L3, measured at Tuulikylä: both the direct pulse and the reflected pulses are shown.*

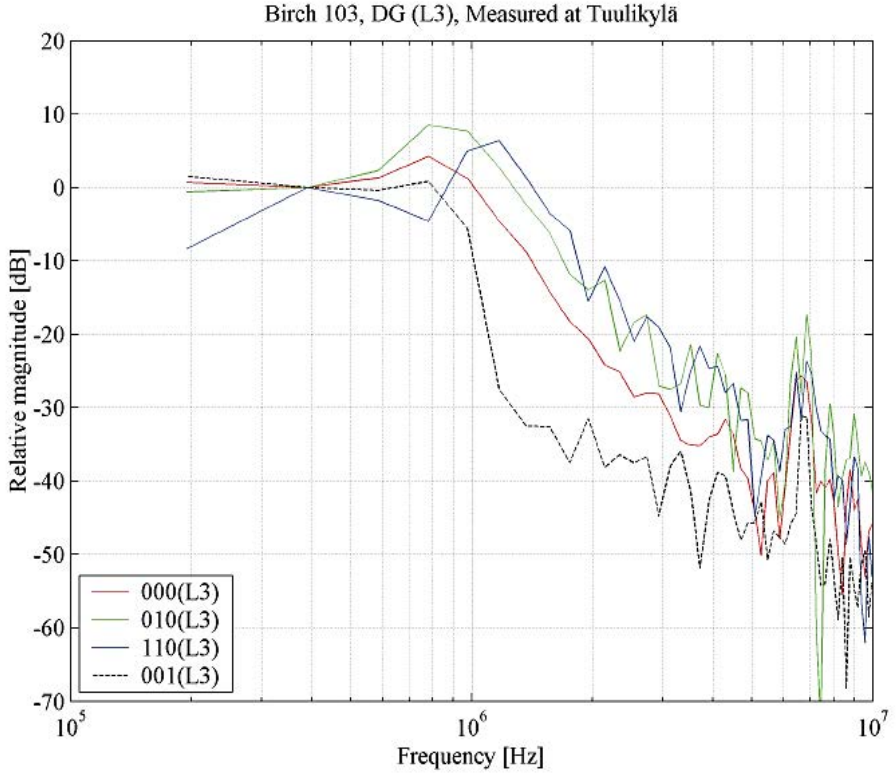

Figure 3.15 *Power spectral densities of an incipient earth fault, related to the phase L3, measured at Tuulikylä: both the direct pulse and the reflected pulses are shown.*

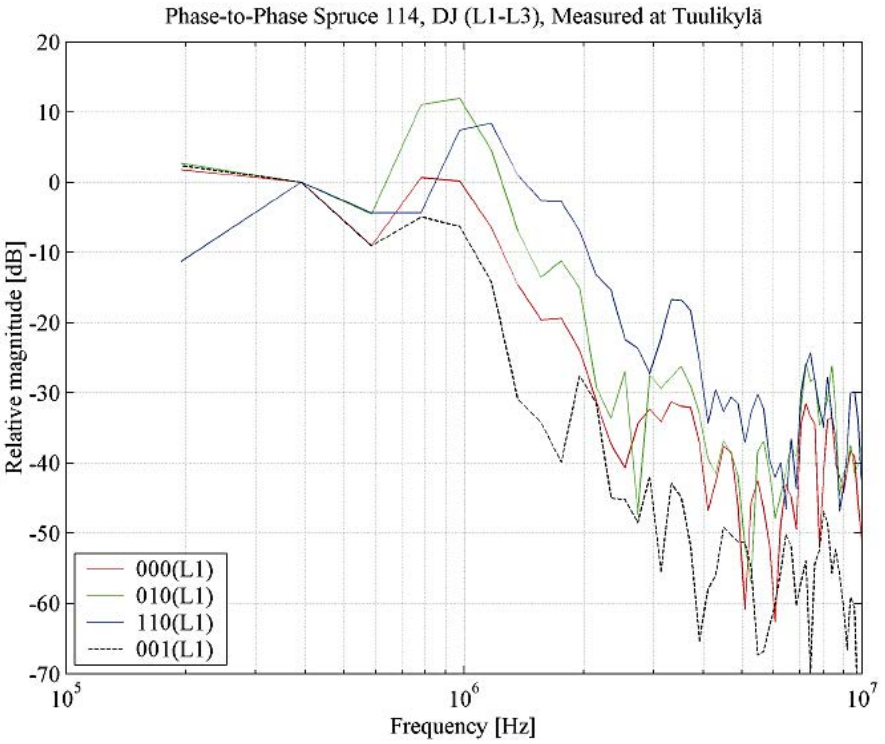

Figure 3.16 *Power spectral densities of an incipient short circuit fault, related to the phase L1, measured at Tuulikylä: both the direct pulse and the reflected pulses are shown.*

For comparison, in Figure 3.17 and 3.18 the PSD's of a direct pulse and its associated pulse reflected from the line end and the PD sensor in Noormarkku (pulse "001") are presented; the pulses were all measured at Pyntösjärvenaukee PD sensor. Figure 3.17 presents an incipient earth fault, while Figure 3.18 presents an incipient short circuit fault. In these cases, the differences between the PSD of the direct pulse and the reflected one is much smaller than the previous figures (Figures 3.14-3.16) conducted at Tuulikylä PD sensor: the deviation between two pulses occurs at high frequencies, mainly above 2 MHz. This is due to a short distance between the discharge source and the measurement point, in the order of 10 km: this suggests that, in generally, in the shorter distances, the effect on the PSD of a travelling wave is smaller respect to the pulses that have travelled for long distances. All the results obtained support the assumption that the impedances of the PD sensors are dependant from the frequency, and moreover, that the reflection coefficient of the sensors increase with the increasing of the frequency. In the refracted wave (pulse "001") the slope of the front decreases more compared to in that travelling directly from the discharge source; in other words, the high frequencies are attenuated more in the refracted waves.

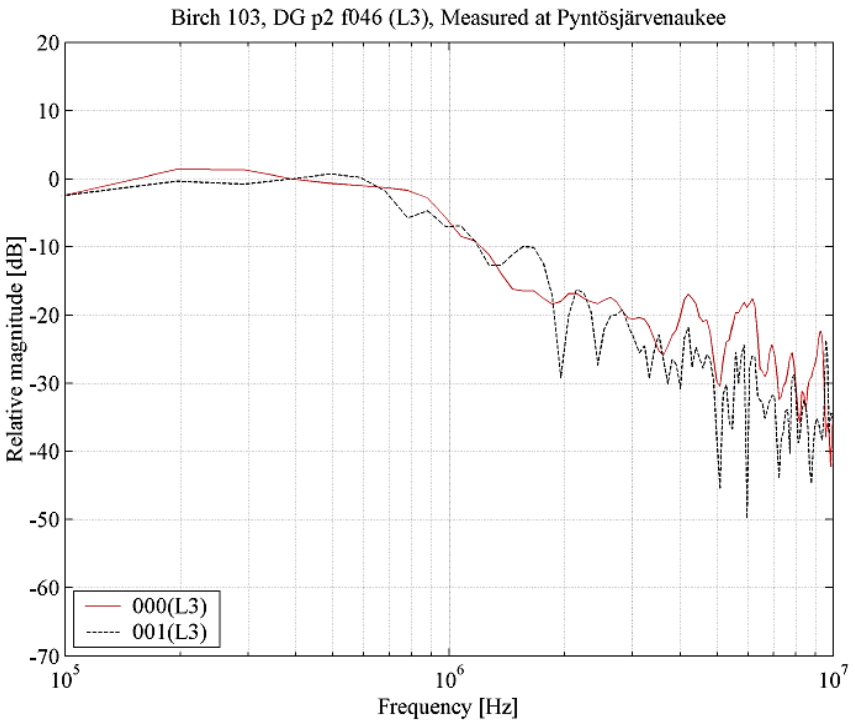

Figure 3.17 *Power spectral densities of a PD pulse in phase L3, related to an incipient earth fault and its reflection, travelling from the line end at Noormarkku to measurement location in Pyntösjärvenaukee.*

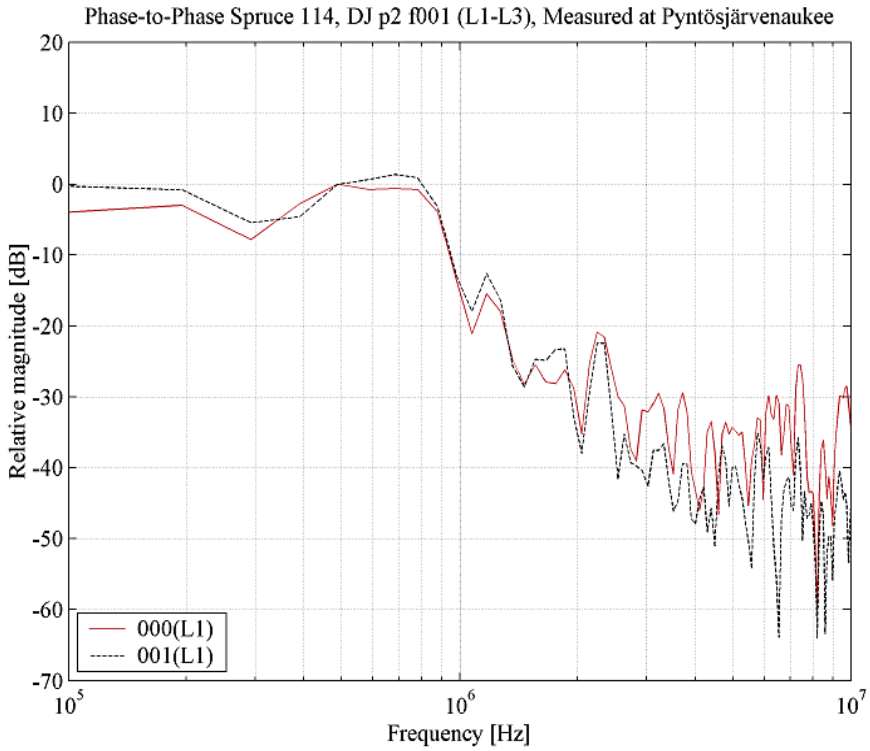

Figure 3.18 *Power spectral densities of a PD pulse in phase L1, related to an incipient short circuit fault between the phases L1 and L3, and its reflection, travelling from the line end at Noormarkku to measurement location in Pyntösjärvenaukee.*

The results presented suggest that, at high frequencies, the sensor segment the line in shorter portions, which facilities the location of the incipient tree faults. As it will be seen in the next chapter, the pulses reflected from a surge impedance discontinuity is utilized in order to locate the incipient tree fault, using the TDR method.

3.4 Propagation attenuation of PD pulses travelling on the line

The phase clearance in high voltage covered conductor overhead lines are smaller than those of high voltage bare conductor overhead lines: this leads a great advantageous in reducing the attenuation of the signal, which is propagating on the line. In particular, the Forest-SAX trial line has a conductor configuration arranged in the triangular, the conductors are covered by a polymeric insulation and a semi-conducting screen on the external surface of the inner conductor, all of which contribute to the propagation attenuation of the line.

In order to estimate the propagation attenuation in the Forest-SAX trial line in this work, pairs of pulses are considered and they are measured in the same location at different time. The first pulse comes to the PD sensor directly from the source of discharge, while the second pulse, that reach the same PD sensor later, is the counterpart of the direct pulse: initially travels in opposite direction, and then, after the reflection in a surge discontinuity point, changes direction toward the measurement location. With this method, the estimation of the attenuation results higher than the real attenuation of the line, due to only a part of the energy of the wave is transferred with the reflection: a part is dissipated at the discontinuity and the rest is transferred in the transmission wave.

In the specific case of Forest-SAX trial line, the most realistic estimation of the attenuation can be obtained on the basis of the measurements conducted at Pyntösjärvenaukee on PD originated between Tuulikylä and Pyntösjärvenaukee. An estimation of the propagation attenuation can be obtained by measuring a pulse travelling directly from the discharge point to Pyntösjärvenaukee and an estimation of the propagation attenuation on a line twice long can be obtained by using the same pulse after it has reflected back in the open line end at Noormarkku toward the PD sensor in Pyntösjärvenaukee, since this pulse has travelled a distance double respect the distance between the locations.

The transfer function of a power line can be presented as:

$$H(\omega, s) = e^{-\gamma(\omega)d} \tag{3.20}$$

where d is the distance travelled by the signal, γ is the propagation constant (determinate in Equation 3.1 in §3.1.1) and ω is the angular frequency. On a logarithmic scale it is possible represent the magnitude of the signal as a function of distance of propagation: for the Forest-SAX trial line the function is almost a straight line, if the line has not any considerable surge impedance discontinuities and assuming the frequency response of the measuring system flat on the frequency range of interest for the signals. The frequency response of the measuring system does not cause great distortion to the signal in the frequency range from hundreds of kHz to few MHz: therefore, the approximation of the propagation attenuation on a log-log scale with a straight line is justified.

Figure 3.19 presents the attenuation profile of different incipient tree fault, both incipient earth and short circuit fault, determined on the measurements conducted in Pyntösjärvenaukee. The pulses, in fact, have experienced only one reflection at the open line end in Noormarkku and at its PD sensor, and these attenuations on the line are regarded reliable enough in order to estimate the greatest distance at which an incipient tree fault can be detected, as it will be seen in the next paragraph.

The attenuation profiles are normalized to 0.1 V at a distance of 2.1 km, which is the average distance between the test site 1 (in which partial discharges occur) and the measuring location in Pyntösjärvenaukee. The profiles of the attenuation are very different for the several incipient tree faults: in general, the incipient short circuit faults are characterised by a lower attenuation respect the incipient earth fault. In Figure 3.19 an incipient short circuit fault (DK p2 f001) has the lowest attenuation, while an incipient earth fault (DF p1 f006) has the highest attenuation, approximately of 3.726 dB. The attenuation between the points at 1.228 km and 10.566 km, that correspond to a distance of 9.338 km, is about 0.3697 dB. If the data are normalized to a distance of 1 km, the attenuation would be 0.03958 dB and 0.3990 dB. Compared with a normal bare line with the same triangular configuration, the lowest attenuation is 0.04 dB/km at 100 kHz, while the higher attenuation is 04 dB/km at 100 kHz; making the same comparison, but at 500 kHz, the measurements conducted on a covered conductor trial line are approximately 60% smaller. The reason is the phase clearance in Forest-SAX line are 20-30% smaller than in a conventional bare line, and it reduces the propagation attenuation.

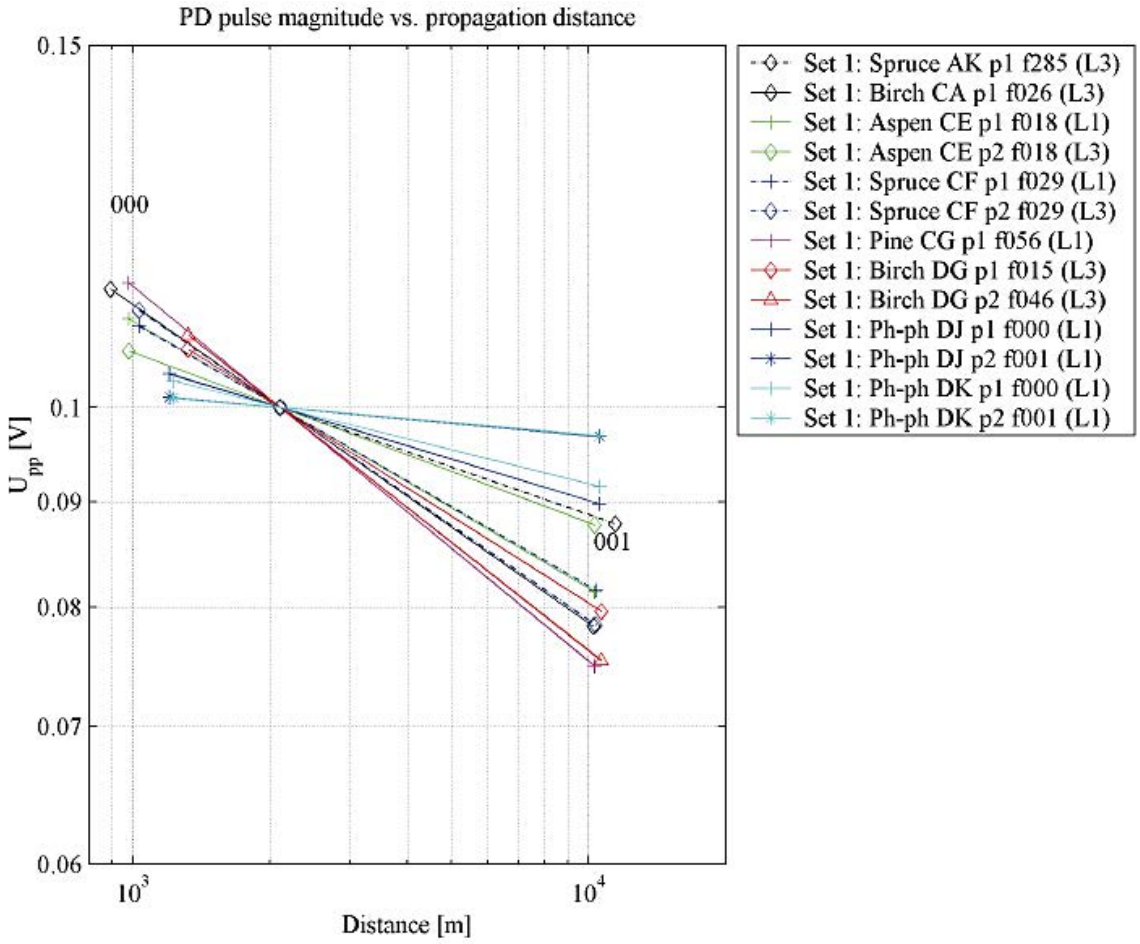

Figure 3.19 *Attenuation profiles, based on measurements conducted at Pyntösjärvenaukee measuring location, on a set of different incipient tree fault.*

This study is made to have a rough estimation of the values of attenuation in case of incipient tree fault on the line, using an appropriate frequency which depends on the frequency content of the partial discharges, generated by an incipient tree fault, and on the frequency response of the measuring system. Usually, in literature there are a lot of example relative to narrowband signals at various frequencies, making complicate a direct comparison with the results of the measurements, which are broadband signals. In fact, in case of broadband signals, the attenuation per unit length depending on the distance from the signal source, due to the signals with high frequency content decrease as the signals travel along the line. A comparison between broadband and narrowband measurements, made in the range of 100-500 kHz, is possible because the PSD of these incipient faults are almost flat below 1 MHz, before decreasing rapidly. In conclusion, the signals with broader frequency content, mainly caused by an incipient earth fault, attenuate more steeply than the signals with narrower frequency content as a function of the distance.

3.4.1 Estimation of the maximum line length using a single IFD unit

At the line end, the impedance may change depending on the frequency characteristic and the number of power apparatus connected to the line: this affect the results of partial discharges measurements taken at the line end.

The magnitude of partial discharges originated from twenty incipient earth fault are studied in terms of peak-to-peak voltage. However, the PD magnitude were measured in different test sites and a comparison on a magnitude scale is not easy. In Figure 3.20 the PD magnitude of 7 incipient earth faults, situated in test site 1 and measured in Pyntösjärvenaukee, are present in order of magnitude to get a rough estimation of the probabilities of magnitude in different discharges. Looking at the graph, it can be assumed 20% of the PD magnitude associated to incipient earth faults, measured at 2 km of distance, are below 0.1 V (peak-to-peak).

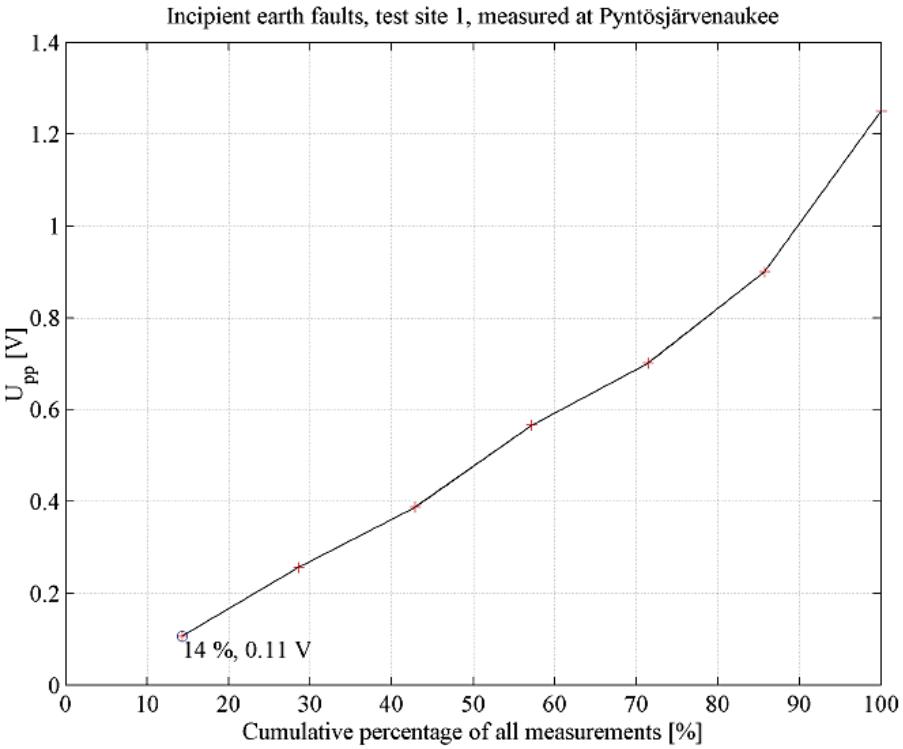

Figure 3.20 *PD magnitudes of incipient earth faults, on test site 1, measured at Pyntösjärvenaukee, in order of magnitude.*

In the studies of the incipient tree faults in site 2, a large number of ITF occurring in freezing conditions and in winter are included. The PD magnitude of several incipient earth faults conducted in test site 2 are present in Figure 3.21: 3 incipient faults are measured in September, 3 in November and 4 in March. In test site 2, the PD magnitudes were measured at short distance

from the incipient fault, only 104-210 meters, therefore, to estimate the distance at which an ITF could be detected, some errors are expected.

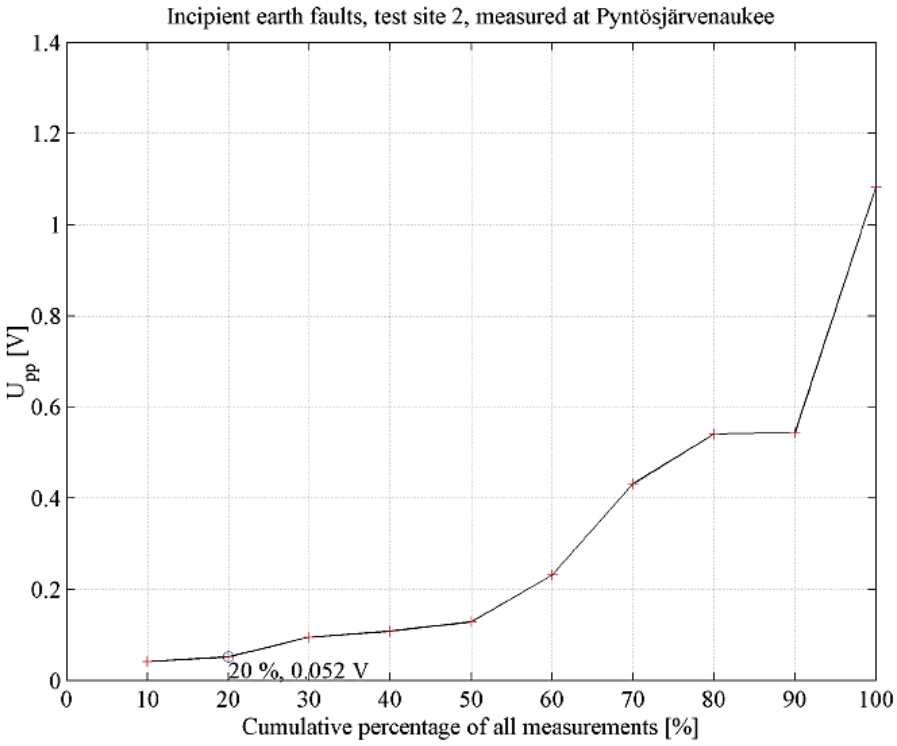

Figure 3.21 *PD magnitudes of incipient earth faults, on test site 2, measured at Pyntösjärvenaukee, in order of magnitude.*

Considering the attenuation lines relative to the incipient tree fault presented in Figure 3.19 as an estimate of the propagation attenuation, the maximum line length that can be monitored using a single incipient fault detection unit, with its specific sensitivity, can be estimated. For two incipient earth fault (DG and DH) the background noise level is around 10 mV peak-to-peak, as showed by the 90% percentile in the background noise. The incipient tree faults, to be detected and picked up, must exceed a certain threshold level, called "pulse detection threshold": in this case, a certain percentile of detected pulses must exceed another threshold level, called "sensitivity of the ITF detection unit", which is higher than normal pulse detection threshold. Assuming that 80% of the partial discharge magnitudes of the incipient tree faults to be greater than 0.1 V peak-to-peak (not in freezing conditions), and 0.5 V peak-to-peak (in freezing conditions), and assuming that incipient tree fault detection unit sensitivity of 2 or 6 times the background noise level (20-60 mV peak-to-peak), a rough estimation of the distance at which an incipient tree fault could be detected,

can be estimated, as presented in Table 3.3. The estimated distance *d* is calculated used the follow equation:

$$d = d_0 \cdot 10^{\frac{\log(s)-\log(u_{ref})}{k}} \tag{3.21}$$

where d_0 is the reference distance (2.103 km) at which the partial discharge magnitude u_{ref} (in terms of peak-to-peak voltage) is defined, *s* is the incipient tree fault detection unit sensitivity and finally *k* is the attenuation line slope as in Figure 3.19.

The most realistic assumption for the sensitivity of the detection unit is in the order of 40 mV, assuming the pulse detection threshold twice of background noise level, which is 10 mV, and the incipient tree fault detection unit sensitivity twice the previous pulse detection threshold, which is 20 mV. The margin to consider between the background noise level and the incipient tree fault detection unit sensitivity depends on the performance of the ITF detection algorithm.

Table 3.3 *Estimates of the line length (km) which can be monitored using a single incipient tree fault detection unit.*

	Slope of the attenuation line	***Distance assuming u_{ref}=0.1 V* (km)**			***Distance assuming u_{ref}=0.05 V* (km)**		
***Sensitivity* (V)**		**0.02**	**0.04**	**0.06**	**0.02**	**0.03**	**0.04**
Spruce AK p1f285 (L3)	-0.0769	2.6E+09	3.2E+05	1.6E+03	3.2E+05	1.6E+03	38
Birch CA p1 f026 (L3)	-0.1548	6.9E+04	7.8E+02	57	7.8E+02	57	8.9
Aspen CE p1 f018 (L1)	-0.1297	5.1E+05	2.5E+03	1.0E+02	2.5E+03	1.1E+02	12
Aspen CE p2 f018 (L3)	-0.0827	6.0E+08	1.4E+05	1.0E+03	1.4E+05	1.0E+03	31
Spruce CF p1f029 (L1)	-0.1282	6.0E+05	2.7E+03	1.0E+02	2.7E+03	1.1E+02	12
Spruce CF p2 f029 (L3)	-0.1526	8.0E+04	8.5E+02	60	8.5E+02	60	9.1
Pine CG p1 f056 (L1)	-0.1822	1.4E+05	3.2E+02	35	3.2E+02	35	7.2
Birch DG p1 f015 (L3)	-0.1406	2.0E+05	1.4E+03	79	1.4E+03	79	10
Birch DG p2 f046 (L3)	-0.1746	2.1E+04	4.0E+02	39	4.0E+02	39	7.5
Ph-ph DJ p1 f000 (L1)	-0.0669	5.8E+10	1.9E+06	4.3E+03	1.9E+06	4.3E+03	59
Ph-ph DJ p2 f001 (L1)	-0.0203	6.7E+34	9.2E+19	1.9E+11	9.2E+190	1.9E+11	1.3E+05
Ph-ph DK p1 f000 (L1)	-0.0547	1.2E+13	3.9E+07	2.4E+04	3.9E+07	2.4E+04	1.2E+02
Ph-ph DK p2 f001 (L1)	-0.0198	4.7E+35	2.8E+20	3.5E+11	2.8E+20	3.5E+11	1.7E+05

The propose of these studies is to understand the different factors to take in consideration in designing the partial discharge monitoring system for the Forest-SAX trial line and to estimate the distance at which an incipient tree fault can be detected. It seems the magnitude of the partial

discharges pulses in the incipient tree fault location depend a lot on seasonal condition; on the other hand, the propagation attenuation of the partial discharges pulses as a function of the distance of propagation depends a lot on the frequency content of the pulses; finally, the sensitivity of the incipient tree fault detection system at the measuring location determines the magnitude threshold level, which must be exceed by the incipient tree fault pulse to be detected. The estimation of the maximum distance detectable for the incipient tree faults is quite complicate due to the different factors that affect the results. The maximum distance at which the incipient tree fault could be detected on the Forest-SAX trial line should be considered case by case: considering the seasonal conditions, the propagation modes and the pulses shapes, the percentage of incipient tree faults to detect and the sensitivity of the incipient tree fault detection system. The incipient tree fault to be detected would be at least in the range of 30 km, in not freezing conditions; if freezing conditions occur in a significant part of the fault, the distance will be reduced to few kilometres.

3.5 Coupling of PD pulses between the phase conductors

A power line can be considered as a multiconductor transmission line, with mutual coupling between the conductors of the three phases and the ground wire; a knowledge of the coupling factor between the phases is relevant in order to interpret the results of the partial discharges measurements conducted on the line. The coupling phenomena are relevant in partial discharge recognitions with the possibility of using a single measurement in only one phase, in order to monitor the incipient tree faults the occur in all three phases. However, the propagation modes vary between the different incipient tree faults depending on the line geometry and the between the conductors and the trees. Additionally, the partial discharge pulses associated to a single incipient tree fault could be represented by different combinations of propagation modes, due to the several ways in which the discharges occur, with different distance between the tree and each phases and with the possibility one or more conductors are in contact or in proximity to the tree or with another conductor. Therefore, discharges in each phase could have different coupling with the neighbour phases.

In case of incipient tree faults, coupling occurs at the ITF location, through the low impedance between the tree in contact with one or more phase conductors. Both the AC conductivity of the tree and the capacitive susceptance of the covering of the conductor increase as a function of the frequency, increasing also the capacitive coupling between the phases during an incipient tree fault. The wave produced by a partial discharge may be injected in all three phases with different

energies in each phases, but there is the possibility to detect the partial discharges that occurs in all three phases by measuring only a single phase. However, the coupling between phases is considered more a problem than a benefit, because the pattern of the pulse, that is coupled from neighbouring phases, may be modified: this tends to decrease the reliability and the accuracy of the atrial discharges recognition.

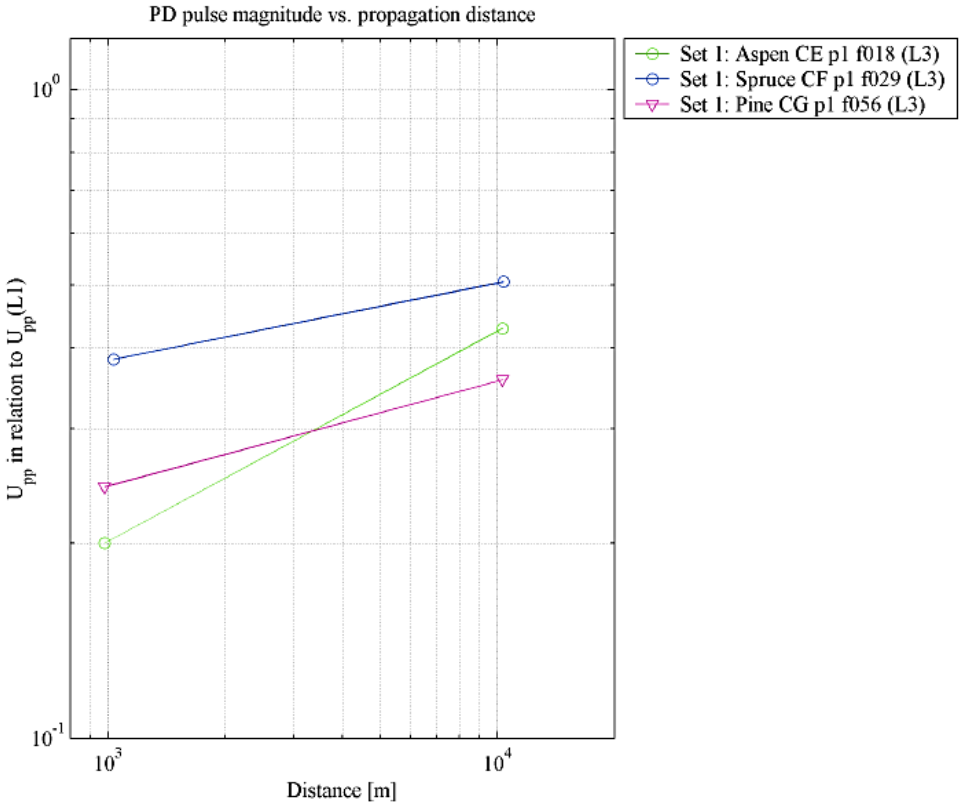

Figure 3.22 *Pulse magnitude in L3, in relation to pulse magnitude in L1, as a function of propagation distance in the case of three incipient earth faults; the measurements were conducted at Pyntösjärvenaukee.*

The coupling between the phases is studied measuring simultaneously a single partial discharge pulse in three phases conductors, and its counterpart pulses reflected in the surge impedance discontinuities along the line. Besides, the coupling is studied in three different incipient tree fault: the incipient short circuit fault, the incipient earth fault in phase L1 and the incipient earth fault in phase L3. The relative pulse magnitudes of the neighbouring phases, in relation to the phase in which the discharge occurs, as a function of the distance, for few incipient earth fault, are presented in Figure 3.22 and 3.23. In case of the incipient earth faults studied here, the magnitudes of the pulses in the neighbouring phases show a clear increase as increasing the propagation distance. At a distance of 1 km from the ITF, the magnitude of the coupled pulse is approximately 20-40%

more, and at a distance of 10 km, it is 30-50% more than the pulse magnitude in the phase in which the discharge occurs.

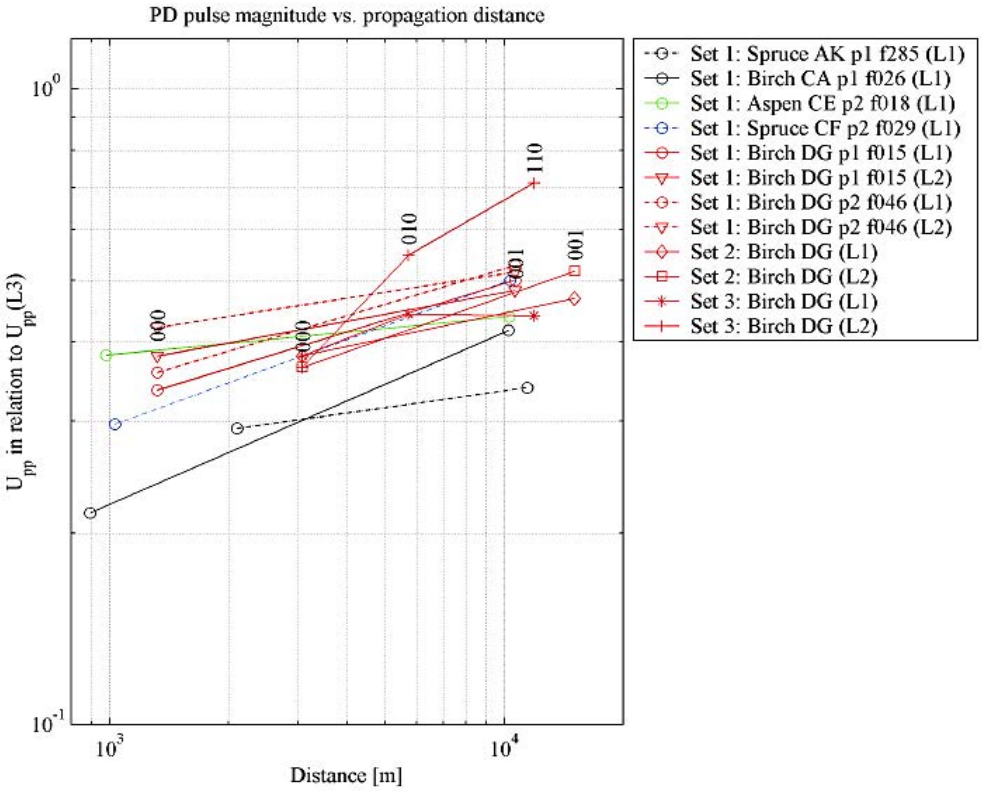

Figure 3.23 *Pulse magnitude in L1 and L2, in relation to pulse magnitude in L3, as a function of propagation distance in the case of three incipient earth faults; Set 1 is measured at Pyntösjärvenaukee, while Set 2 and 3 at Tuulikylä.*

In Figure 3.22, the incipient tree fault "CE" has a considerably steeper increase: this different behaviour in the steepness of the graphs, is likely to be explained in different modal composition.

In case of incipient short circuit fault, discharges occur both between phase conductors and between each conductor and the tree. If the discharge occurs between phase conductors, a current pulse of equivalent magnitude but opposite polarity appears in both the phases involved in the discharge: the relation between the signal magnitude in the phases may be preserved at long distance if there are not any surge impedance discontinuities; in Figure 3.24 PD magnitude profiles of several incipient short circuit are represented. The pulse magnitudes in the phase L2, related to the phase L1, increase with increasing the distance travelled: this is attributed to the PD sensors, which have slightly reflection coefficients for each phases. In case of incipient short circuit fault, the phase conductor not involved in the contact does not show much increase in the magnitude of

the pulse in relation to the discharge phase with the increasing of the distance: this complicates the detection of an incipient short circuit fault, using a single phase measurement.

Thanks to the coupling between phases, the incipient tree faults occurring in the three phases are detected by a single phase measurement, although the ITF sensibility on the neighbouring phases is smaller than in which the measurement sensor is collocated.

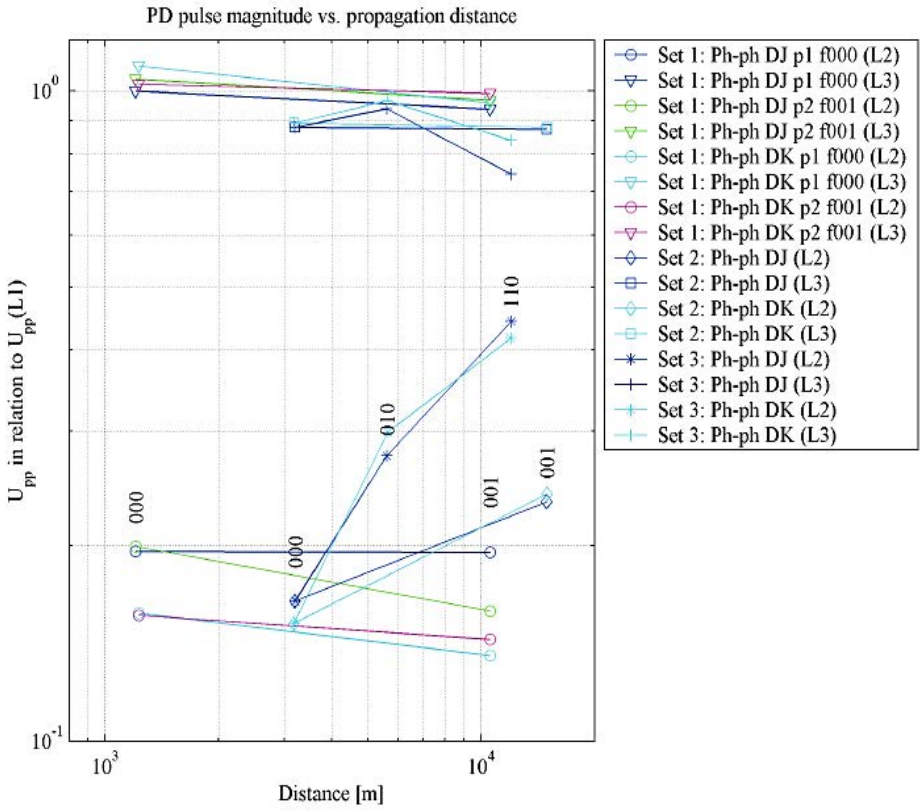

Figure 3.24 *Pulse magnitude in phases L2 and L3 in relation to the phase L1, as a function of propagation distance in case of incipient short circuit faults "DJ" and "DK". The discharges occurred between the phase conductors L1 and L3. Set 1 was measured at Pyntösjärvenaukee, while sets 2 and 3 at Tuulikylä.*

Chapter 4

Partial discharge measurements and detection of falling trees on a covered conductor line

This chapter presents the techniques used in order to measure the partial discharges on a high voltage power line, due to a fallen tree on a covered conductor line, using on-line measurement equipment, which does not disturb the power supply. Particular attention is put on the characteristics of the measurements instruments, as the bandwidth, the sampling or the quantization of the analogue signal. Then, the Rogowski sensor is presented: it is a current sensor which is able to pick up the partial discharges from the current waveforms, with good accuracy, without disturb the power service. After a clearing step, in which the interference noise is remove from the coming signal, which has travelled from the fault point to the sensor location, the signal of interest is analysed by an automatic method. The partial discharges are in fact analysed and their magnitudes and pulse waveforms are interpreted by one of the several statistic methods, in order to detect if in the line an incipient tree fault is happened. The last part focuses on the location of these incipient tree faults, through the study of the partial discharges, which are seen by the PD sensor as travelling wave. The study of the time, taken by the waves to run across the line, give an indication of the distance at which the PD is generated.

4.1 On-line partial discharge measuring system

Measuring of partial discharge has been used for several time as a test technique in order to evaluate the insulation design of a new high voltage insulator device; it was a quality control after the manufacture step of power apparatus. Lately, partial discharges measurements were used as a diagnostic technique to evaluate the conditions of the high voltage insulations; at first as a periodic measurement and then as a continuous on-line. These on-line measurements do not need to interrupt the power supply or interfere with any operations. Continuous on-line measurements need an automatic analysis of the measured data and communication with the monitoring unit. The on-line instruments are permanently installed in the proximity of the site which has to be

monitored. As seen in the previous chapter, if the distance between the PD source and the sensor is high, the frequency dependant attenuation and the potential reflections on impedance changes will distort the signals produced by the partial discharges sources. Of course, these phenomena cause problems in the interpretation of the measurement results and affect the design of the measurement system. For this reason, the PD measurements and interpretations of the results should be automatic: the external intervention of a user is necessary only if the instruments detect an abnormal PD activity. In this case, the communication functions between the instruments and the network operator are essential to allow to take the right actions.

In this work, the on-line partial discharges measuring system is used in order to detect fallen trees on a high voltage covered conductor line. In Figure 4.1 is represent a simplified block diagram which shows the electrical on-line partial discharges measuring system. The system consists of a PD sensor, that is a coupling device between the power line and the measuring system, a transmission system to transmit the signals, a PD instrument, a data analysis system and a communication system.

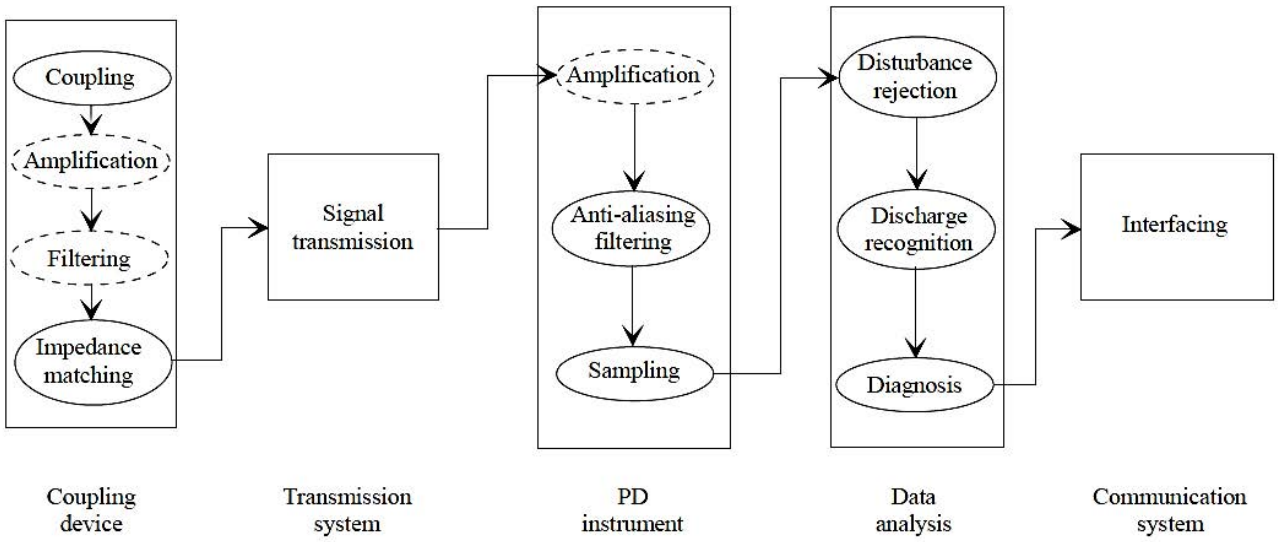

Figure 4.1 *Simplified block diagram of a digital on-line PD measuring system.*

The cost of the whole device tends to be high, if the coupling device has high voltage insulations; it dominates the total cost of the system, especially for high voltage levels. A solution could utilize the existing network components. Instead, the electronics devices used for the measurement and the analysis of the data are usually easier to scale down in costs respect to a coupling device with high voltage insulation.

The parameters that characterized a digital on-line partial discharges measuring system are:

1. The frequency ranges of the measuring system, that is the range between the lower and the upper cut-off frequencies (f_1 and f_2): the bandwidth Δf is defined as $\Delta f=f_2-f_1$. At these frequencies, the transfer function of the system falls by 6 dB from the pass-band value;
2. The sampling frequency of the measured signal;
3. The number of levels used in the digital conversion of the signal from the analogue;
4. The sensitivity of the system, that is, in this case, the magnitude of the smallest PD pulse the system can detect.

4.1.1 Bandwidth of the measuring system

The optimal bandwidth of the measuring system depends on a number of factors like the location and the type of the incipient tree fault monitored, or the disturbance signals at the measuring site. Usually, in practical applications, the bandwidth is fixed and it is a compromise between different factors. The most relevant information to keep in consideration in the bandwidth choice is the information about the frequency characteristic of the signals which are measured. Therefore, the frequency at which PD pulses occur has to be considered to avoid errors caused by the superposition of some consecutive pulses; a correct registration of the PD magnitudes is relevant in their recognition and detection. In addition to these technical strains, the optimization is also affected by economic constrains. An increase of the bandwidth of the measuring system means an increase of the price of the system, due to the higher quality devices.

In a lossless system, the spectrum of the partial discharges signals is preserved from the point of generation to the point of detection. In case of real power lines, the signals are attenuated and distorted when they travel from the generation point to the measuring sensor. For a power line, the attenuations and the distortions depend on the power line characteristics, the location of the origin and the measuring sensors. Approximately, at 10 MHz the attenuation is 25 dB/km, assuming the ideal rectangular filter. The optimum detection bandwidth varies with the position of the PD source: increasing the distance between the PD source and the sensor, the best sensitivity is achieved decreasing the bandwidth. With an adequately small bandwidth, few tens or hundreds of kHz, the sensitivity seems to be independent from the distance between the PD origin and the detector. On the other hand, with a large bandwidth, a more accurate discrimination between partial discharges of a closer source and interference pulses of a remoter source is achieved.

An approach in order to optimize the bandwidth of the measuring system in designing filters, according with the IEC 60270, is based on the integration of the PD current pulses and is the follow:

1. The spectrum of the current pulse, that has to be integrated, should exceed the upper cut-off frequency of the filter f_2 by a factor of ten or more;
2. The bandwidth of the filter Δf should be larger twice the highest repetition rate of the input pulses.

In an on-line measurement, these requirements are difficult to achieve, since the PD signal is considerably distorted. Therefore, the spectrum of the pulses is narrowed caused by the attenuation of the high frequencies during the propagation, as seen in previous chapter.

Generally, in on-line measurements the bandwidth is larger than in the laboratory. The lower cut-off frequency f_1 is tens or hundreds of kHz, while the upper cut-off frequency f_2 varies from hundreds of kHz to tens MHz. A large bandwidth increases the sensitivity provided the PD is measured close to its origin, so that high frequencies of the signal are not attenuated excessively. A frequency ranges from 20 to 100 MHz discriminates between the PD signals of interest and stochastic disturbances. The selection of the bandwidth is in fact one of the most crucial decision in designing the on-line PD measurements system: it has effects on the measuring system both from technical and economical point of view. The technical performance of the measuring system in detection of PD are affected by the bandwidth selection: an excessively narrow bandwidth could cause superposition of pulses causing errors. The optimal frequency range for the measuring system depends on the characteristics of signals, both that to be measured and expected interference signals. The magnitude and the frequency of disturbance originated from the network or from the measuring system itself are relevant factor to keep in consideration. In addition, there are economic constrain, related to the high price of insulation system: if the PD measuring system is just integrated into some other system, as an existing network components, it is used as coupling device, but this may limit the bandwidth choices.

4.1.2 Sampling and quantization of the analogue signal

The output signals from the coupling devices are typically in an analogue form, continuous both in amplitude and in time. However, an automatic analysis requires the signals are in digital form: thus, a conversion from analogue to digital (A/D) is necessary. In the first step, the analogue signals are converted into discrete-time signals, but continuous in amplitude. Each signal sampled is quantized in amplitude in one of the 2^B levels, where B represents the number of bits used in A/D

conversion. The result is a digital signal which exists only in a discrete point in time and in that time point only in a discrete value.

In PD measuring system, the signals are sampled continuously with a constant interval of sampling. Provided the sampling frequency is high enough, in order to register with a good accuracy both the pulse shape and the peak value. In PD measurements, the method would require a lot of memory and a lot of data processing capacity cause the high number of pulses processed, but it performs well even in a noisy environment.

Another method used is the sequence triggering mode. It is available in some oscilloscopes; the sampling starts when the signal meets the trigger conditions. As soon as it meets these trigger conditions, the sampling starts with n equidistant samples, for a duration of one PD pulse approximately, after which the sampling stops. The sampling restarts only when the signal meets again the trigger conditions. In this way, setting the trigger conditions, the background noise and the interference do not meet the level of the trigger conditions, thus it is possible to record the PD pulses and ignore the background noise. The method uses in more efficient way the memory capability, since background noise and interference are not stored. However, it is necessary some priori information about the duration of the pulses and the highest frequency components, in order to predefine the sampling frequency and the memory of each segment to optimize the total memory consumption, ensuring the essential information of the PD pulses are recorded.

4.1.3 Anti-aliasing filter

The sampling theorem states that for describe the signal completely, if the highest frequency component in the signal is f_{max}, the signal should be sampled with a rate of $2\ f_{max}$. If the sampling is low than the specific rate, it leads to aliasing and thus the original signal is not able to be recovered if the data are reconverted from digital to analogue. In the case of PD measurements, aliasing causes errors in peak registration of the value of the PD pulses: this could also cause mistakes in the location of the PD source using the method based on the time reflectometry or on the pulse travel times.

To fulfil the sampling theorem, the signals and the noise that stay outside from the frequency band of interest are removed. In order to accomplish it, the signal, before the sampling, goes through a filtering with an analogue low pass filter, so called anti-aliasing. In the practice, the aliasing phenomenon cannot be completely avoided since the noise is present and because an anti-aliasing filter does not remove completely the signal energy outside the interest band. In Figure 4.2 an anti-aliasing filter is presented, where f_c is the cut-off frequency, while f_s is the stopband frequency:

the signal components greater than f_s are attenuated by A_{min}, whereas the signal components between f_c and f_s are reduced in amplitude monotonically in function of their frequencies. An excessive transmission or an insufficient attenuation of frequencies greater than f_s could cause errors in the amplitude estimation of PD pulses in the input of A/D converter. In PD measuring system, the oversampling is commonly used, to keep the filter simple and to minimize the aliasing error when the PD pulse peak value is determined. The sampling frequency of about 6 or 8 times the Nyquist frequency is recommended.

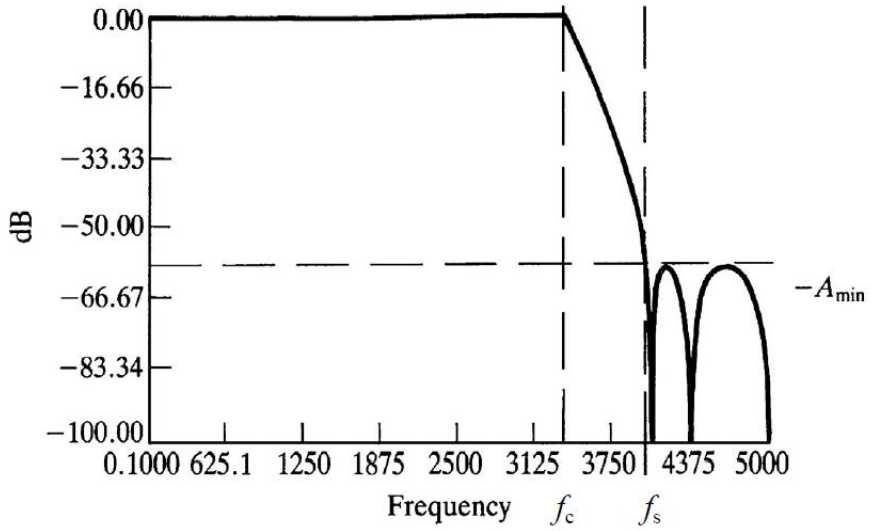

Figure 4.2 *Practical frequency response of an anti-aliasing filter.*

The dynamic range of the measuring system is defined as the ratio of a specific maximum level of the input signal and the minimum detectable level of the input signal. In a PD measuring system, the dynamic range is important, because the magnitude of pulses varies greatly in most cases, so it is necessary to register both high and low magnitude with the same amplification setting. The dynamic range in a digital PD measuring system is therefore affected by the A/D converter resolution, by noise generated in amplifiers and by imperfections of anti-aliasing filter. In available on-line measuring system and in PD instruments, the resolution communally used goes from 8 to 12 bits.

The bandwidth, the sampling rate and the dynamic range are relevant factors to consider in evaluation of performance of the measuring system.

4.2 Partial discharges sensor

The sensor used in PD detection can be divided in capacitive and inductive sensors, which measure respectively the voltage and the current. Research has produced several devices used for PD diagnostic that have been commercialized. In this work, the Rogowski coil has been chosen as PD sensor, for its proprieties as a wide bandwidth frequency needed for the PD detection and its non-intrusive method in the line. Besides, the Rogowski coil has a good linearity due to its structure without an iron core or magnetic materials; it is simple and it has a low cost. In table 4.1 the Rogowski coil is comprised with other type of sensors. Other different sensors were tested in order to determine the optimal one for the on-line partial discharges detection in high voltage power lines. Three different type of sensors have been compared and the results show Rogowski coil sensor is the favoured both in terms of sensitivity, frequency response and installation feasibility.

Table 4.1 *Features comparison of partial discharges sensor.*

	Capacitive sensor	**Axial magnetic field sensor**	**Rogowski coil**
Sensitivity	Low	Low	High
Universal applicability	Wide	Limited	Wide
Frequency response	High (up to 200 MHz)	Low (up to few MHz)	High (up to 40 MHz)
Time resolution	A few ns	Tens of ns	A few ns
Installation difficulty	Easy	Easy	Easy

Partial discharges that occour in a power line can be monitored measuring either the current flow or the voltage charge. The purpose of the coupling devices is to pick up either the current or the voltage wave related to a PD pulse, or even both of them separately, without any distortion in transforming it into a different form that can be register by the instruments. From the point of view of the PD pulses, the power frequency current and voltage waveforms can be considered like a disturbance, which can reduce the dynamic range of the instruments available for the register of PD pulses. For this reason, the power frequency current or voltage with its harmonics have essentially to be removed or separated from the signals either by a coupling device or by a high pass filter put before the instrument. From the point of view of the interpretation of the measuremnt results, the power frequency voltage waveform is a relevant information if this information is provided to the PD instrument by the PD coupling device, thus the PD pulses can be recorder separatly from the frequency voltage.

The partial discharges sensors are divided into three groups: voltage sensor, current sensor and directional couplers. A directional coupler is a combination of current and voltage sensors with small distance between them, allowing to find the direction of the pulse propagation; however, directional couplers are not explained in this thesis. Voltage sensor is a voltage divider made of two impedences (Z_a and Z_b) connected in series, as shown in Figure 4.3 a). The voltage divider used in PD measurements consists of a coupling capacitor C_k and a impedance Z, with a resistive, capacitive and inductive elements as in Figure 4.3 b). These voltage sensors are used usually in the on-line PD monitoring in rotation machines.

Coupling capacitors designed for PD measurements exhibit a good high frequency characteristics. A drawback of a PD coupling capacitor is that it tends to decrease the reliability of the power network due to its additional components and its high voltage components tends to make the sensor relative expensive. The last can be overcome using capacitances just existing in the power network. The main capacitance, Z_a in the Figure 4.3 a), is usually 100-600 pF, and the other, Z_b in the Figure 4.3 a), is about ten times larger. The problem is that existing power components have not specified by the manufacturer their high frequency characteristics.

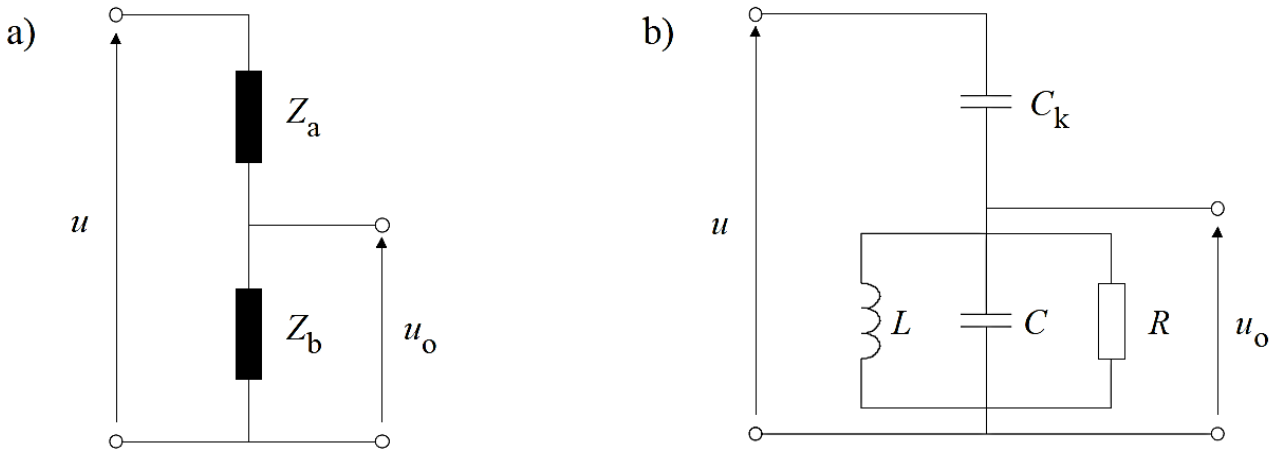

Figure 4.3 a) *A voltage divider and* **b)** *a coupling capacitor and a LCR impedance.*

4.2.1 Rogowski coils

The current sensors used in on-line PD measurements can be divided in two groups: the high frequency current transformers and Rogowski coils. Radio frequency current transformers (RFCT) or high frequency current transformers (HFCT) are wound on the iron powder core, while the Rogowski coil is air cored. Both of them (RFCT and HFCT) have been used in on-line PD

monitoring application, but due to their characteristics the iron core materials saturate at high currents: this can be a problem if the pulses to monitored are superimposed on high power frequency current. Rogowski coils, instead, have a very good linearity, without any effects of saturation or mutual inductance, so it is independent from the current measured. An example of Rogowski coil and its equivalent circuit is represented in Figure 4.4.

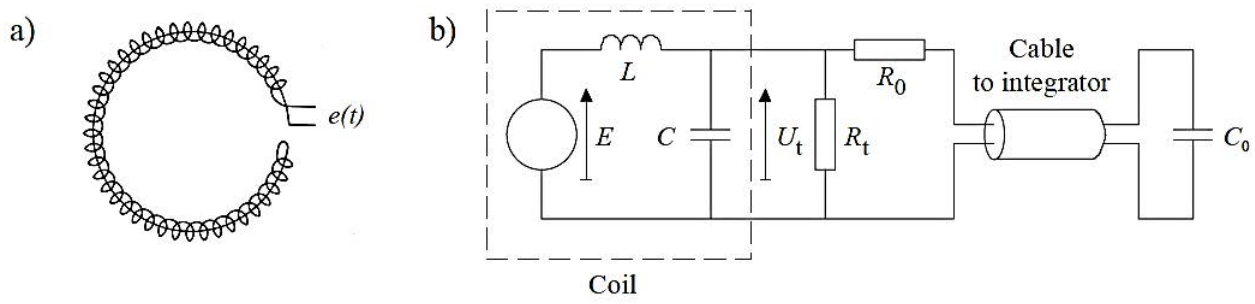

Figure 4.4 a) *A Rogowski coil and* **b)** *its equivalent circuit with a passive integrator.*

The Rogowski coil is used to measure fast and high-frequency transient currents in the range of mega-amperes. Thanks to its advantages of reduced size and low insertion loss, compared to a current transformer, Rogowski coils is a popular method of measuring current with power electronics equipment. The installation of the coil does not require any disconnection and thus it becomes a non-intrusive sensor, that is a very important for online monitoring method in PD measurements. Therefore, there is no saturation thanks to the air-cored coil, due to the absence of magnetic materials, and it also permit to have a very good linearity. Its light weight allows to be implemented as a low cost solution. Rogowski coils, in fact, are preferred as PD sensors in order to take measurements for detecting fallen trees on covered conductor overhead power lines.

A Rogowski coil has N turns, each with an area A and length l_c; the voltage output $u(t)$ induced in the coil by a current $i(t)$ is given by the Equation 4.1 of change of flux:

$$u(t) = -M\frac{di(t)}{|dt|} = -\frac{\mu_0 NA}{l_c}\frac{di}{dt}, \tag{4.1}$$

where M is the mutual inductance between the coil and the main current.

The self-inductance of a toroid L is:

$$L = \frac{\mu_0 N^2 A}{l_c}. \tag{4.2}$$

The self-inductance L and the self-capacitance C of the coil cause resonance, which may restrict the frequency range of the Rogowski coil usable at high frequency. Decreasing the turns in the coil, also reduce L and C, increasing the resonance frequency but decreasing the sensitivity. Therefore, in the dimensioning of the coil, it needs to do a compromise between sensitivity and bandwidth. If the measurements are done close to the resonance frequency, the resonance effects can be damped by the resistance R_t. The damping is achieved with a resistance R_t:

$$R_t = \frac{\pi}{2}\sqrt{\frac{L}{C}}. \tag{4.3}$$

The Rogowski coil can works in two different modes. The first method is done making the L/R_t time constant short, compared with the pulse in the primary current. This is called "differentiating coil", because the current flows in the coil and the voltage in resistor R_t is proportional to the differential in the primary current. The second method is done making the L/R_t time constant long: in this case the coil is called "self-integrating". In this case the voltage across R_t is proportional to the primary current, with the coil that acts as an air-cored transformer. An example of the effects of R_t on the impedance of the Rogowski coil is shown in Figure 4.5. With R_t = 100 Ω, the frequency ranges between 200 kHz and 20 MHz is the "self-integrating" region, where it can be used directly for the measurements. The frequency below the 200 kHz is the "differentiating coil" region, where instead it need an integrator in order to produce a flat response.

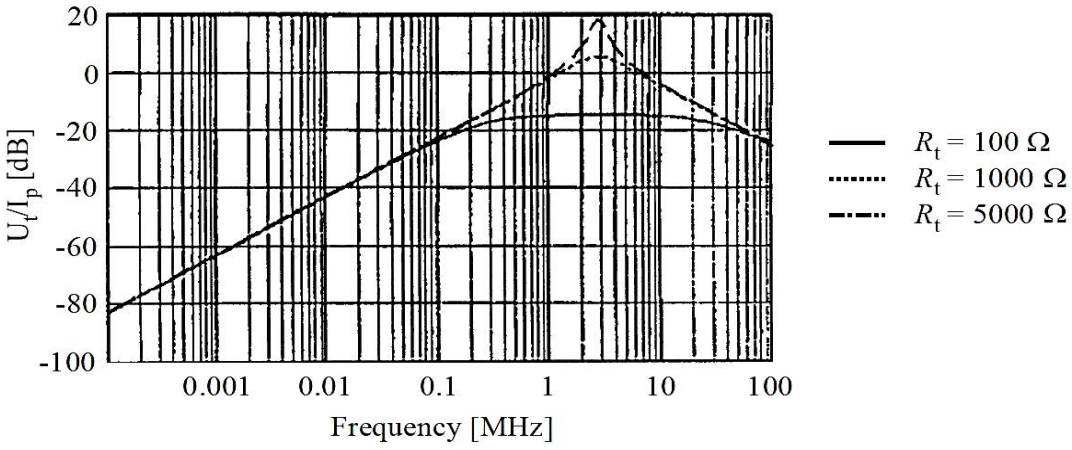

Figure 4.5 *Impedance of a Rogowski coil with different resistances R_t.*

The capacitance of the ending cable increases the coil capacitance, reducing the resonance frequency of the coil and also the bandwidth. In order to avoid this effect, a resistance R_0 in series, with $R_0 >> R_t$, is connected to the end of the coil, as shown in Figure 4.4 b). This resistor, therefore,

forms part of the integrator, which can be a passive RC circuit, formed by R_0 and C_0. However, this RC integrator can be only applicable in high frequency currents or in short duration pulses.

4.3 Interference signals and noise suppression

Partial discharges measurements with AC on the line are always affected by noise and electromagnetic disturbance (EMD). The best way to delete the noise problem affecting the PD measuring signals is a post-processing noise reduction technique. Disturbances, inevitably present in on-line PD measurements, increase the level of background noise and therefore reduce the measurement sensitivity. Generally, the noise sources can be divided into four groups:

1. Narrow-band signals, caused by radio transmission, as broadcasting or radio communication networks, or by power communication system;
2. Periodical pulse shaped signals, caused by switching in power electronics;
3. Stochastic pulse shaped signals, as partial discharges in power system, arcing between close metallic components, or lighting and switching operations;
4. Broadband random noise generated, for example, in amplifiers.

Narrow-band signals can be eliminated using a frequency domain filtering: since the frequencies of the narrow-band signals change often over time, the filter automatically adjust itself, according with the interference conditions. The filters can be based on Fast Fourier Transform (FFT), infinite impulse resonance (IIR) filters or finite impulse response (FIR) filters. In the method which uses FFT, the measured signal is firstly transformed in frequency domain. In the frequency domain, the PD pulses produce a spectrum relatively constant over a wide ranges of frequencies, while the narrow-band interferences appear as discrete spectral lines high intensity: these narrow interferences can be removed setting them to zero. One of the advantages of filtering using FFT/IFFT is the easy configuration in order to remove the narrow-band interferences and the stopband can be narrow. Instead, a drawback of these methods is the long calculation time, due to the extensive transforming of the signals from the time domain to the frequency one and vice versa. However, an advantage of IIR and FIR filters is the shorter calculation time, operating in real time and filtering the data stream from the analogue-to-digital converter. The advantage, in fact, is that it can be applied to the signal before the digitalization, so the dynamic ranges of the digitizer can be exploited only for PD pulses, instead of for the mixture of interference signals and PD, where interference signals could consume a great part of the dynamic range.

After the disturbance signals are removed, the next step is to collect the PD pulses in the measured signal. However, if there is not a priori information about the characteristics of the pulses, all the pulses are collected and only after the decision if is a PD or disturbance is made. The detection of pulses is accomplished by setting a threshold, positive or negative, representing the background noise level, and considering any exceeding of this level as a pulse. Other several methods are developed to suppress of stochastic and periodical pulse shaped disturbances.

4.4 Analysis and interpretation of PD signal

The use of partial discharges measurements to the detection of fallen trees on a covered conductor line is different from other partial discharges measurements application, due to the physical distance between the PD measurement location and the PD source (a tree fallen on the line) which can be several kilometres. This factor has to be considered in the interpretation of the measurement results. The aim of the analysis and interpretation pf the PD pulses is to identify and localize the site in which the partial discharges are originated. The localization of a discharge can help in deducing the reason for its generation and, in case of an incipient tree fault, it can help in clearing the fault. There is the need to distinguish the ITF that could cause a short-circuit (caused by a direct contact between the phase conductors) from that could cause an earth fault with less disastrous risk.

In order to understand if the pulses measured are caused by a fallen tree over the line or other PD source of interference, several methods are used to distinguish the different types of PD sources: these methods are based on the statistical analysis of the phase and magnitude in individual pulses. Due to the stochastic phenomena of PD process, the magnitude ranges of the PD may be very large; not only the highest PD pulses is sufficient to detect, but a significant portion of smaller ones have to be detect, to justify the statistical analysis of pulse magnitudes.

In the past, the PD identification was performed by a visual observation of discharge patterns on a power frequency ellipse of an oscilloscope screen. However, this method cannot be used in monitoring partial discharges automatically. Since the digital recording of PD data became possible, the research in the field has been very active using automated analysis and interpretation of PD pulses. The method that could be used in order to analyse the PD data are:

- Phase resolved partial discharge analysis (PRPDA);
- Time resolved analysis (TRA);

- Pulse sequence analysis (PSA).

In all these method, the general procedure is very similar and the steps can be described in Figure 4.6:

1. In the first step, PD patterns are selected and distinguished between PD of interest;
2. The extraction of features with sufficient discriminatory power;
3. The use of a database with the PD source of interest;
4. Finally, a classification algorithm is able to classify and recognise a known fault as one of interest included in the database.

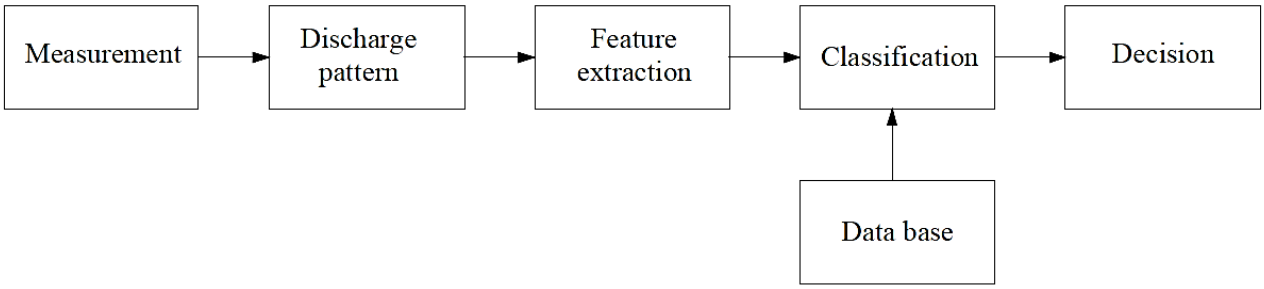

Figure 4.6 *A general recognition procedure.*

The first method seen is the PRPDA: the basic idea of this method is to superimpose all the discharges accumulated during the recording time on a reference cycle, which is synchronized with the beginning of the cycle, as shown in Figure 4.7 a). The range of phase angles is between 0° and 360°, but there is no correlation between pulses in different cycles. With this method information about propagation effects are lost, but the memory is saved. The parameters of interest are the pulse magnitude q_i or the voltage u_i and the phase angle φ_i of discharge occurrence.

The second method seen is PSA: the method aim is to analyse the change of the local electric field at the discharge site between consecutive discharges. As in Figure 4.7 b), the voltage change Δu_1, Δu_2, …, Δu_5 between consecutive discharges is a significant parameter, due to the local electric field change in a discharge site could influence the start of the next pulse. other relevant parameters are the phase angle (or time) difference between consecutive discharges $\Delta\varphi_1, \Delta\varphi_2, \ldots, \Delta\varphi_5$ and their magnitude. The PD patterns are based on these three parameters.

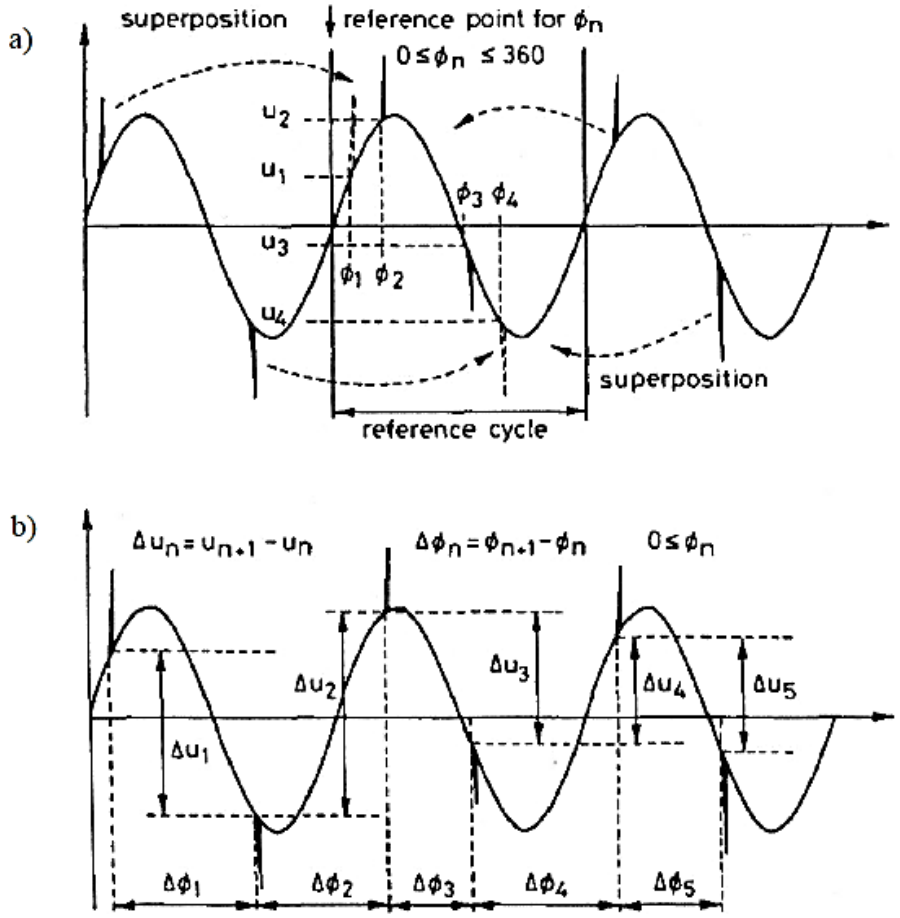

Figure 4.7 *Basic principle of* **a)** *PRPDA method* **b)** *PSA method.*

However, all this method presented before have the same problems:

1. Interference signals can modify the recorded discharges pattern;
2. Also signal attenuation and distortion due to the propagation between the PD location and the measurement sensor can modify the discharges pattern;
3. Multiple simultaneously discharges are superimposed in one discharge pattern, but the signals have to be discriminated on each PD source separately.
4. Any distortions of the power frequency voltage waveforms (voltage harmonics) can modify the PD parameters.

4.5 Location of an incipient tree fault

The aim of this work is to study a function for the PD source locating in order to localize the faults and develop an efficient technique for the online monitoring of these partial discharges, generated

due to a leaning tree on a covered conductor overhead transmission line. The knowledge of the PD source location is useful in planning the maintenance and repair actions and in the risk assessment. On a CC line, the knowledge of the PD source location can help to verify the origin of the PD signal and clear rapidly the incipient tree faults.

Single-end and double-end online detection and location have shown good results in PD detection, but errors in determining the source location of the PD. These errors are due to the dependency on the propagation velocity, which is affected by physical parameters, as the temperature or the height of the phases respect to the ground. Moreover, the propagation velocity is frequency-dependant, and the dependency increases with the increasing of the propagated signals frequencies. The best accuracy for the PD location is the multi-end travelling waves locator, with synchronized measuring methods.

There are several methods for PD measurement. The most known methods for measurement of PD are:

- *Optical detection method*: during the appearance of the discharge, the light is dissipated as an ionization excitation process. A transparent insulating material is functional for this detection method;
- *Acoustic detection method*: the method perceives and encodes the acoustic signal generated during a PD occurrence. It is not affected by electromagnetic disturbances (EMD), which reduce the sensitivity of electrical methods, but it is complicated to apply;
- *Chemical detection method*: PD are detected observing the chemical changes in the insulating material used in HV power equipment. The method does not provide the information about PD characteristics and its location. Furthermore, complicated instrumentations are required during online monitoring PD;
- *Electrical detection method*: the method is the most popular methods for PD measurement in HV power equipment. It is based on the appearance of the voltage and current pulse: the pulses last less than one second and have a variation frequency in the range of kHz to MHz. The shape of the pulses gives the information about the PD. To observe PD impulses, a time domain recording device is used. Various processing methods are applicable to identify and locate the PD signals.

The location of the PD source can be done, using the time domain reflectometry, i.e. by the pulses arrival times measured in one or more locations in the network. Time domain reflectometry is the most commonly method applied for locating a PD source in the cables. The method is presented

in Figure 4.8, where a PD occurs in the point *C*, along a cable *AB*, with the measuring system connected to the point *A*. At point C, two identical travelling waves are formed and they travel in opposite directions along the cable. The pulse travelling towards the point *A* is recorded in *A* as the first pulse, while the pulse that is travelling in the opposite direction is completely reflected at point *B* (assuming the cable end open) and it travels back towards the point *A*, where the pulse is recorded as the second one. The pulse that had reached the point *A* first, after the reflection at *B*, returns back to *A* and is recorded as the third pulse.

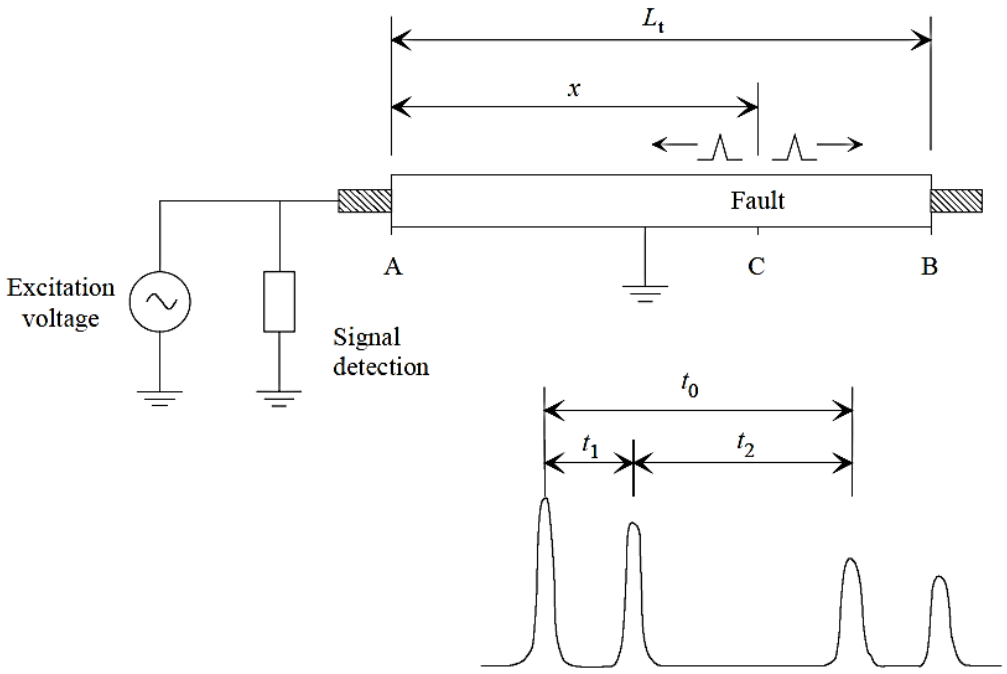

Figure 4.8 *The principle of PD location using the time domain reflectometry.*

The unknown distance is called *x*, between *B* and *C*, and can be determined by the Equation 4.3, measuring the pulse intervals t_0 and t_2, in addition to the known length L_t of the cable:

$$x = \frac{t_2}{t_0} L_t \tag{4.3}$$

or, whether the propagation velocity v_p of the pulse is known, it can be determined by the Equation 4.4, measuring the interval t_1, among the first and second pulse:

$$x = L_t - \frac{v_p t_1}{2}. \tag{4.4}$$

Generally, the time domain reflectometry method is suited for off line PD measurements, in which both cables are disconnected from the network. However, in long cables, the attenuation of the reflected pulses, which have travelled for to two times the whole cable length, may result too high for the detection and the determination of the time of arrival (TOA) of the pulses. Therefore, with a measuring system located at both ends in the cable, the TOA of a pulse are measured at both ends and only the first pulse is analysed. An advantage of this method is the propagation distance of the pulses is smaller and so there are no reflections at the far cable ends. A disadvantage of this method is the more complex measuring system and it needs some tools (for example, GPS) in order to synchronize the separate measuring systems.

Because of the frequency dependent attenuation, the PD pulse is distorted when it travels along an overhead or cable line: the different frequency components, in fact, travel at different speeds. This dispersion spreads makes difficult to select a reference point on the waveform and determine the TOA of the pulses. In addition, the pulse shapes are distorted cause of the frequency-dependent reflection coefficients at the end of the cables. Additional errors in PD source location could be introduced due to the propagation velocity which is not uniform along the line: the propagation velocity variations, in fact, occur due to some variations in ground resistivity or, in cables, due to some variations in the semiconducting material composition. Added errors could be introduced due to the imperfections in the measuring system.

4.5.1 Location accuracy

On HVCC lines, the request for the location accuracy is not so high as in cables, thanks to the visibility of the fault. The accuracy of one-line span (100-200 m) is adequate to help the maintenance to find in the quickest way the incipient tree fault site and remove the tree. Since the time domain reflectometry (TDR) method is based on the time of arrival of the first pulse, which travels directly from the incipient tree fault to the measuring location, and then its counterpart pulse which travels in the opposite direction and is reflected from an impedance discontinuity on the line, become interesting to study the attenuation of the reflected pulses when they meet different surge impedance discontinuities.

In the time domain reflectometry method, the location of the PD is based on the time intervals between two or three pulses which arrive from the discharge source, directly and after reflections at the end of the line or at impedance changes along the line. The simplest way to determine the intervals is to consider the pulse highest peaks. In Tables 4.1 and 4.2 are present the estimates of PD source location, calculated from Equation 4.3, conducted at Tuulikylä and Pyntösjärvenaukee.

Table 4.1 *PD source location estimates of test trees, calculated on TDR method conducted in Tuulikylä.*

Tree ID	***Phase***	***Tree species***	***Distance on line map* (m)**	***Distance estimated by TDR* (m)**	***Deviation* (m)**	***Deviation w. correction* (m)**
AK	L3	Spruce	2299	2260	-10	-10
AL	L3	Spruce	2297	2356	39	39
AM	L3	Spruce	2289	2244	-45	-19
DG	L3	Birch	3079	3016	-63	-17
DH	L2	Pine	3068	2997	-71	-13
DJ	L1	Spruce	3198	3125	-73	19
DK	L1	Spruce	3175	3108	-67	-9

Table 4.2 *PD source location estimates of test trees, calculated on TDR method conducted in Pyntösjärvenaukee.*

Tree ID	***Phase***	***Tree species***	***Distance on line map* (m)**	***Distance estimated by TDR* (m)**	***Deviation* (m)**	***Deviation w. correction* (m)**
AK	L3	Spruce	2104	2154	50	-16
AL	L3	Spruce	2106	2188	82	130
AM	L3	Spruce	2114	2256	142	142
DG	L3	Birch	1324	1351	27	27
DH	L2	Pine	1335	1348	13	13
DJ	L1	Spruce	1205	1278	73	-53
DK	L1	Spruce	1228	1333	105	26

The time intervals are definite according to Figure 4.9, based on the highest peak (absolute value, using the "*abs*" and "*max*" functions in Matlab) from the 5 µs time windows which contain the pulses. The time steps resolution of the pulse peaks is 0.1 µs, which correspond to a sampling frequency of 10 MS/s. The first peak, in the direct pulse, is the largest, but the second pulses, the reflected one, has opposite polarity. In Table 4.1, the time stamp of second and third pulses, was determined erroneously: due to this error, both the time interval t_0 and t_2 are 0.25-0.5 µs too short. Thus, the estimated distance from Tuulikylä is too large respect to the distance determined by the line map. However, if a manually correction is done, the difference between the map location and the location estimated by the TDR measurement is reduced to less than 20 meters. These errors may be partly attributed to the low noise ratio of the signal, the inaccuracies of the line map and

the variations of the signal propagation velocity on the line. Looking at the Table 4.2, the location accuracy in Pyntösjärvenaukee is of the same order of magnitude of Tuulikylä, but in this case the estimated distances are larger than those from the line map.

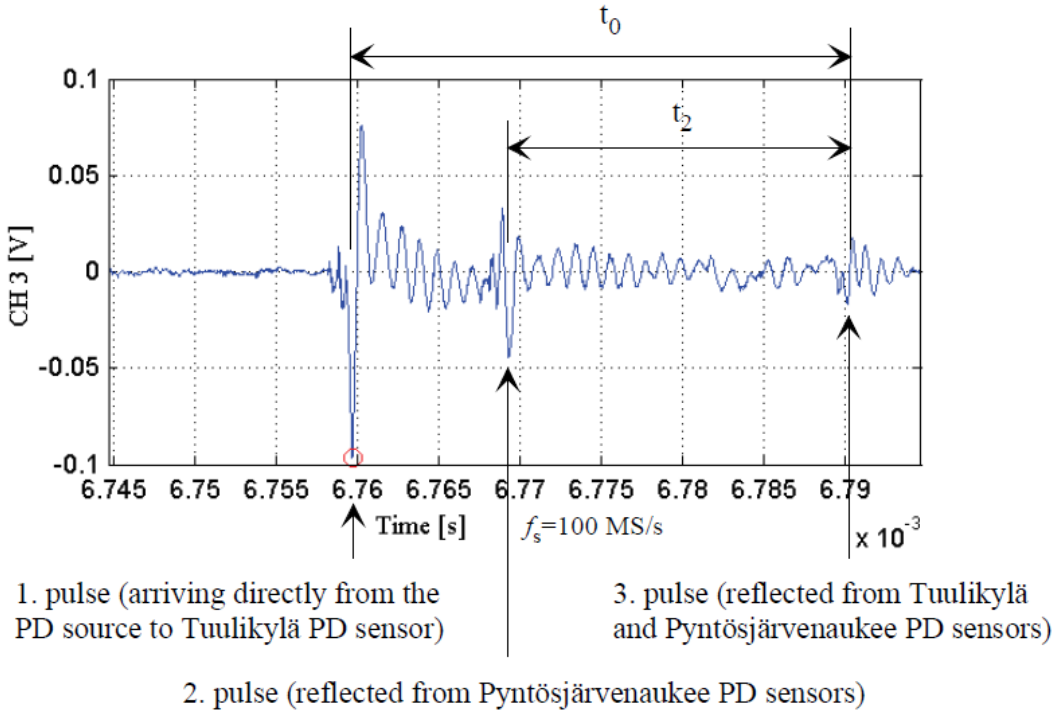

Figure 4.9 *Determination of the time intervals t_0 and t_2, for the estimation of the location for the incipient earth fault.*

Placing the measuring locations at the end of the line is suitable for the PD location. Instead, placing the measuring locations away from the line end could cause additional reflections, that complicate the PD location. Also the measuring location in the middle of the line is problematic, in case the first and the second pulses are superimposed due to the small distance (few hundred metres) between the PD sensor and the fault.

Generally, the TDR method is suitable to incipient tree fault location on a 110 kV covered conductor line for the following reasons:

- The structure of high voltage networks is very straightforward (few branches and transformers along the line than in medium voltage networks): branches in fact cause additional reflections, complicating the results interpretation;
- The attenuation on the line is small;
- The short branch lines which permit to monitor the whole line by using only one PD monitoring system at the substation. Methods of location based on two measuring locations

are necessitate where no infrastructure exists for communicate (GPS), in order to synchronize two separate measuring systems.

4.5.2 Measurement at the line end

It results useful to install the PD sensor in the substation, at the end of the CC line. At the substation, in fact, the power supply and the communications infrastructure are available and, usually, there is already present high voltage apparatus in which PD sensor can be integrated. However, the presence of the substation could introduce high frequency interference. Besides, the substation introduces a further impedance to the line, causing pulse reflections and distortion in the PD pulses waveforms.

During normal operation, the substation includes the 110 kV power transformer, the switching and the measuring apparatus. In some cases, the line operates without a load, with a PD sensor and an open switch (or disconnector). The PD sensor, in fact, is always connected to the line, to permit the PD monitoring of the line also if the line is not energized; the PD monitoring is in function regardless if the power transformer is connected or not to the line. The one phase configuration of the Noormarkku substation is presented in Figure 4.10, where the disconnector *S2* separates the equipment from the line and from the PD sensor. During the field test, disconnector *S2* was normally open, separating the substation from the line. An imagine of the Noormarkku substation in presented in Figure 4.11.

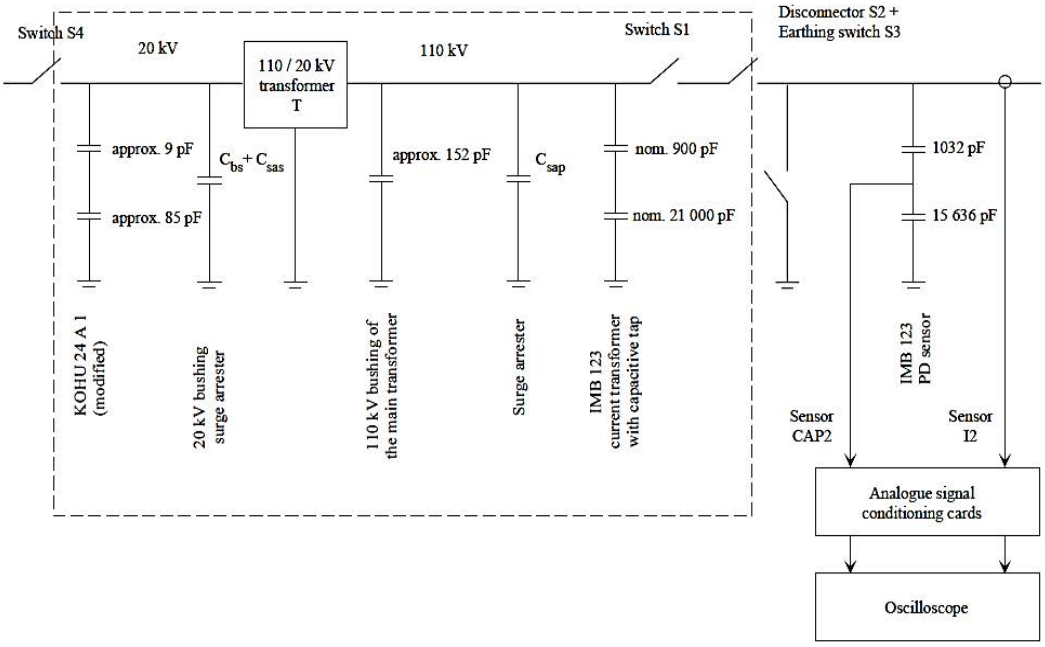

Figure 4.10 *Simplified capacitance model of the PD sensor and the phase L3HV apparatus at Noormarkku 110/20 kV substation.*

Some tests were arranged when the disconnector *S2* was closed during an ITF test, so the substation equipment could be connected or disconnected from the CC line, operating the switch *S1*. The inductive sensor (*I2*) is the PD sensor used in the pilot installation and the *IMB 123* is a current transformer with a built-in Rogowski coil: it measures the PD current pulses travelling in the Forest-SAX line. The capacitive sensor (*CAP2*) is the capacitive divider, in the primary winding insulation it is formed by the capacitive layers of the same *IMB 123* current transformer. The signals from the capacitive divider are available in a tap terminal (outside the transformer), where it can monitor the conditions of the paper insulation by a dielectric loss angle test. The sensor *CAP2* measures the PD voltage pulse travelling in the Forest-SAX line.

Figure 4.11 *Switches, disconnector, earthing disconnector, PD sensors and support insulators located in Noormarkku 110/20 kV substation.*

The first test started with the transformer disconnected from the trial line and it was connected about 40 minutes after the incipient earth fault. The second test, instead, started with the transformer connected and it was disconnected about 1 hour and 20 minutes after the incipient earth fault. In each test, four sets of 102 PD pulses, which exceed the trigger level, are measured;

two sets are done before and two after the connection (or disconnection) of the transformer. For each set of pulses, the standard deviation and the mean pulse values, in phase L3, are determined. The results from the first and the second tests are presented respectively in Figure 4.12 and Figure 4.13. The figures present the mean values per unit (p.u.), normalized respect to the mean value of the last pulse measurement before the disconnection of the transformer (Figure 4.12) or of the first measurement after the connection of the transformer (Figure 4.13).

The PD magnitude, with the transformer disconnected, is only about 0.25-0.30 times the magnitude with the transformer connected. The sensitivity of the incipient tree faults detection decrease and should be taken in account when the line has the transformer disconnected. Besides, disconnecting the transformer from the line, the background noise increases by 10-20 %. However, in case of an inductive sensor, no considerable noise can be observed: this is due to the small signal level of the Rogowski coil. The noise level from the IMB 123 capacitive divider, instead, is considerably higher.

Typical PD waveforms measured before and after the transformer connection to the line by the sensor are shown in Figures 4.14 and 4.15 respectively. The PD waveform is relevant, since it affects the implementation of the ITF detection algorithm. A simple method to achieve this is to set a certain “dead time” after the detection of pulse peak, after which additional oscillations are ignored.

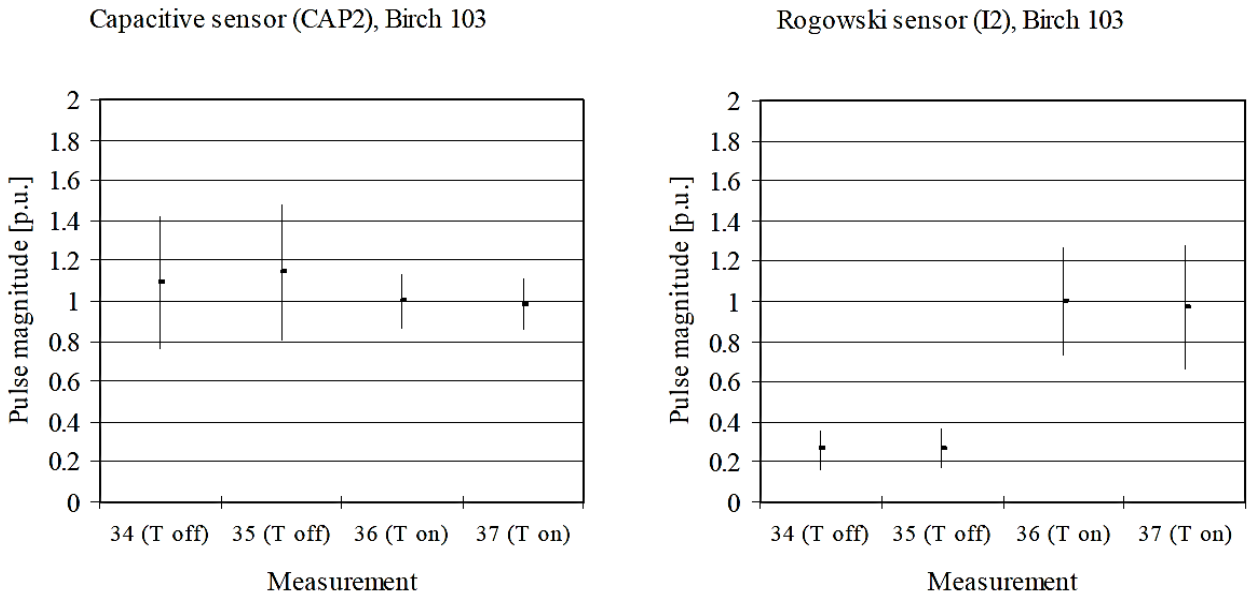

Figure 4.12 *Mean pulse magnitudes measured with a capacitive sensor (CAP2) and Rogowski sensor (I2), with the transformer disconnected (T off) and then connected (T on). PD pulses are represented per unit (p.u.), respect the mean value of first measurement after the connection of the transformer to the line (measurement number 36).*

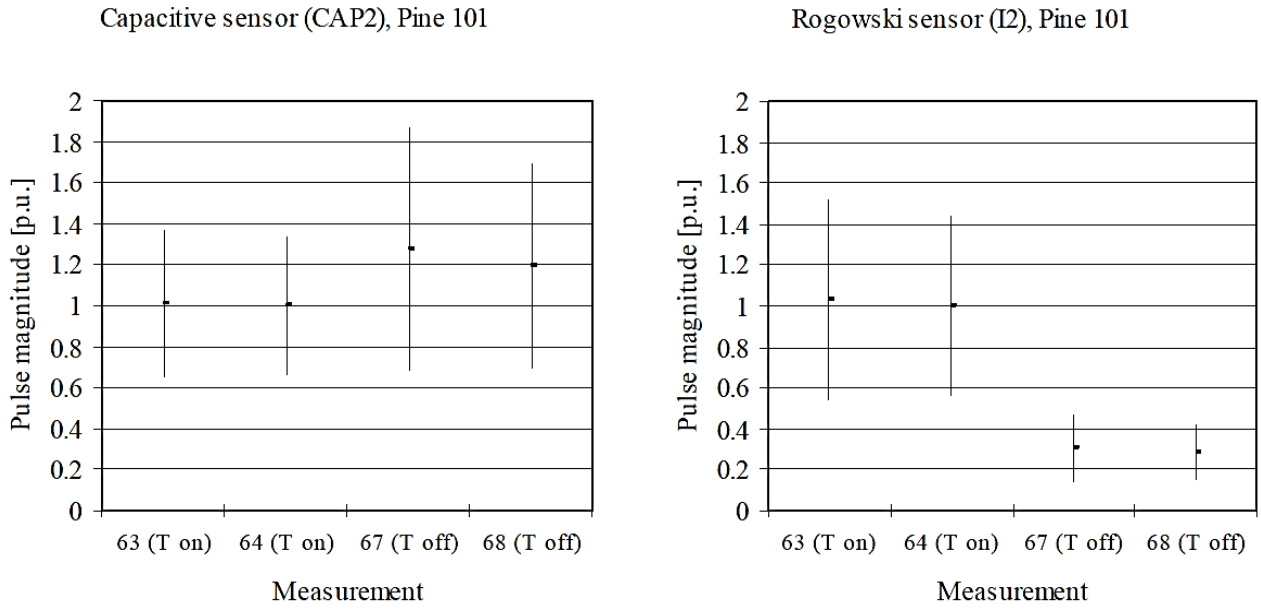

Figure 4.13 *Mean pulse magnitudes measured with a capacitive sensor (CAP2) and Rogowski sensor (I2), with the transformer connected (T on) and then disconnected (T off). PD pulses are represented per unit (p.u.), respect the mean value of last measurement before the disconnection of the transformer to the line (measurement number 64).*

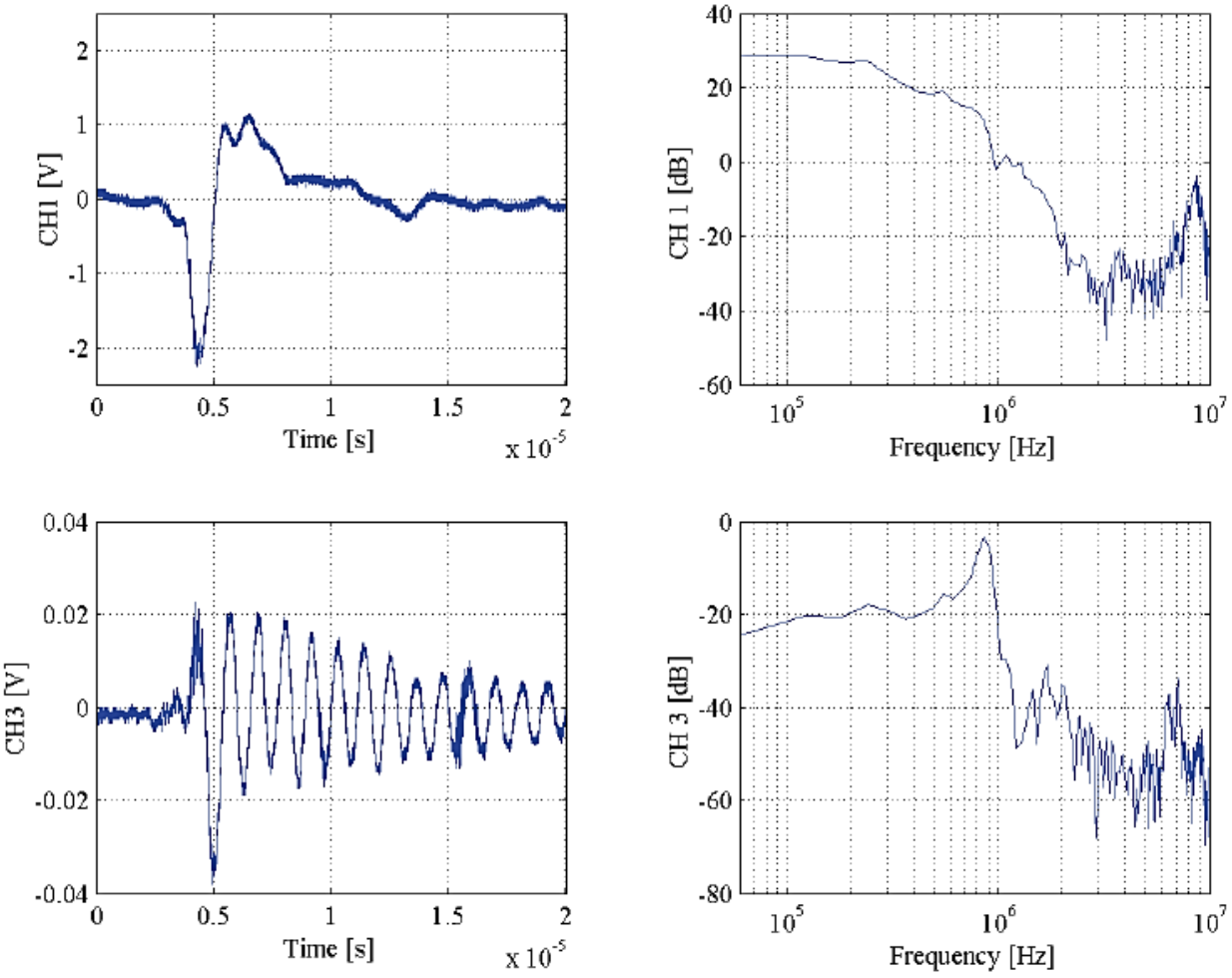

Figure 4.14 *PD waveforms and PSD from the capacitive (CH1) and inductive (CH3) sensors, with the transformer disconnected from the line.*

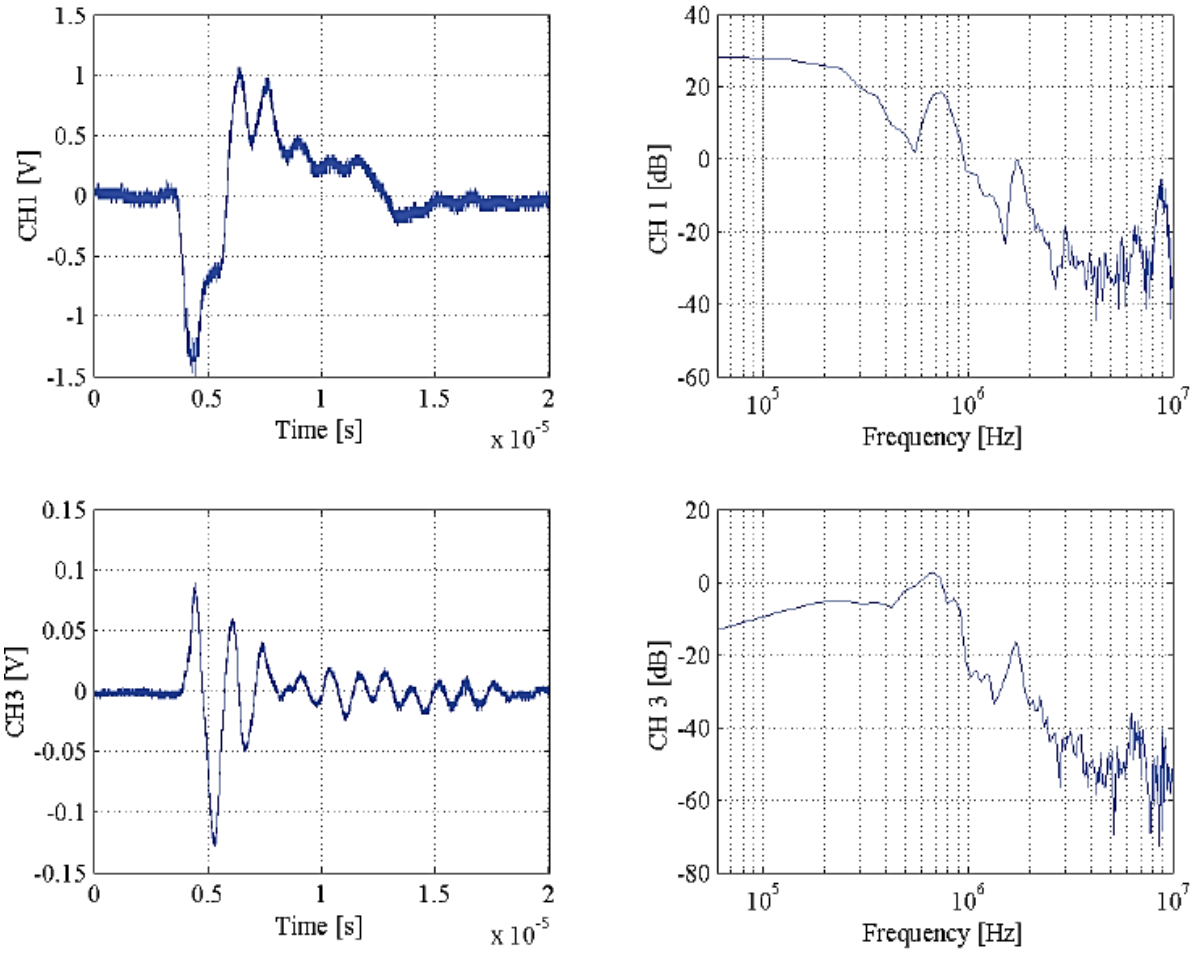

Figure 4.15 *PD waveforms and PSD from the capacitive (CH1) and inductive (CH3) sensors, with the transformer connected from the line.*

The transformer connection introduces additional oscillations in the waveform measured from the capacitive sensor, nevertheless the effect is small. The additional oscillations are exhibited however on the PSD at frequencies of about 700 kHz and slightly at less than 2 MHz. Moreover, the attenuation of the PSD seems to be steeper with increasing frequency when the transformer is connected. Otherwise the behaviour of the capacitive sensor, where the PD waveforms obtained from the inductive sensor are very oscillatory with the transformer disconnected from the line.

Chapter 5

Covered conductor lines modelling on EMTP

In this chapter the theoretical part is over, and the practical work is presented. The aim of this chapter is, in fact, to modelling the high voltage overhead covered conductor line by the use of an electromagnetic software, in which it will be possible to simulate the PD generation and to study their propagation along the line. The covered conductor line is model, as will be seen in this chapter, as a cable line but it will be put above the ground, like an overhead line, simulating a very large layer of air around the CC line. Then, the Rogowski coil is presented: it will be put at the ends of the line and this sensor will detect the PD pulses. Finally, the rest of the line is presented, with a particular attention to the discharge site.

5.1 EMTP-RV software

The software used in this work is EMTP, an Electromagnetic Transients Program: it is a computer program for the simulation of both electromagnetic and electromechanical control system transients on the multiphase electric power systems. EMTP-RV is the redesigned latest version: RV means Restructured Version. EMTP is a software used to study transients in electrical networks and in power systems: it is possible to perform simulations and analysis of transient in power system. The major advantages of EMTP-RV are the flexibility in modelling, with a wide variety of studies: in this simulation environment it is possible to create from small electrical circuit to a large network, with also the possibility to create subcircuit with unlimited levels. A library of simple devices is used to build specialized control functions. Besides to a large library of electrical and electronic devices, EMTP-RV can solve control systems, by the using of block-diagrams. Power circuits can be solved both using macro models and detailed nonlinear functions. Moreover, EMTP-RV can find steady-state solution and offers unique and advanced multiphase load-flow solution option.

Line or cable modelling is also included: the user specifies the geometry and material data. In this work, EMPT-RV is used to model a simple network, made by an overhead covered conductor line

in high voltage, 110 kV, putting the geometry and the material used in that kind of conductor. The aim is to simulate several partial discharges formations on the phases of this type of new conductor and the propagation of these pulses along the line as travelling wave. The PD phenomena are current pulses in high frequency, with a propagation velocity slightly lower to that of the light, with propagation time quite short. Then, with the Scope View tool, it is possible to see the waveform of the PD pulses, in this case, or in general the waveforms of any signals.

5.2 Line model

The EMTP-RV contains several models to represent CC overhead lines. The user, in modelling step, can select any of these models, such as lumped or distributed parameters, frequency independent or frequency-dependent models. In case of CC overhead line, the choice of the model depends on a number of factors, such as the length of the lines, the nature of the simulation and the fidelity of the results. The following three options are possible for CC overhead line models in the EMTP environment:

1. *Constant parameters model (CP)*: this model is also named Bergeron or Clark model. This distributed parameter model includes all the traveling wave phenomena; however, it represents the line resistances as a lumped element, making some problems, as will be seen late.
2. *PI-model*: nominal PI-equivalent model has lumped parameters; it is suitable for the short lines simulations.
3. *Frequency dependent model (FD)*: it is also called JMarti model. This is a frequency-dependent model and has constant transformation matrix suitable for simulating the traveling wave phenomena in long transmission lines.

For this work it was chosen the first model, the constant parameter model. Certainly, the frequency dependant model would have been more accurate, since the line impedance change as frequency changing, being more similar to the reality. The model proposed by J. Marti is adequate for long transmission line, but in this case, the work is based on relatively short covered conductor line (about 9 km), where the use of Clark model is sufficient.

In constant parameter model, the line impedance does not change with the frequency variation, assuming the cable parameters R, C, and L constant: they are calculated at the model frequency setting by the user. In this model L and C are considered distributed as in an ideal cable, while R

is considered lumped at three places (cable middle and cable ends). Finally, the shunt conductance G is assumed to be zero. An advantage of the CP model, respect to the FD model, although the latter is the most accurate, is the computationally speed: in fact, the constant parameter model is faster than the frequency dependant one, and this factor is to be consider when a lot of different simulations are to be executed. In order to be so speed, the line is assumed lossless in the first stage, the losses are included only in a second stage. The losses are in fact modelled separating the line in two separate lines, where the propagation time and the total line resistance is halved, as shown in Figure 5.1. with this configuration most of the transmission line are satisfied, but however some problems can be generated, as will see later. This method is acceptable if the R >> Z_c.

Figure 5.1 *Inclusion of losses in the distributed parameter line model.*

The generic version of this device is the "*CP m-phase*". The other versions in the library line are "*CP 3-phase*" (only for a 3-phase line) and CP double (double-circuit) transmission line.

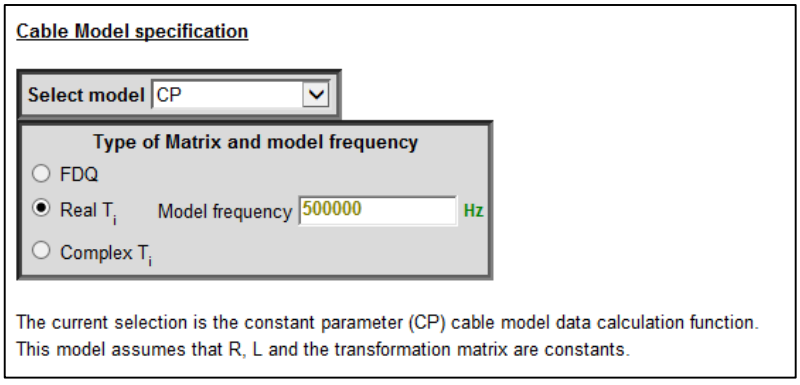

Figure 5.2 *Selection of cable model in the 3-phase line, with real transformation matrix at a specific frequency.*

As seen in Figure 5.2, the CP-line uses a constant real transformation matrix "*Real T_i*", that is a transformation matrix calculated at the given model frequency, chosen by the user, in this case 500 kHz.

5.3 Covered conductor line modelling

In EMPT-RV it is not possible to directly model a covered conductor line; EMTP-RV interface only supports overhead lines with bare conductors or underground cables. The covered conductor line is not a classical overhead line, due to its XLPE covering layer, as seen in the first chapter; however, it is not even a typical underground, since it has not an electrostatic sheath. The first problem met in covered conductor line modelling was in fact understanding which kind of line use.

Certainly, the only possibility is to represent the insulation layer around the metallic conductor was to use the cable representation. So, the first thing to do in built any line on EMTP-RV is to introduce the cable data in a tab. This data tab allows the user to insert manually the geometrical and electrical characteristics of the cable to represent. The user has to specify the geometrical dimension of the cable, for each layer, the electrical data of the conductor and the electrical proprieties of the insulation material. Moreover, there is a possibility to distinguish the cable type between single-core coaxial cable and pipe-type cable. In the single core the cables are coaxial, while in the pipe-type the coaxial cables are enclosed by a metallic pipe.

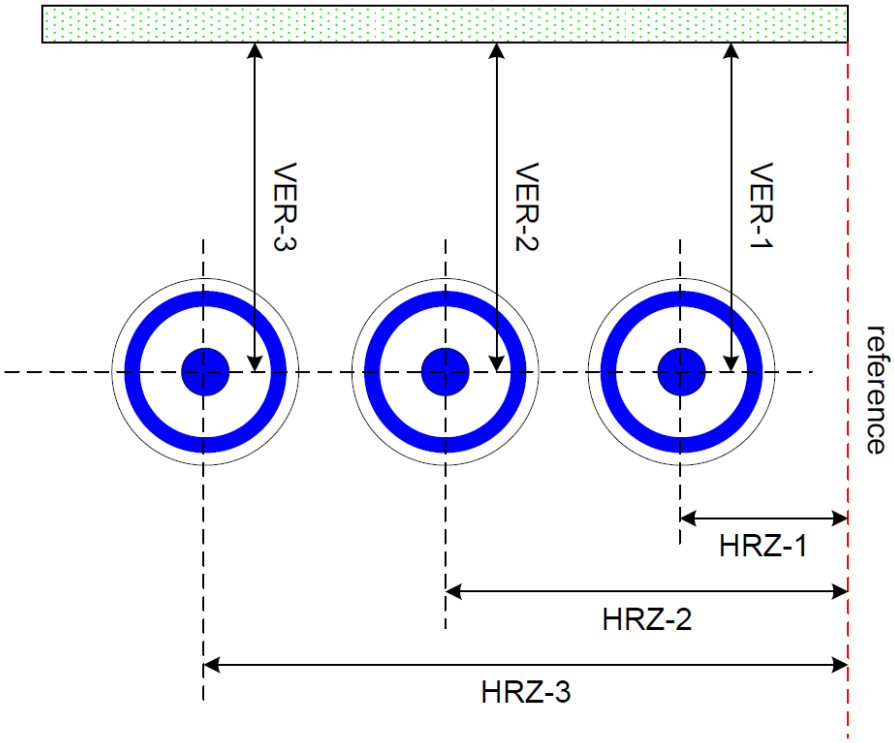

Figure 5.3 *Single-Core cable system.*

At the beginning, it was chosen to use the single-core coaxial cable, as in Figure 5.3, but with the possibility to remove the shield and put only an insulation XLPE layer around the metal conductor. The only problem is the assignment of the vertical height. The software accepts only positive value of the vertical height, but in default it considers the cable undergrounding, with no possibility to locate the cable in air, as an overhead line. Clearly, the results of the PD simulation would have been wrong, due to the different resistivity of the air and of the ground.

So it was decided to change the type of cable, choosing a pipe-type cable. Certainly the representation is not the best and the most accurate, but it is a good simplification in order to represent the overhead covered conductor line in EMTP-RV. The pipe-type permits to represent the three phases, with the conductor and its protecting layer, and also an air layer which encircles all the cables: all the cables are located inside a conductive pipe, as shown in Figure 5.4. To represent all of this, the dimension of the external tube is very large, so that the radius of curvature can be neglected. The model is not real, but it is a simplification, that respects the real characteristic of the covered conductor line.

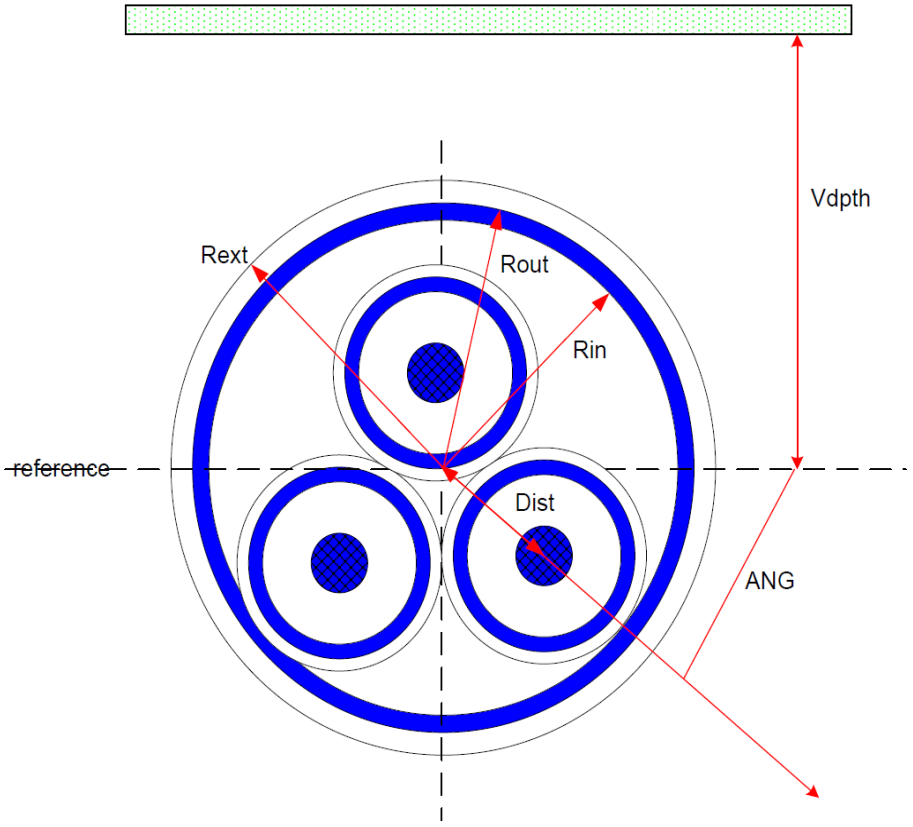

Figure 5.4 *Pipe-type cable*

The first step, after choosing the cable model, is to insert the value of the internal conductor cables, which represent the three phases of the system, both from geometrical point of view and

from electrical one. For the geometrical dimension, it needs to referenced to value of the Figure 5.5, which represent a generic cable with several layers: in this case the layer needed are two, that are the inner metal conductor and the insulation XLPE layer, removing other layers as the metallic shield.

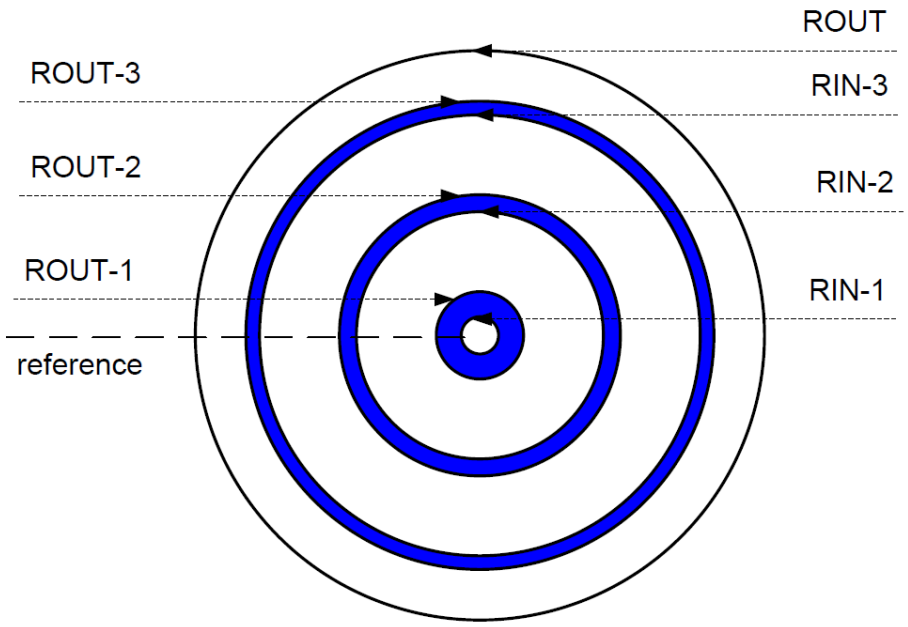

Figure 5.5 *A single coaxial cable with 3 conductors.*

In the following table, Table 5.1, the values used for modelling the internal cable conductors are presented.

Table 5.1 *Geometrical data of cable conductors.*

Cable number	***Number of conductors***	***Distance from center of pipe*** **(m)**	***Position angle*** **(deg)**	***Outer insulation radius*** **(m)**	***Inside radius R_{in}*** **(m)**	***Outside radius R_{out}*** **(m)**
1	1	11.2	0	0.0195	0	0.00525
2	1	13.19	6.9	0.0195	0	0.01125
3	1	14.14	6.4	0.0195	0	0.01125
4	1	15.08	6	0.0195	0	0.01125

In addition to the three cable phases, the other conductor to model is the ground wire, which is part of the covered conductor line system. The first cable of the Table 5.1, in fact, is the ground wire; the other three are the phase conductors. For each cable the number of conductors are one, in fact both the covered conductors and the ground wire have only one conductor, with no metal shield around. Putting the value 1, the metal shield is removed, and only two layers remain: the conductor and the insulation layer (XLPE for the covered conductor, and air for the ground wire). As said before, the dimension of the pipe is very large, unlikely with the reality. In this work, the radius pipe dimension is 30 meters, with the centre of the pipe put at 30 m above the level of the ground. For this reason, the cables have distance about 15 m from the centre of the pipe. The first cable (the ground wire) is 11 m distant from the centre of the pipe, it is the closest to the centre, and thus the most distant from the ground level. At the same way, the fourth cable is the phase closest to the ground, but the most distant from the centre of the pipe (15.8 m). In Figure 5.6 a representation with exact dimension of tower-top considered in this work is shown. Then, considered the ground wire as reference, looking at the Figure 5.6, the other phases are positioned different respect the centre of the pipe and the reference, which passes from the ground wire. The phases, in fact, have a little angle of displacement respect to the reference, about 6 degrees, calculated using simple trigonometrical formulas. The outer insulation radius is the radius of the whole covered conductor,

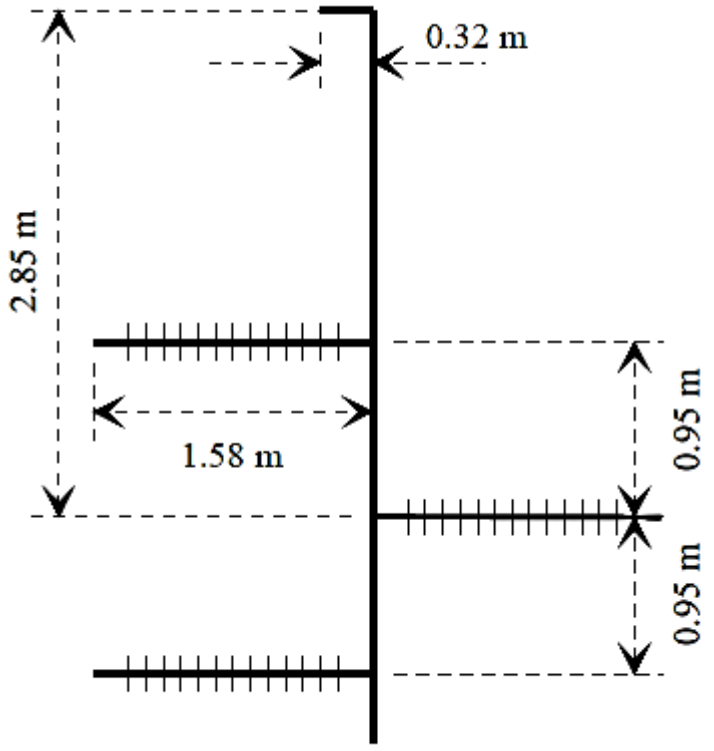

Figure 5.6 *Real dimensions of the tower-top of the Forest-SAX CC line, considered in this work.*

considering the conductor and the insulation, as seen in chapter §1.1; for the ground wire, it is considered an air layer with a radius of the same dimensions of the XLPE layer, in order to have the same outer dimension for all the cables. The metallic conductor is made by only one metal material: aluminium alloy for the covered conductor and steel for the ground wire. Thus, the inside radius R_{in} can be considered 0, and the outside radius R_{out} is the effective radius of the conductor.

The second step is to insert the electrical parameter of the line, both relative to the conductors and to the insulation layers. In the Table 5.2 the electrical values are shown.

Table 5.2 *Electrical data of cable conductors.*

Cable number	***Resistivity*** **ρ (Ω m)**	***Relative permeability*** **μ**	***Insulator relative permeability*** **μ_{in}**	***Insulator relative permittivity*** **ε_{in}**	***Insulator loss factor*** ***$LFTC_{in}$***	***Phase number KPH***
1	4e-7	100	1	1	1.e-6	0
2	4e-8	1	1	2.3	1.e-4	1
3	4e-8	1	1	2.3	1.e-4	2
4	4e-8	1	1	2.3	1.e-4	3

The resistivity for the steel conductor is considered $4 \cdot 10^{-7}$ and $4 \cdot 10^{-8}$ for the aluminium alloy. Instead, the relative permeability μ is considered 100 for the steel and 1 for the aluminium. For the insulation layers, both for the air and for the polymeric sheath the relative permeability is always 1. For the relative permittivity, instead, obviously is 1 for the air, while for the XLPE layer it is considered 2.3. The insulator loss factor for the material used is $1 \cdot 10^{-6}$ for the air and $1 \cdot 10^{-4}$ for the sheath. Finally, in the last column, the phases are numerated, assigning the three cables closest to the ground as system phases, while the highest wire as grounding wire, since the wires with KPH 0 are considered grounding.

The third step is to insert the data relative to the geometrical dimension of the pipe. As said before, the dimensions of the pipe are extremes, in order to model the covered conductor line as an overhead line. In the Table 5.3, the geometrical data of the pipe are reported (the parameters are referred to the Figure 5.4).

Table 5.3 *Geometrical data of pipe.*

Inside radius of pipe (Rin) **(m)**	***Outside radius of pipe (Rout)*** **(m)**	***Outside radius of tubular insulator (Rext)*** **(m)**	***Vertical distance of the pipe's center from the surface of the earth (Vdpth)*** **(m)**	***Phase number of the pipe (0 if grounded)***
30	32	32.05	100	0

As said before, the radius of the pipe is approximately of 30 meters, thus though the software sees the pipe underground at 100 m, the cables are put in an air environment, wide enough to consider them isolated from the ground and isolated only by the air.

The fourth step is to insert the electrical data of the pipe: this process is quite simple, since the pipe is considered made by air, with air insulation and finally surrounding by another layer of air. In Table 5.4 the electrical data of the pipe are shown.

Table 5.4 *Electrical data of pipe.*

Resistivity **ρ (Ω·m)**	100	***Insulation loss factor (LFCT-IN)***	$1 \cdot 10^{-5}$
Relative permeability of the pipe **μ**	1	***Relative permeability of the insulation surrounding the pipe*** μ_{out}	1
Relative permeability of the insulation inside the pipe μ_{in}	1	***Relative permettivity of the insulation surrounding the pipe*** ε_{out}	1
Relative permettivity of the insulation inside the pipe ε_{in}	1	***Loss factor of the insulation surrounding the pipe (LFCT-OUT)***	$1 \cdot 10^{-5}$

The last step is to insert the length of the line and choose the kind of model. As concern the model, as seen in the previous section, the constant parameters model has been chosen, and the various simulations are done changing the model frequency, in a range from 100 kHz and 2 MHz. As concern the length of the line, the covered conductor line considered is 9 km long, but the line is divided in litter pieces, each one 1 km long. The reason of this choice is due to the fact the CP model is used. The software, as seen in section §5.2 and shown in Figure 5.1, represents the line with a lumped resistance, one quarter in each end line, and half in the centre. With quite long line, as 9 km long, the lumped resistance is of great value, and in the simulation in which travelling waves are studied, it represents a line discontinuity, generating unwanted reflection on the line.

The best thing would be representing the line pieces as a span long (130 m), but for simplification, instead of represent about seventy line pieces, only nine pieces of line are represented.

Once all the covered conductor data are inserted, it is generated a file in which all this data are elaborated in order to compute the constant modal transformation matrix Q. The matrix contains complex values, but for the CP-model in the cable, the modal *R, L* and *C* parameters are determined from exact complex Q, using only the real part of Q. Z_c and the travelling time are determined for the lossless model. For each mode/phases, the kilometric resistance (Ω/km), the characteristic impedance Z_c (Ω) and the travel time (s) are calculated at a certain frequency. At the same time, for each mode/phase a real transformation matrix Q is calculated. These calculated data are uploaded in the cable line as a file, without the need to insert these data manually.

The covered conductor overhead line modelling is finish.

5.4 Rogowski coil modelling

The other important device to modelling in EMTP-RV environment for these simulation works is the Rogowski coil, the sensor used to measure the partial discharges pulses. Referring to the Figure 4.4 b) in the previous chapter, now the modelling of that equivalent circuit is done. The geometric data of the Rogowski coil, represented in Figure 5.7, are given in Table 5.5.

Table 5.5 *Geometry of the Rogowski coil.*

***Inner diameter d_1* (mm)**	162.4
***Outer diameter d_2* (mm)**	191
***Transducer diameter d_{rc}* (mm)**	14.3
***Length of the wire l_w* (m)**	25
***Radius of the wire r* (mm)**	1
***Length of the coil l_{rc}* (mm)**	600

For toroidal coils which have a circular cross-section, the lumped parameters are calculated as follows:

$$R_l = \rho_c \frac{l_w}{\pi r^2}; \tag{5.1}$$

$$L_l = \frac{\mu_0 N_{rc}^2 d_{rc}}{2\pi} log \frac{d_1}{d_2}; \tag{5.2}$$

$$C_l = \frac{4\pi^2 \varepsilon_0 (d_2+d_1)}{log\frac{(d_2+d_1)}{(d_2-d_1)}}; \tag{5.3}$$

where ρ_c is resistivity of the copper and ε_0 is permittivity of the air. To provide an appropriate damping, the value of the Z_{out} can be determined as:

$$Z_{out} = \frac{\pi}{2}\sqrt{\frac{L_l}{C_l}}. \tag{5.4}$$

The parameter data of the Rogowski coil are given in Table 5.6.

Table 5.6 *Parameter of the Rogowski coil.*

Resistance r_l **(Ω)**	0.11
Inductance L_l **(μH)**	0.6
Capacitance C_l **(pF)**	50.3
Terminating impedance Z_{out} **(kΩ)**	2

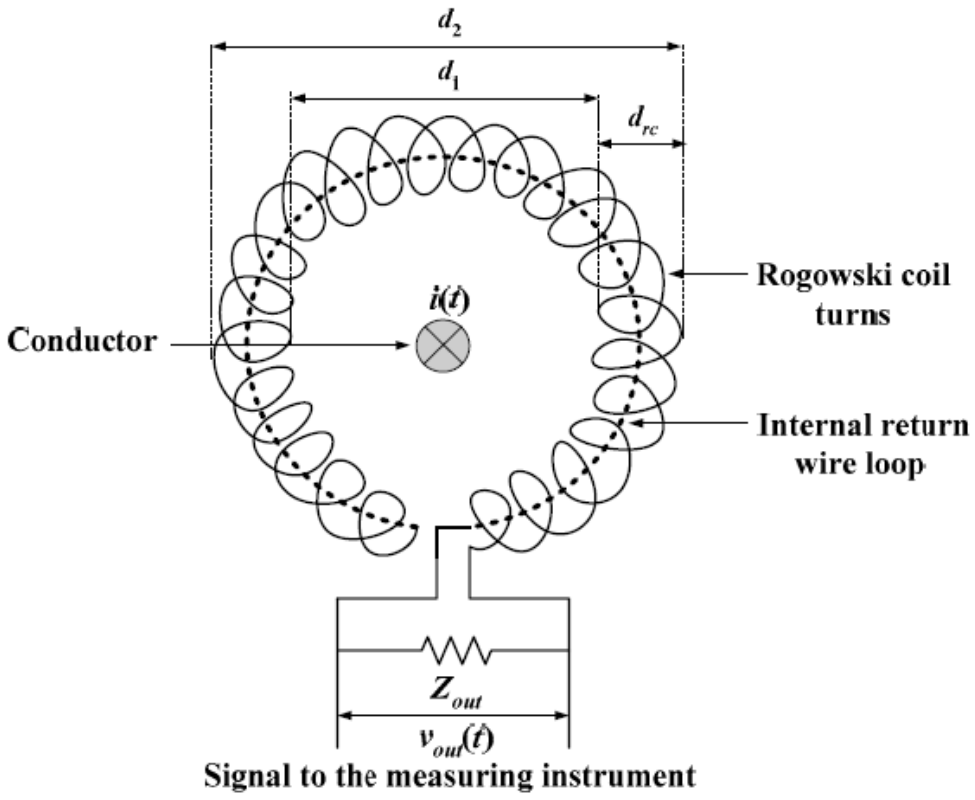

Figure 5.7 *Geometry and construction of the Rogowski coil.*

In the Figure 5.8, the Rogowski modelling in EMTP-RV environment is shown. The connection of the sensor with the phase line is in/out connection. In EMTP-RV simulations, the modelling of the Rogowski coil, in order to simulate the behaviour of an air-cored, is done with an ideal transformer, having a linear magnetizing characteristics. The ideal transformer is 110 kV/200 V, while the magnetization inductance is 10 μH. Then the electric components are insert as explained before, with their values. Respect to the usual representation, it was inserted an additional resistance, called R_b, in series with the line capacitance, as a dissipative element, in order to avoid the beat phenomenon. This phenomenon happens when a frequency resulting from the superposition of other periodic frequencies, as shown in Figure 5.9. The figure shows the waveform seen at the oscilloscope, if the R_b is absent. To justify the value of R_b, the Shannon theorem is used: the time constant τ, that is the product of this resistance R_b and of the capacitance C_l, must be equal to the simulation time step. Considering the time step of the simulations (Δt) of 100 ns, and the value of the capacitance C_l of 0.05 nF, the resistance R_b, put to avoid the beats, has

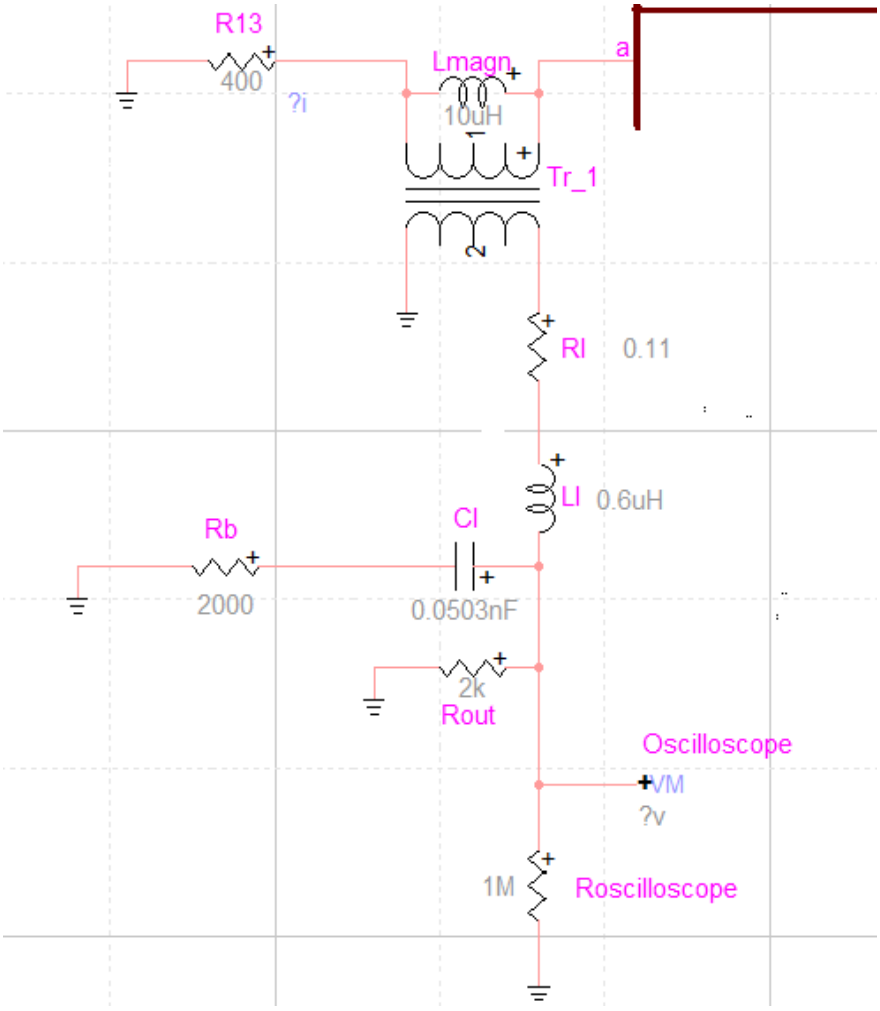

Figure 5.8 *Rogowski coil modelling in EMTP.*

to be 2000 Ω. Finally, between the voltage scope element and the ground, a great resistance (1 MΩ) is put in order to simulate the real resistance of the oscilloscope.

Depending on the kind of simulation, the sensor can be put on only one phase or on all three, or else only at the end of the covered conductor line, simulating the line-end measurement in a substation for example, or at both the extremes of the CC line.

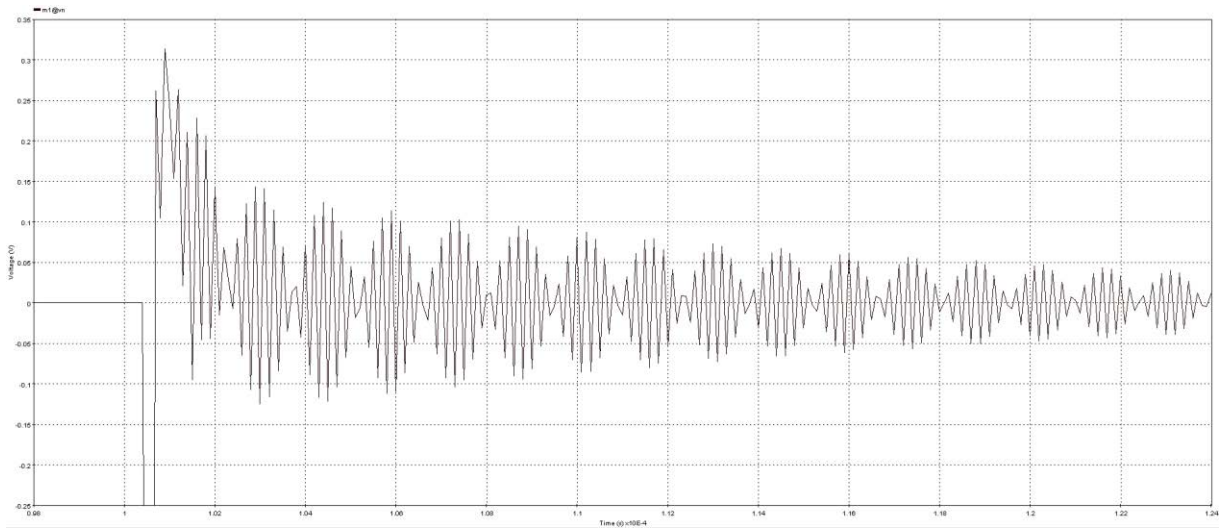

Figure 5.9 *Beat phenomenon if no resistance is put to damp the sensor response.*

5.5 Modelling of the rest of the line

Now the other elements of the network are presented: the voltage source, the line and the partial discharges generator. The source used to supply the line is a simple AC voltage generator, with an amplitude of 110 kV, frequency of 50 Hz and obviously with the phase displacement of 120°. Before and after the covered conductor line some resistances are inserted to simulate a bare overhead power line. Some resistance of 400 Ω are inserted in each phases, before and after the CC line; the value chosen for the resistance is the typical magnitude of a traditional high voltage overhead line with antenna connection. Finally, the partial discharges point of generation is presented. It is located almost at the centre of the line, 5 km distant from the generator and 4 km from the end of the CC line. It is formed by two capacitances, a resistance and an ideal switch. The capacitances are connected in series, their value is 1 nF: the first one, the closest to the line, represents the insulation layer of the covered conductor, the second one, the closest to the ground, represents the ground capacity C_0. In parallel to the second capacitance, there are the series of a switch and a resistance. The ideal switch is set to close after 0.1 ms after the start of the simulation,

in order to simulate an earth fault between a phase and the ground. The resistance is set to 100 kΩ, a typical value of the sum of the tree resistance and the earth tree resistant (R_{tx}+R_{te}), taken from Table 2.2 of the section §2.4.2. After the switch closing, the parallel between the capacitance and the great resistant simulates the formation of the partial discharges caused by a tree fallen on the covered conductor line.

Now, all the network design is done and in the next chapter the simulation of the PD generation, their propagation along the line and the results of their measurements by the Rogowski coil are presented.

Chapter 6

Partial discharges simulations on EMTP-RV

In this last chapter the results of the simulations are shown. Using the EMTP-RV software, the incipient tree fault on a 110 kV covered conductor line is simulated, and using the Rogowski coil it is possible to see the magnitudes of the partial discharges generated from a tree in contact with the insulated line. Besides, it is possible to see them as travelling waves and, looking at the time of arriving of the pulses, verifying with the lattice diagram the distance at which the discharges take place along the line. The simulations that are presented are:

1. An incipient earth fault in the phase A, with the Rogowski coil connected in all three phases, in order to see the magnitude of the discharges pulses in the different phases, both that subject to the discharge and those adjacent;
2. An incipient earth fault in the phase A, but with the PD sensor put only in the phase subject to the discharge (phase A), in this case in both the line end, in order to verify the time taken by the travelling waves to travel along the line after various reflection in the discontinuity points;
3. Two incipient earth faults in the phases A and B, without contact between them. The configuration and the aim is the same of that in 1;
4. An incipient short circuit fault between the phases A and B. As in the first point, the Rogowski coil is put in all three phases in order to see the differences between them in pulses magnitudes.

Some of these cases are repeat varying the frequency of the model, from 100 kHz to 2 MHz. With the frequency variation, the magnitudes and the waveforms of the pulses will change, but the time of arrival of the pulses at the sensors will be the same.

Finally, some of these cases are repeat varying the neutral management. Varying the grounding of the neutral conductor, it is possible to see if the previous cases change depending on the management of the neutral.

6.1 Incipient earth fault in the phase A, with the PD sensor in A, B e C

As seen in the previous chapter (§5.5), the arrangement is with a simple AC voltage source, set to 110 kV and put in the beginner of the line, a covered conductor line 9 km long, made by nine pieces of shorter line and with the discharge generation point located approximately in the middle of the CC line. In this case, a tree falling on the line and the incipient fault involving only a phase is simulated (case 1. in the section §2.6); for simplicity, the phase involved is the phase A, the closest to the ground. The sensors are located at the line end and in this simulation they are put in every phase, in order to see the differences in magnitude in each phase, both that involved by the discharges and in those not involved.

In every simulation, the "Simulation time" t_{max} is 32 ms, while the "Main time-step" Δt is 0.1 μs. Inside the network, some oscilloscopes are insert in order to verify the magnitudes and the waveforms expected. The first waveform shown in Figure 6.1 is the voltage waveform of the high voltage generator, in the phase A. All the following plot in this chapter are done used the tool MPLOT, a Matlab tool used in EMTP-RV to plot the waveform of the scopes put in the network.

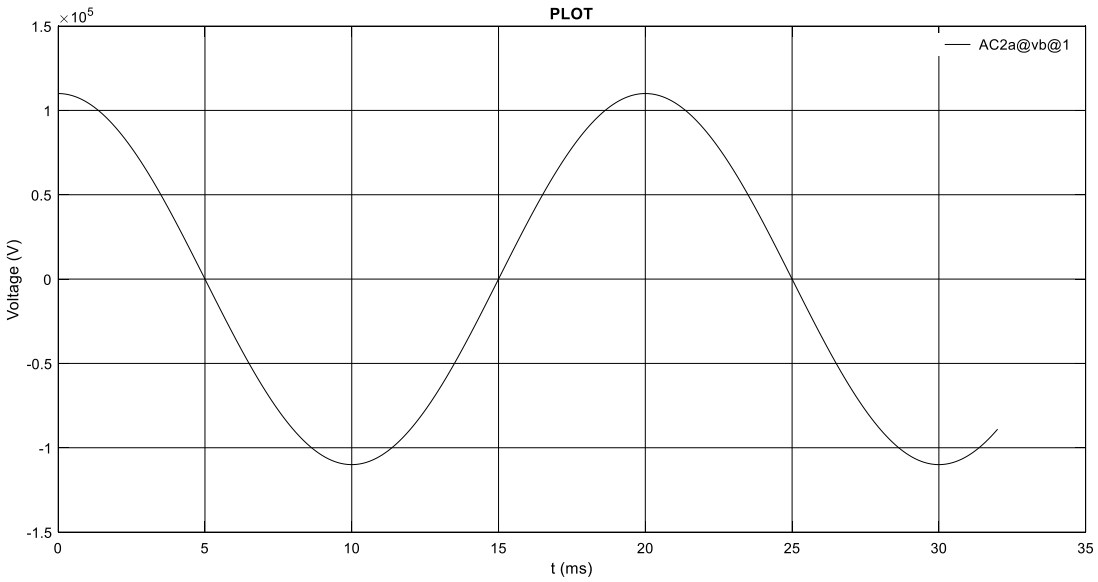

Figure 6.1 *Voltage waveform in 110 kV AC source.*

In the following figures (Figure 6.2, 6.3 and 6.4) it is possible to see the partial discharge pulses which arrive at the sensor at the line end. The Rogowski coil, as explained in the previous chapter (§5.4), has the aim to delete the frequency voltage (or current) and to show only the pulses present in the signal. Considering the first instants after the discharges (from 0.1 to 0.2 ms), the first pulses

can be seen; besides, the magnitudes of the discharges and the time taken to travel along the line can be calculated looking at the plot. The tool used in EMPT-RV to plot the voltage and the current is “Scope View”, and using a cursor setting on the graph, it is possible to measure with precision the point coordinate. In this way, the magnitudes of the pulses are estimated; in this work, the voltage magnitude of the PD pulses are considered as voltage peak-to-peak. Besides, in addition to the pulse magnitude, using the cursor, the time of arriving of the pulses can be estimated, in order to verify the lattice diagram or to calculate the discharge distance when the fault point is unknown.

In the Table 6.1 are summarized the value of the first five pulses in each phases, in order to compare their magnitudes.

Table 6.1. *PD magnitudes (mV) in the three phases.*

Phases	***1st pulse* (mV)**	***2nd pulse* (mV)**	***3rd pulse* (mV)**	***4th pulse* (mV)**	***5th pulse* (mV)**
Phase A	539	11	201	10	33
Phase B	384	5	174	14	20
Phase C	202	3	176	36	24

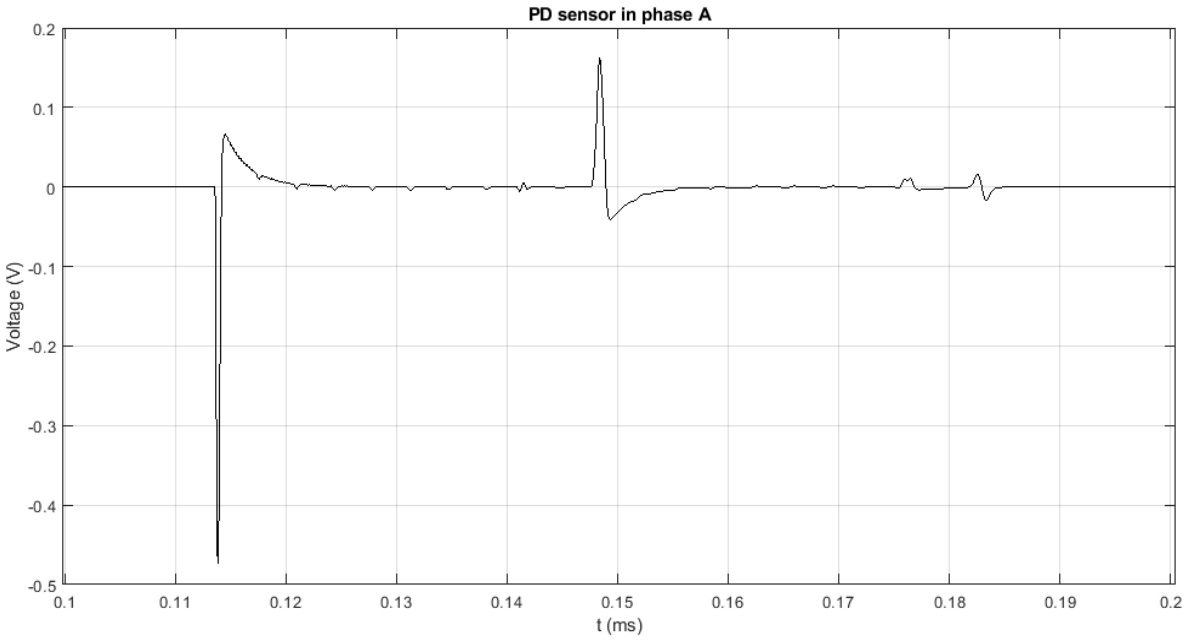

Figure 6.2 *PD pulses in phase A. Sensor at the line-end and the discharge is occurred in the same phase.*

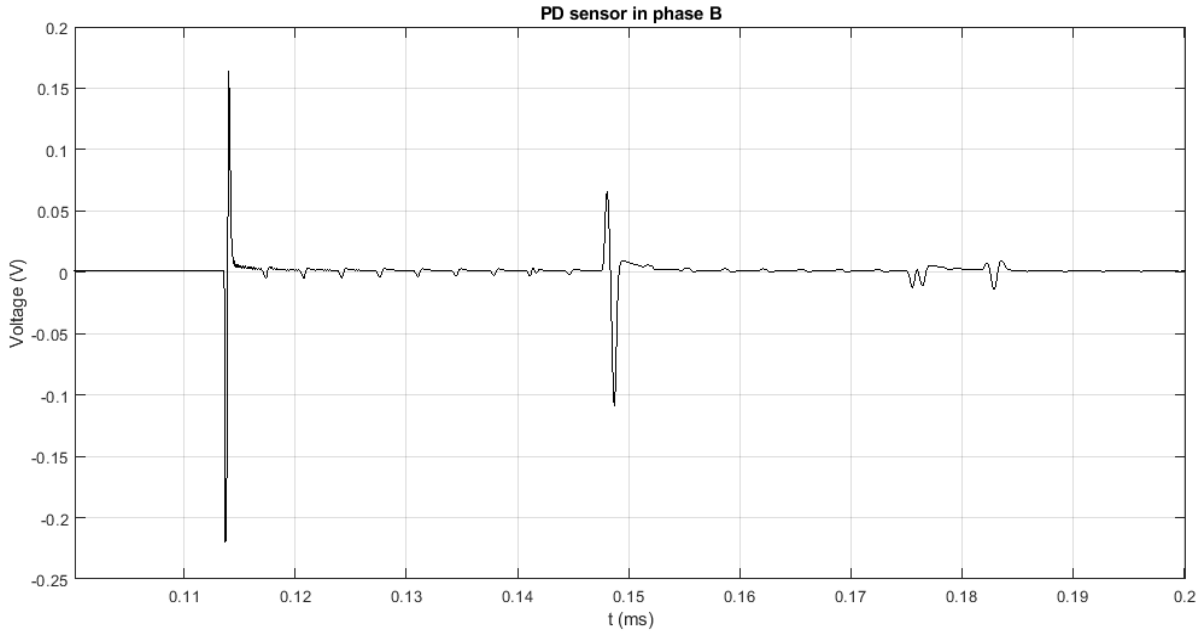

Figure 6.3 *PD pulses in phase B. Sensor at the line-end and the discharge is occurred in the close phase.*

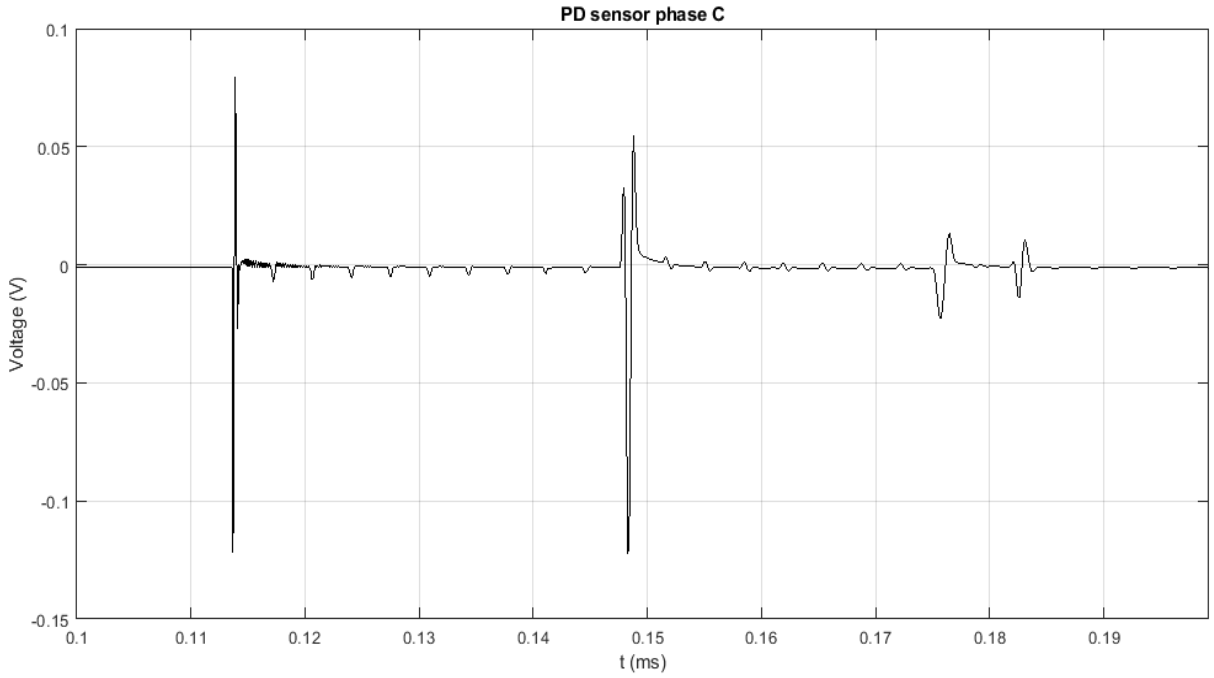

Figure 6.3 *PD pulses in phase C. Sensor at the line-end and the discharge is occurred in another phase.*

As expected, the phase A, in which the discharge occurs, presents the largest magnitudes of the pulses. As concern the direct pulses, obviously the largest pulse is that of the phase A, and the smallest is that of phase C, which is the most distant from the discharge. For the other pulses (the

second, the third, the fourth and the following) this correlation cannot be preserve. May happen that pulses in the sane phases can be larger than in the fault phase, as in the fourth pulses, where the phase C is also larger than in phase B, cause the different behaviour of the pulses after a reflection on the line. Moreover, in the sane phases, the polarity of the pulses is the same of that in the phase A, with a first negative polarity and then a positive one. The second pulses, instead, have the opposite polarity respect the direct pulse. Between the main pulses, there are 9 smaller pulses. They are a consequence of the CP model used to modelling the line. As explained in the previous chapter (§5.3), the line is made by 9 pieces, in which the losses are model with lumped resistance. These resistances are little points of discontinuity for the signals, thus in the plot it is possible to see them as very little pulses.

From this simulation, the use of only one sensor in order to detect PD pulses in the phases is verified: in fact, if the fault happens in only a phase, in the other phases is possible to see the pulses thanks to the couple between them. Only one sensor is sufficient to understand the distant at which the fault happens, and with a visual inspection clear up the damage. This can reduce the cost of the monitoring system and the disturbance to the power supply.

6.2 Incipient earth fault in the phase A, with the PD sensor in A at the both line ends

In this second simulation, the setup of the network changes a bit: the Rogowski coil is inserted only in the phase A, but in this case in both the line ends. The aim of this simulation is to verify the lattice diagram and therefore the time of arrive of the PD pulses at the sensors. In Figure 6.4 a representation of lattice diagram of the CC line is shown: the discharge starts in the middle of the line and a pair of waves travel in opposite direction. After the reflection, they change direction and so on. Using this graph, it is possible to calculate the expected time at which the pulse arrives at the sensor. The three number used in the graph, as in the chapter 3, are the number of times in which a pulse is reflected in one of the three discontinuity points (the start, the sensor and the end of the line).

In the Table 6.2 the time in which the pulses arrive in the sensors are calculated and summed.

Table 6.2 *The arrival time of the reflected pulses at the sensor.*

Line of 4 km		***Line of 5 km***	
Pulses	***Time of arrive* (μs)**	***Pulses***	***Time of arrive* (μs)**
000	13.6	000	17
110	40.8	100	44.2
001	47.6	011	51
220	68	210	71.4
101	74.8	101	78.2

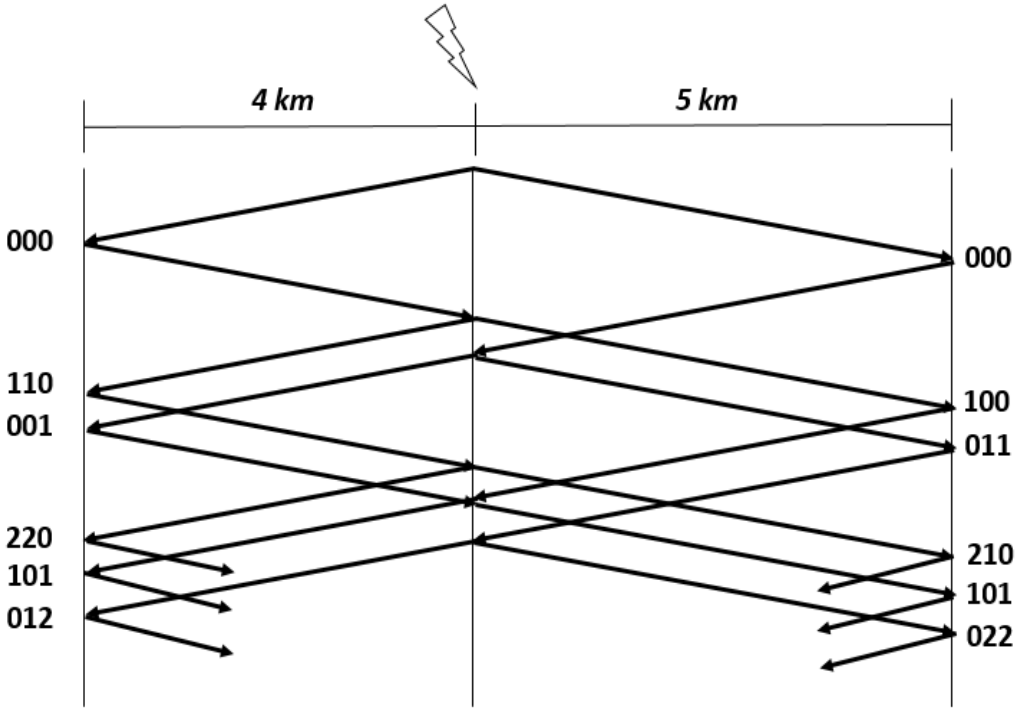

Figure 6.4 *Lattice diagram of the partial discharges along the line studied.*

The velocity of the pulses on the line is calculated on the base of the first pulse arrival time. Looking at the scope of the sensor, considering the first pulse (the direct, 000), it is possible to know the time in which the pulse arrives at the sensor, using the tracking cursor mode on the viewer, which shows the exact coordinates on the time-axis. In the left sensor, which is 4 km distant from the discharge location, the first pulse arrives 13.6 μs after the generation of the pulse; therefore, the pulse travels at a velocity of 294118 kilometres per second. Using this value for the pulse velocity and knowing the length of the line in which the pulses travel, the Table 6.2 was completed referring to the lattice diagram in Figure 6.4.

Now the interest thing is to verify if the time of arrive calculated in the table correspond to the time that is possible to see manually in the scope. In the Figure 6.5 a zoom on the pulses is done, in order to appreciate better the peak pulses. The plot is relative to a sensor put at the end of the line, on the phase A, the same in which the discharge happens. The usual peaks due to the nine pieces of line are always present, but other pulses with different form can be distinguish. These peaks, in fact, are the pulses that arrive at the sensor after the reflection in the discontinuity point of the line. In the Figure 6.6, instead, the plot of the PD pulses presented in the sensor put at the beginning of the line, near at the AC source, 5 km distant from the discharges point is shown. In both the plots, arrows are positioned in correspondence of the PD beginning of the pulses.

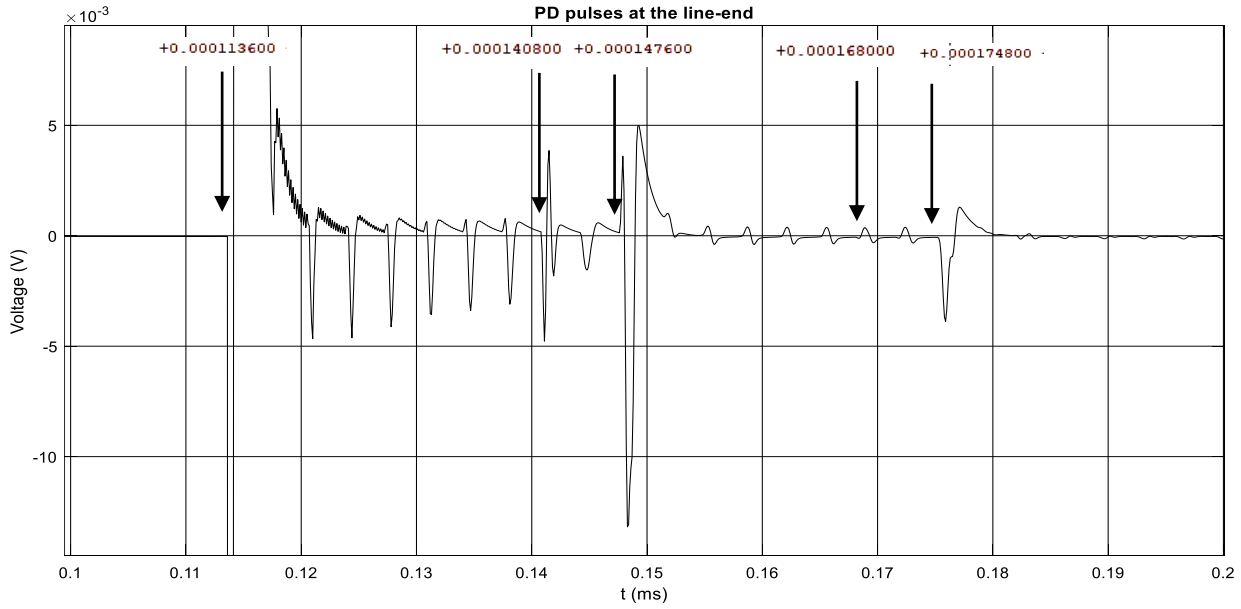

Figure 6.5 *Arrival time (μs) of the PD pulses at the sensor in the end of the line.*

In both cases, the fourth pulses, which have experienced twice reflections in one of the line end, are very attenuated. With this zoom it is impossible to detect, but with further enlargement they get visible. Unfortunately, they are too small to be detectable by trigger level of the measurement system, for this reason, the first 3 pulses are used to calculate the distance at which the incipient tree fault takes place. With the combination of two PD sensors, as in this case, the information can be elaborated together, in order to locate the discharges location. However, with the use of two PD sensor at the extremes of the line, a GPS system is needed to synchronize perfectly the signal data. The solution with two PD sensors is the favourite in order to localize the fault with accuracy, without knowing the exact value of the PD pulses velocity; however, as seen in the previous

chapters (§ 4.5), a solution with only one sensor at the end of the line is sufficient if the line length and the pulses velocity are known.

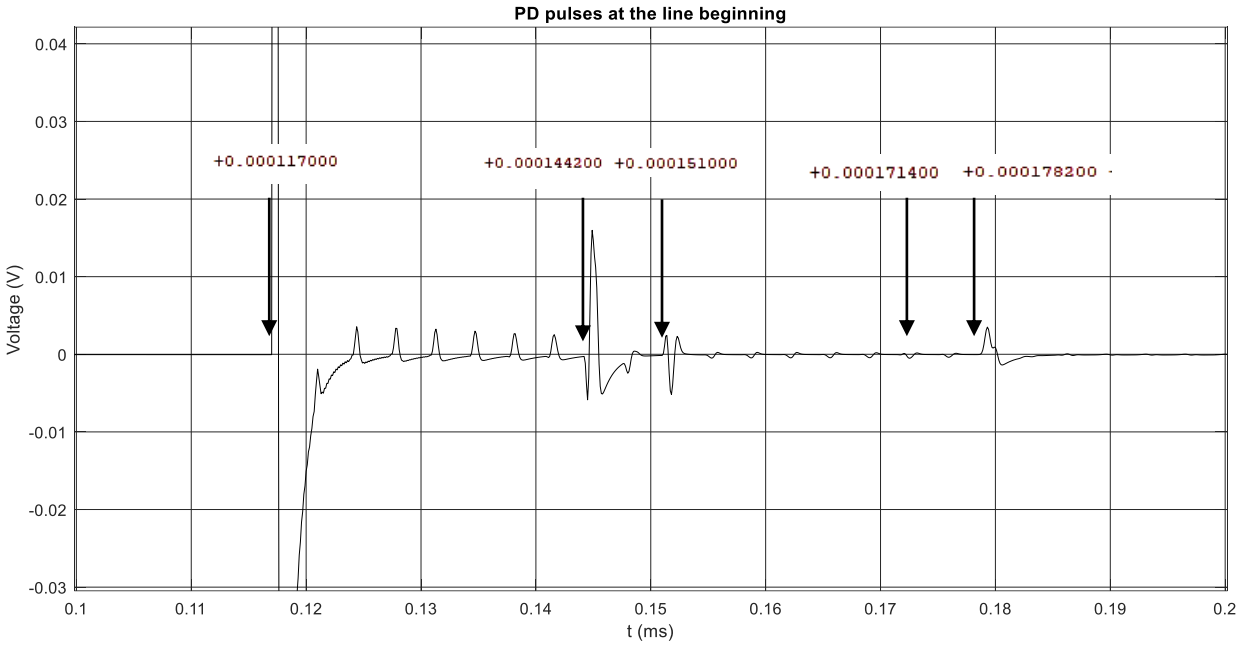

Figure 6.6 *Arrival time (μs) of the PD pulses at the sensor in the beginning of the line.*

6.3 Incipient earth fault in the phases A and B, with the PD sensor in A, B e C

In this simulation the setup of the line is very similar to that in the first simulation. The only difference is that the partial discharges take place in two phases, phase A and B. Considering the case 2) of the section §2.6, the configuration is relative to an incipient earth fault in two phases, without any contact between them. This case simulates the falling of a tree on the CC line, involving two adjacent phases, without any contact between them.

In Figure 6.7, 6.8 and 6.9 are shown the plots of the PD pulses on the three sensors, each one put in the three phases. The aim of this simulation is to make a comparison with the first simulation in which the discharge happens in only one phase.

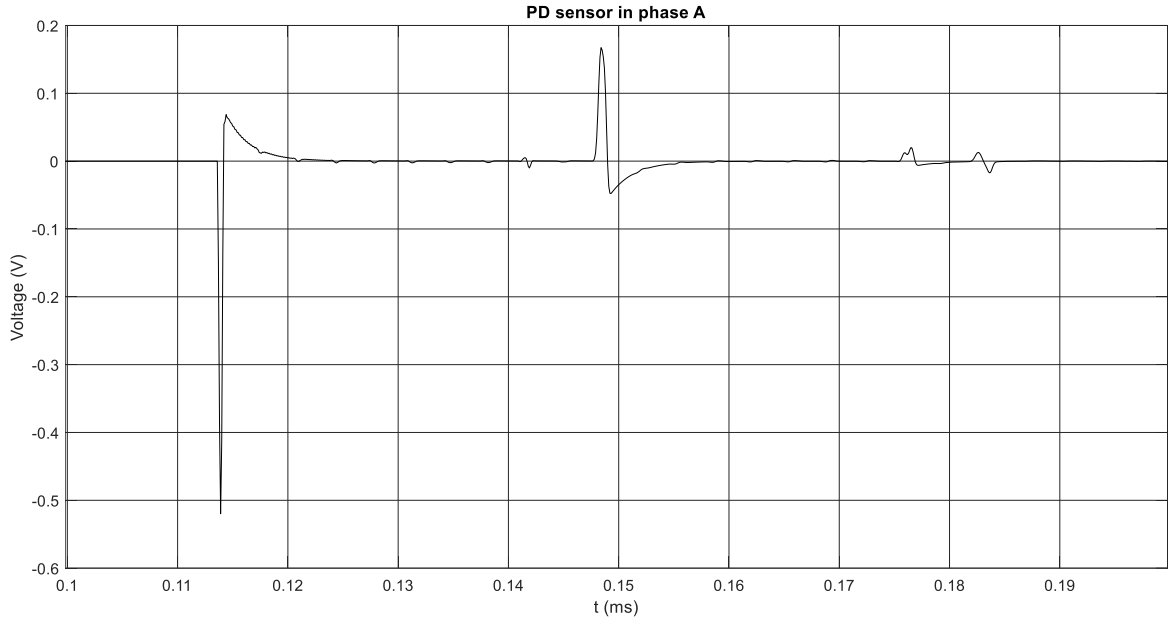

Figure 6.7 *PD pulses in phase A. Sensor at the line-end and the discharge is occurred in the same phase.*

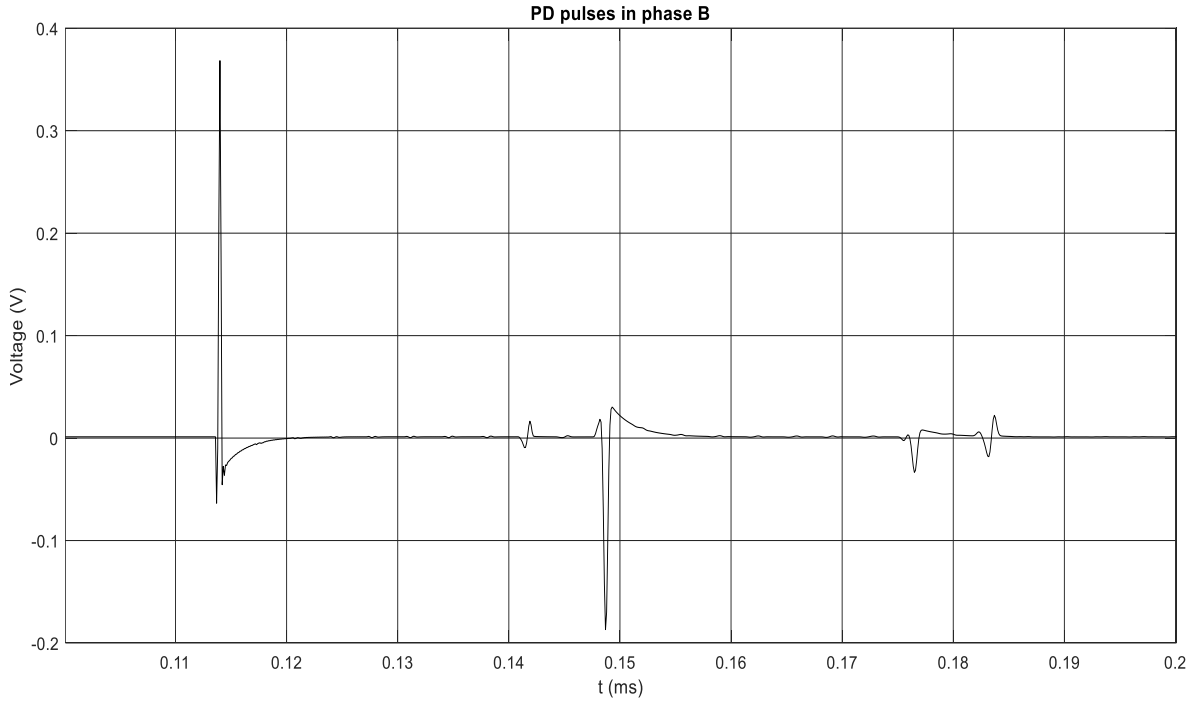

Figure 6.8 *PD pulses in phase B. Sensor at the line-end and the discharge is occurred in the same phase.*

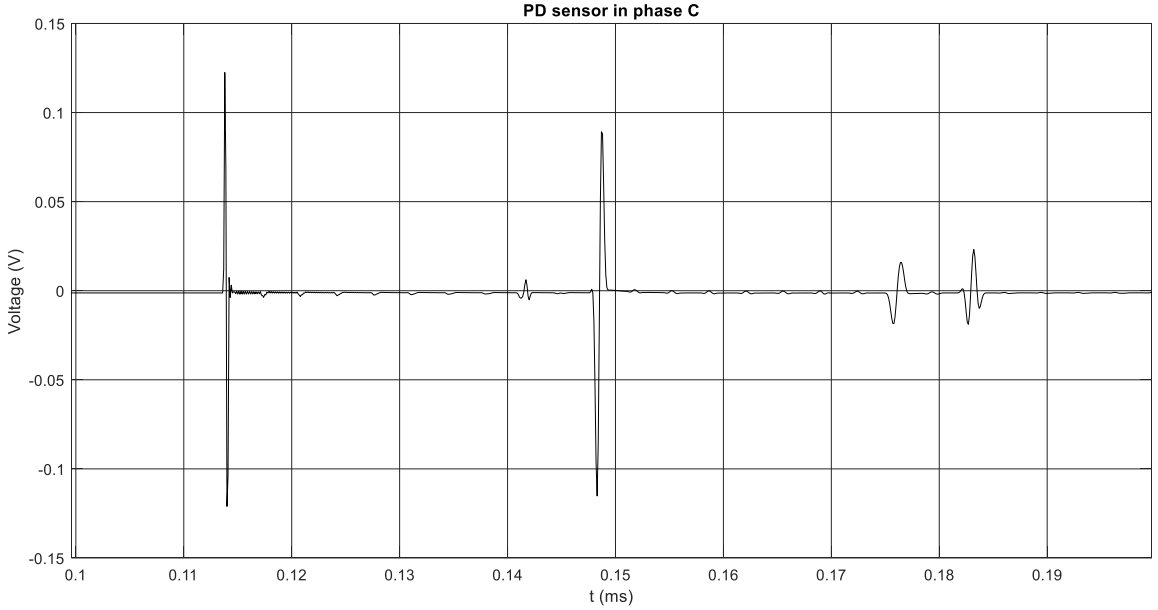

Figure 6.9 *PD pulses in phase C. Sensor at the line-end and the discharge is occurred in the adjacent phases.*

The sum of the pulse magnitudes in the three sensors are presented in the Table 6.3. Besides, in Table 6.3, a comparison between the values of the first case (PD in only phase A) and this third case (PD in two different phases) is presented.

Table 6.3 *Comparison between the PD pulses in the different cases (ITF in one and in two phases).*

Phase	***1st pulse* (mV)**		***2nd pulse* (mV)**		***3rd pulse* (mV)**		***4th pulse* (mV)**		***5th pulse* (mV)**	
Phase A	539	589	11	15	201	215	10	25	33	30
Phase B	384	432	5	26	174	217	14	41	20	40
Phase C	202	244	3	11	176	204	36	34	24	42

As expected, in this case, with two incipient tree faults in two different phases, the magnitude of the PD pulses that are measured in the sensors are larger, respect to the case in which the discharge happens in only one phase. In fact, in this simulation, it can be possible to distinguish the second pulse, which in the first simulation, it has not been clearly visible with a visual inspection. The conclusion of the first simulation, that is the possibility to use only one PD sensor on one of the three phases, remains valid also for this simulation since nothing change, except the magnitude of the sensor due to the two discharges in the adjacent phases.

6.4 Incipient short-circuit fault between the phases A and B, with the PD sensor in phases A, B and C

In this fourth simulation, an incipient short-circuit fault between the phases A and B is simulated, as in point 3) of the section §2.6. A tree falls on the covered conductor line, involving two phases which come in contact with each other, making an incipient short circuit fault. On the line modelling setup, the only change is the insertion of an ideal switch between the two partial discharge points. The switch is connected on a side with the phase A and on the other with the phase B. This is initially open and after 0.1 ms closes, synchronously with the other two switches, which simulate the earth fault on the phases A and B separately.

In the Figure 6.10, 6.11 and 6.12 are shown the plots of the PD pulses on the three sensors, each one put in the three phases. The aim of this simulation is to make a comparison with the last simulation, in which the discharges happen in phases A and B separately, making two different incipient earth faults, and this in which the discharge happens with the phases in contact each other, making an incipient short circuit fault.

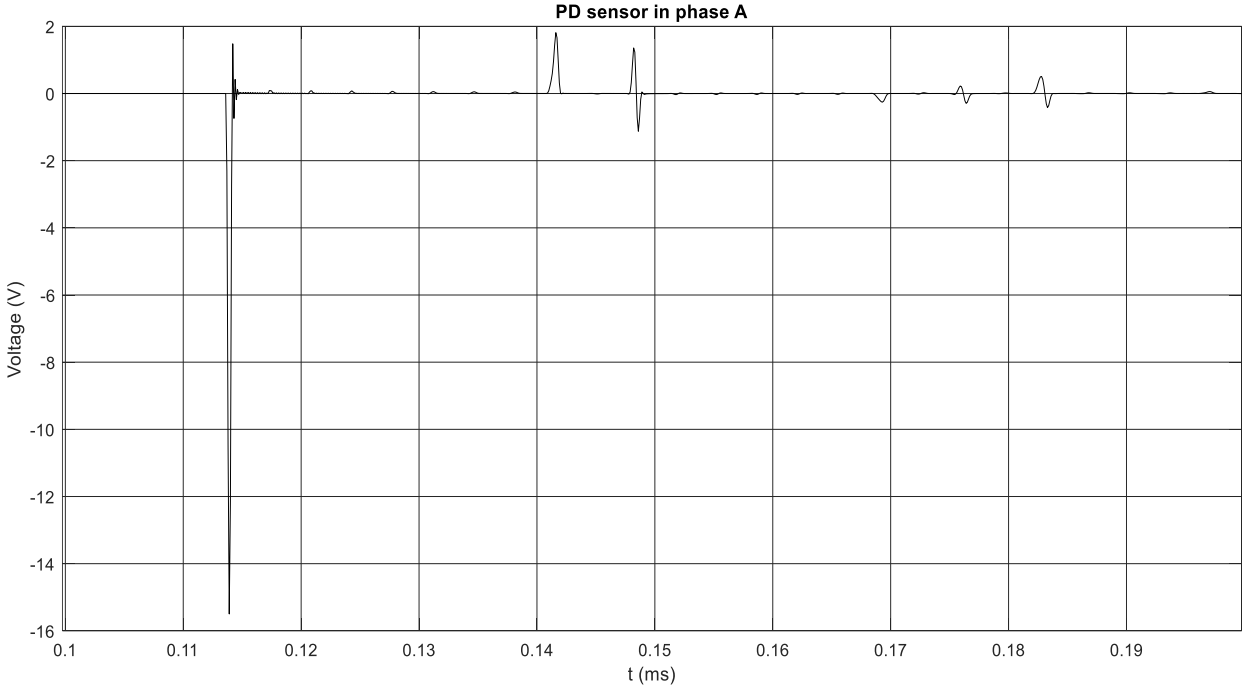

Figure 6.10 *PD pulses in phase A. Short circuit discharge happened in this phase.*

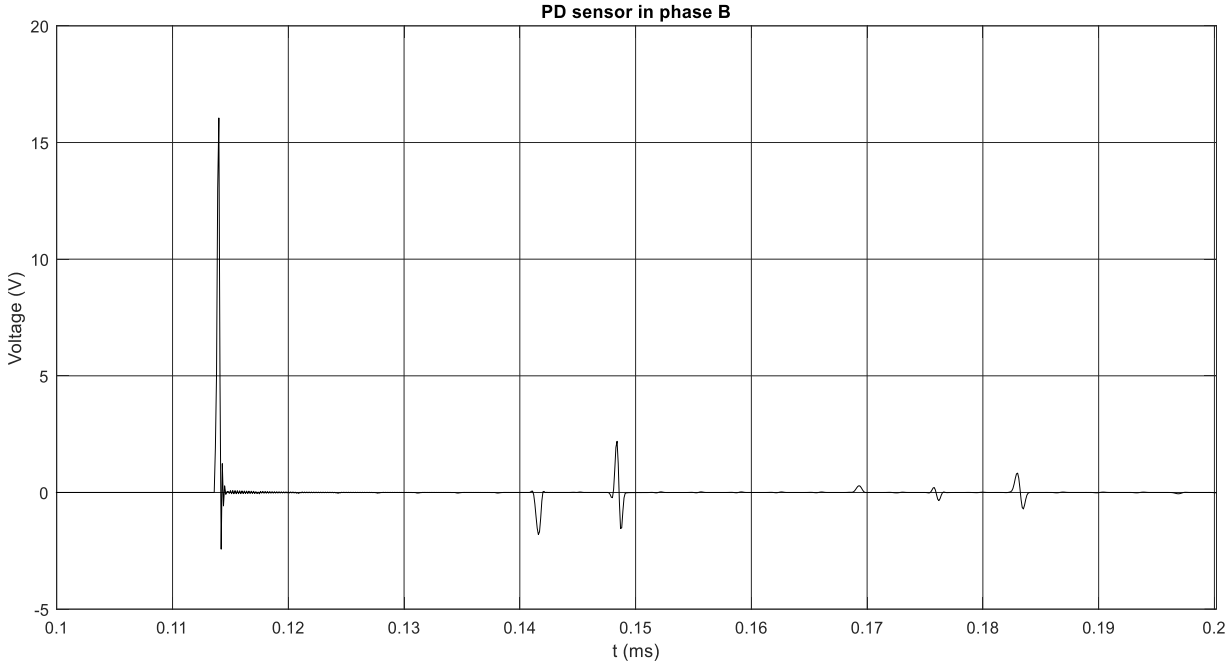

Figure 6.11 *PD pulses in phase B. Short circuit discharge happened in this phase.*

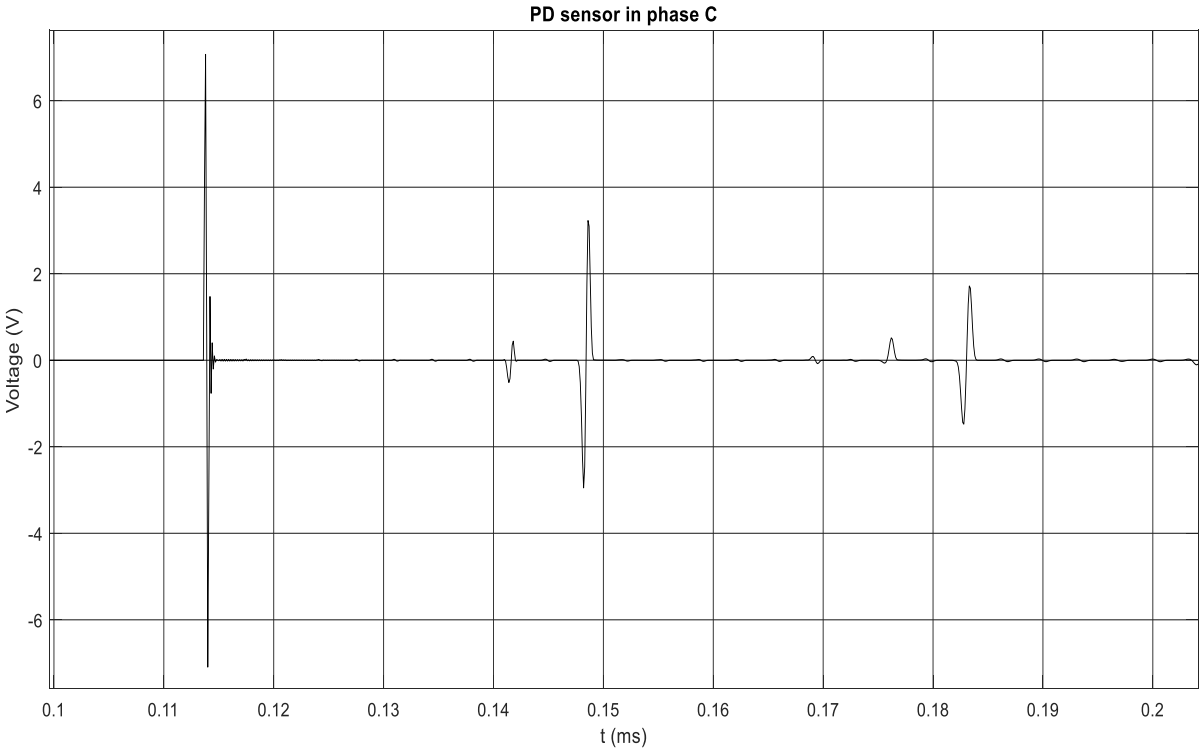

Figure 6.12 *PD pulses in phase C. Short circuit discharge happened in different phases.*

As in the Table 6.3, in the Table 6.4 the sum of the pulse magnitudes in the three sensors is presented. Besides, a comparison between the values of the last case (earth fault in phases A and B) and this fourth case (short circuit fault in the phases A and B) is presented.

Table 6.4 *Comparison between the PD pulses in two different cases (earth fault and short circuit fault in the same phases).*

Phase	***1st pulse* (V)**		***2nd pulse* (V)**		***3rd pulse* (V)**		***4th pulse* (V)**		***5th pulse* (V)**		***6th pulse* (V)**	
Phase A	0.589	16.98	0.15	1.81	0.215	2.48	Low	0.25	0.25	0.52	0.30	0.92
Phase B	0.432	18.48	0.26	1.80	0.217	3.73	Low	0.29	0.41	0.55	0.40	1.53
Phase C	0.244	14.16	0.11	0.96	0.204	6.18	Low	0.09	0.34	0.52	0.42	3.20

As seen from the results in the table, in this case, with a short-circuit between two phases, the orders of magnitude change for the first three pulses. Even for the first pulse, the order of magnitude is increased of two orders of magnitude. Therefore, the incipient short-circuit tree fault has magnitude larger than the incipient earth fault, even if this happens in two phases. This distinction between the two cases (earth fault and short-circuit fault) is useful to recognize if in the incipient tree fault two phases are get in contact with each other. However, if the line is monitored with the automatically sensors and the fault is detected immediately, the damage could be cleaned before the outage of the line with an interruption of the power supply, thanks to the insulation layers of the covered conductors, which permit the contact between the phases without the formation of an electrical arc and the opening of the line protections. In high voltage, however, as in this case, the duration of the withstand of a short-circuit between the phases is not long, it is about two hours before the outage of the line. In any case, these large pulses are an obvious sign of an incipient tree fault along the line.

6.5 Frequency variation of the line model

In the next simulations, the frequency of the line model is changed in order to see the differences in frequency variation. The partial discharges can happen in a large range of frequency: these simulations are done with a variation of the model frequency, in order to simulate the various possibilities. All the previous simulations are done at 500 kHz, while the next will be at 100 kHz, 1 MHz and 2 MHz. To change the frequency of the simulation, the frequency model in the cable data has to be change manually in each simulation.

In the Figure 6.13, 6.14, 6.15 and 6.16 the PD pulses, caused by an incipient earth fault in the phase A, are represent varying the model frequency, 100 kHz, 500 kHz, 1 MHz and 2 MHz respectively.

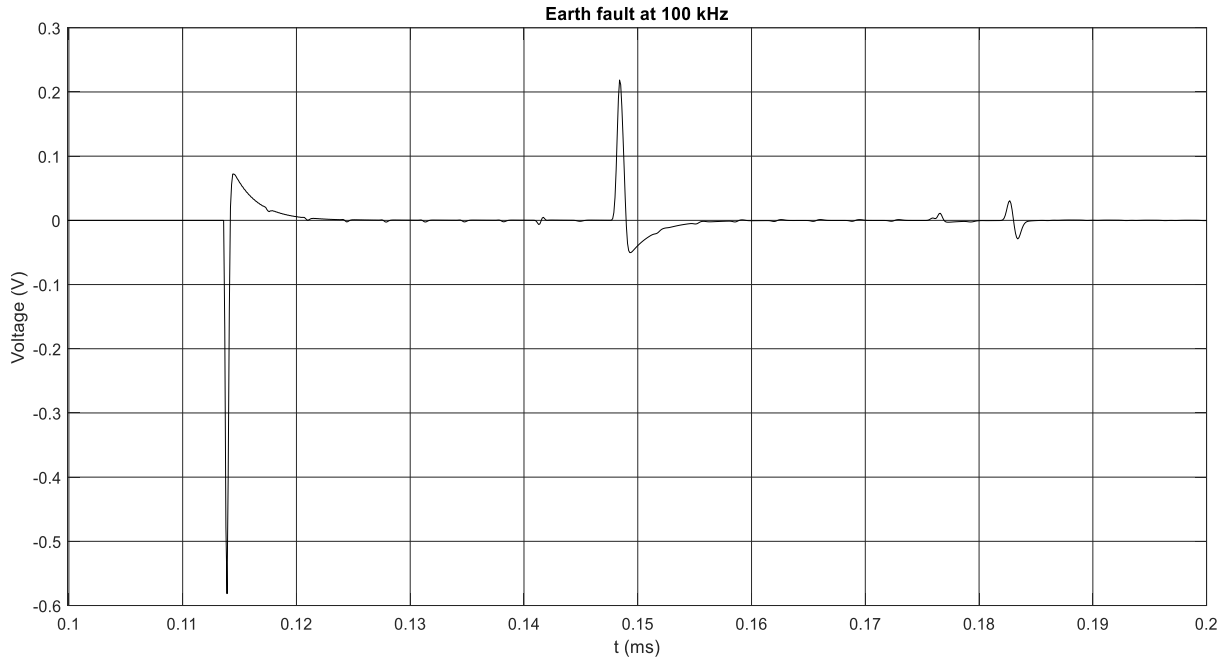

Figure 6.13 *PD pulses at 100 kHz, after an incipient earth fault.*

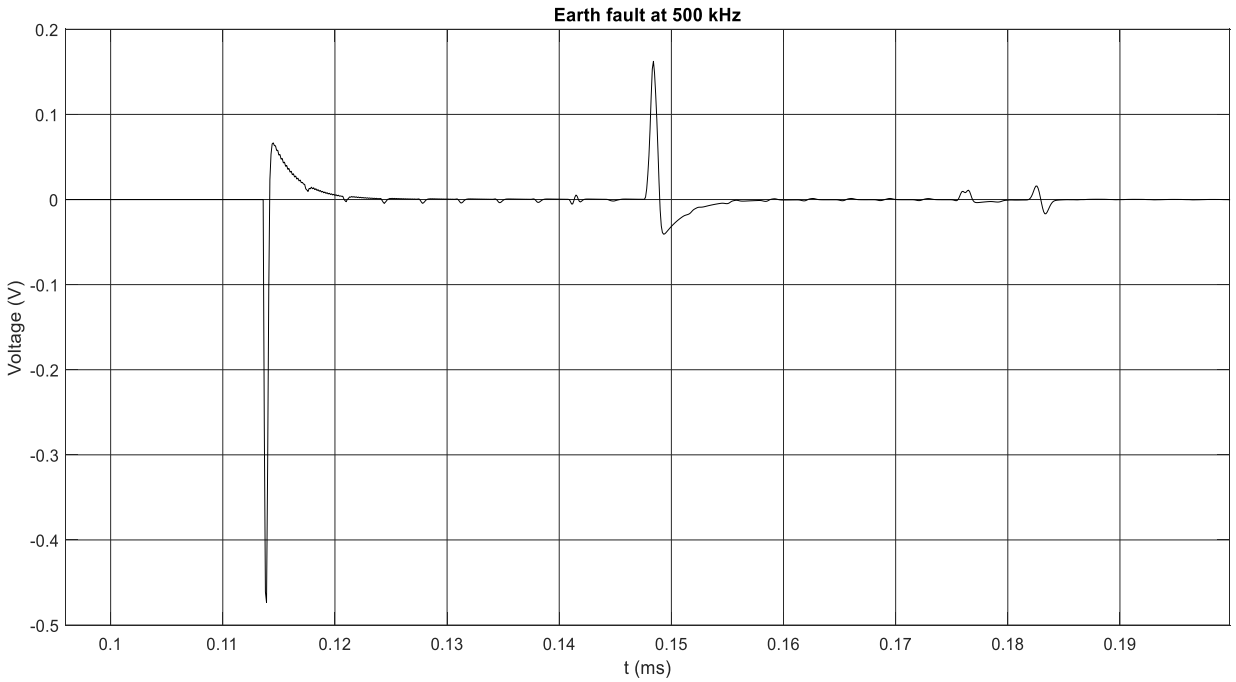

Figure 6.14 *PD pulses at 500 kHz, after an incipient earth fault.*

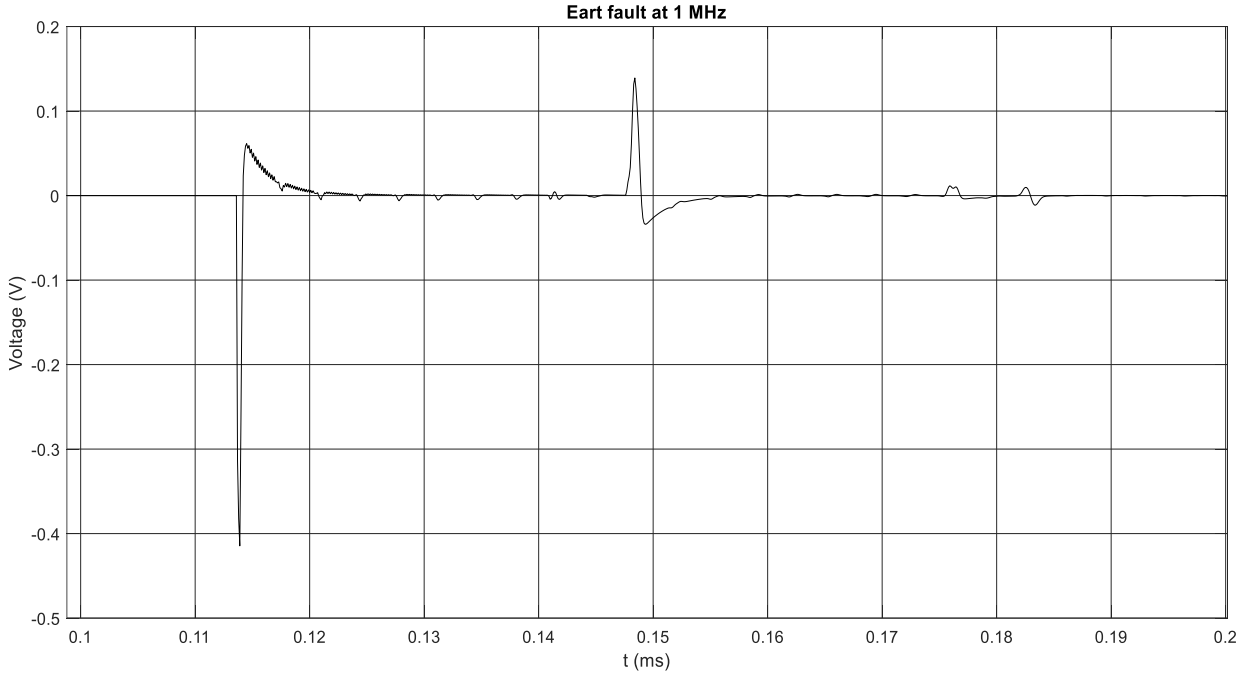

Figure 6.15 *PD pulses at 1 MHz, after an incipient earth fault.*

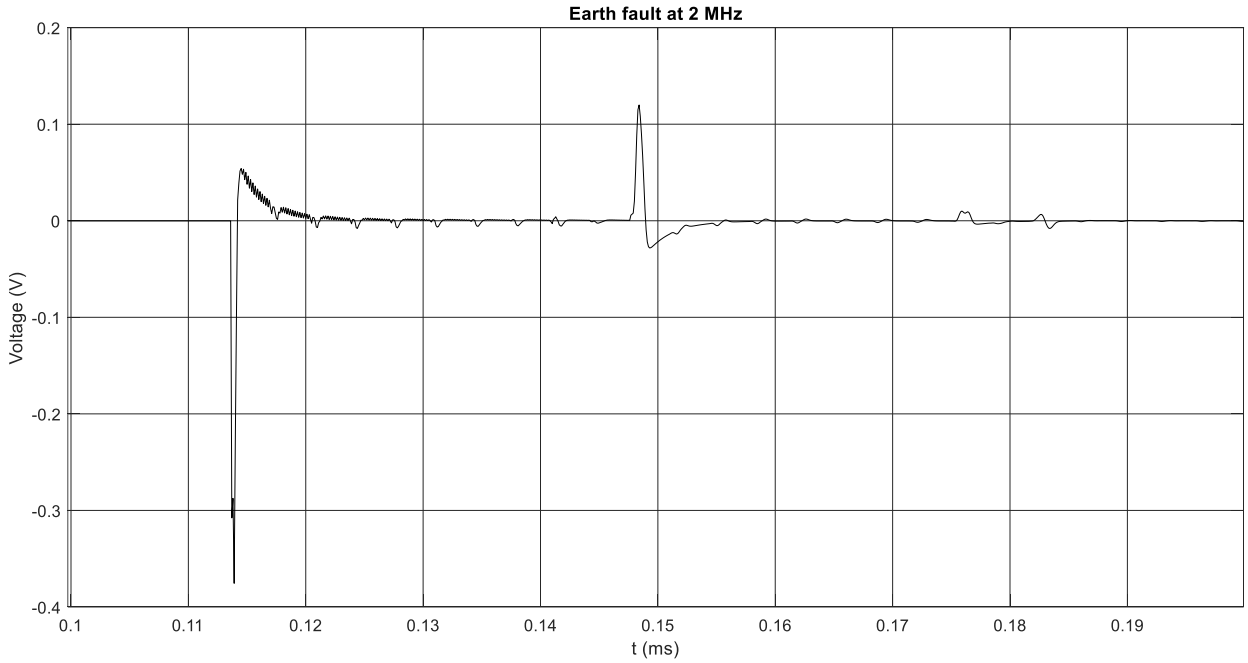

Figure 6.16 *PD pulses at 2 MHz, after an incipient earth fault.*

Instead, in the Figure 6.17, 6.18, 6.19 and 6.20 the PD pulses caused by and incipient short-circuit fault in the phase A and B are represented, looking at the scope sensor in the phase A, varying the model frequency using the same step of the previous simulations. The aim is to make a comparison of the magnitude of the PD pulses with the frequency variation, using the typical partial discharge frequency.

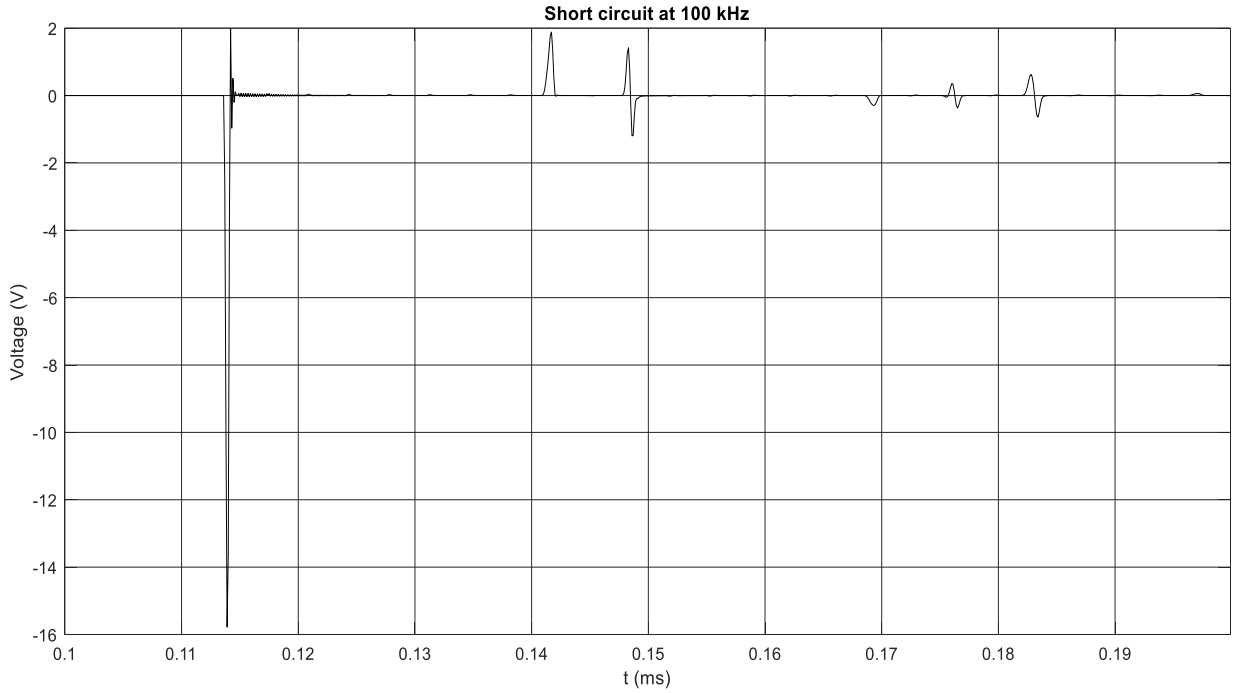

Figure 6.17 *PD pulses at 100 kHz, after an incipient short-circuit fault.*

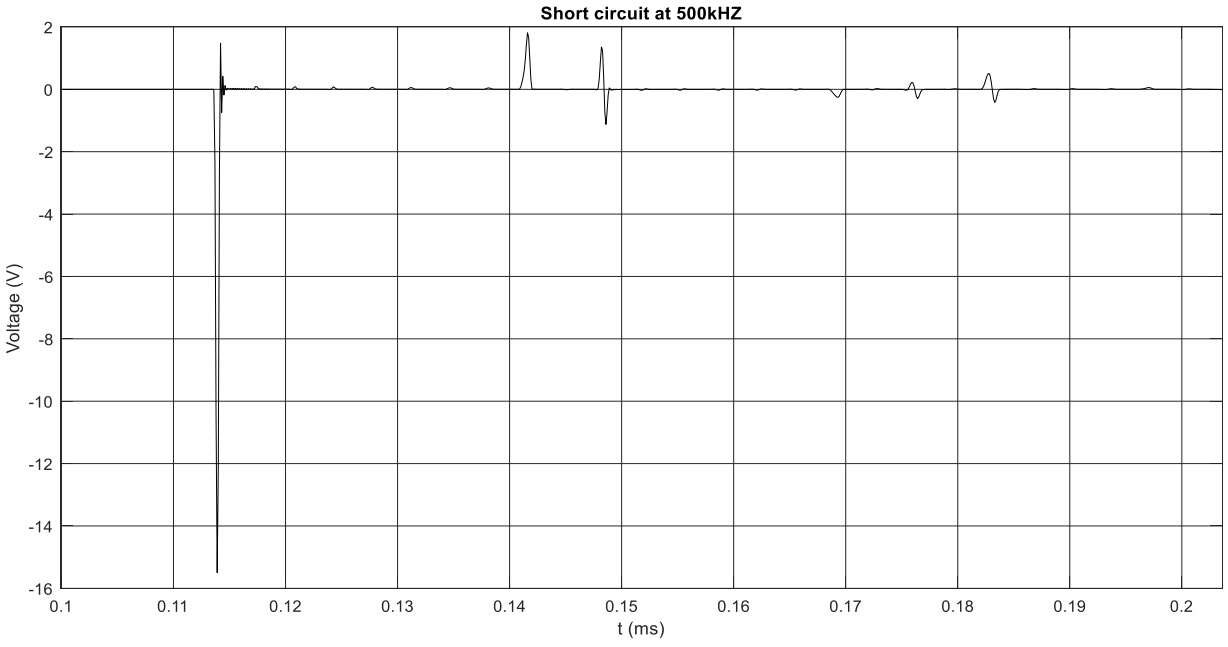

Figure 6.18 *PD pulses at 500 kHz, after an incipient short-circuit fault.*

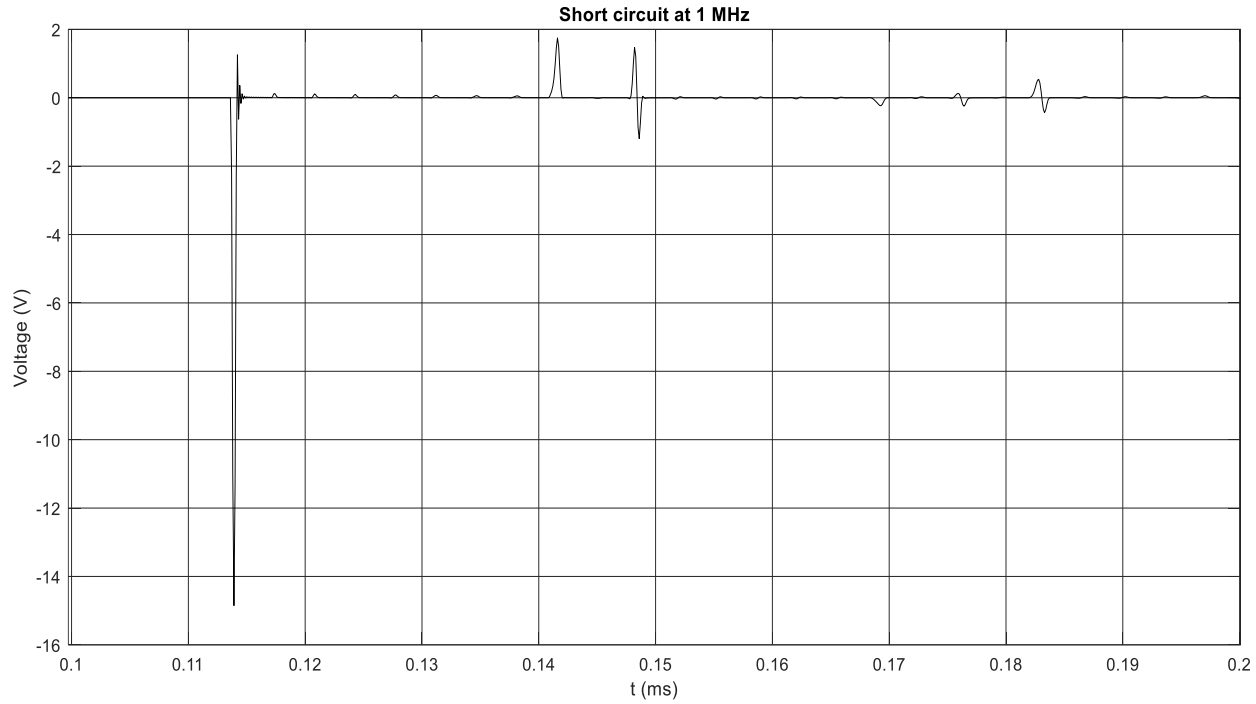

Figure 6.19 *PD pulses at 1 MHz, after an incipient short-circuit fault.*

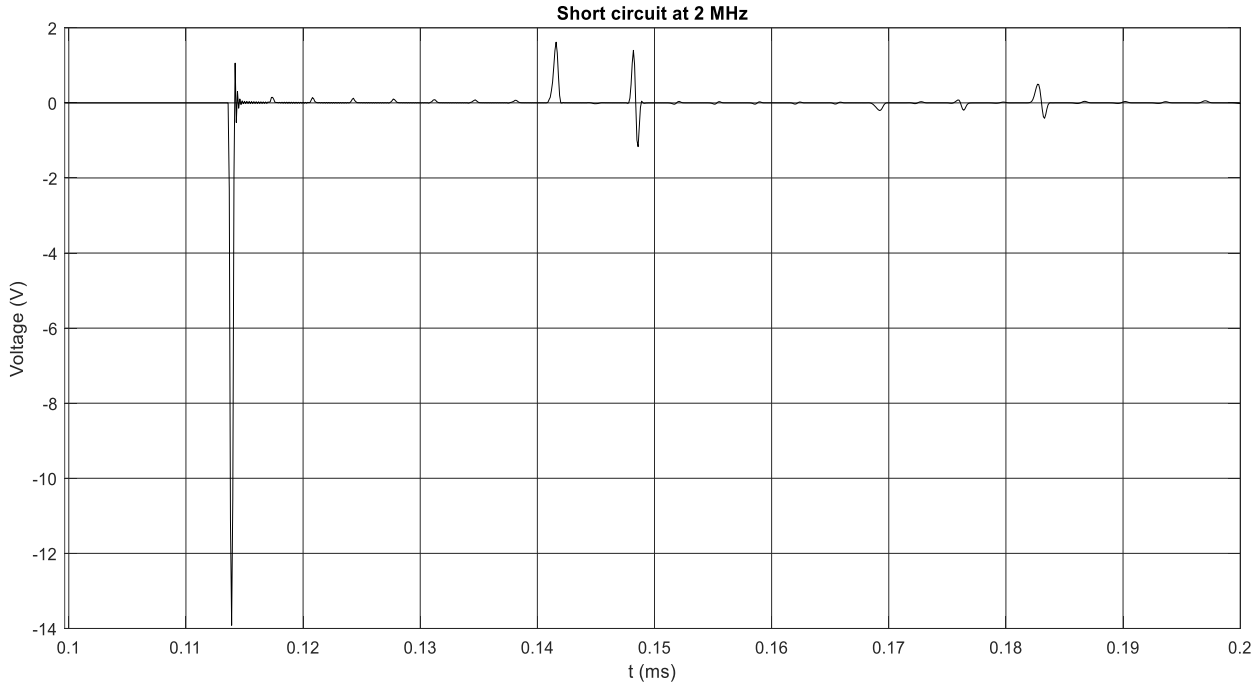

Figure 6.20 *PD pulses at 2 MHz, after an incipient short-circuit fault.*

In the Table 6.5 and 6.6 are summed the first PD pulses magnitudes in the two type of incipient tree fault (incipient earth fault and short circuit fault) at difference frequency.

Table 6.5 *PD pulses magnitude at different frequencies relative at an incipient earth fault.*

Model frequency	***1st pulse* (V)**	***2nd pulse* (V)**	***3rd pulse* (V)**	***4th pulse* (V)**	***5th pulse* (V)**	***6th pulse* (V)**
100 kHz	0.656	0.0011	0.269	0.003	0.014	0.060
500 kHz	0.527	0.018	0.203	0.003	0.014	0.032
1 MHz	0.476	0.009	0.173	0.003	0.015	0.021
2 MHz	0.247	0.010	0.148	0.003	0.013	0.015

Table 6.6 *PD pulses magnitude at different frequencies relative at an incipient short-circuit fault.*

Model frequency	***1st pulse* (V)**	***2nd pulse* (V)**	***3rd pulse* (V)**	***4th pulse* (V)**	***5th pulse* (V)**	***6th pulse* (V)**
100 kHz	17.764	1.885	2.615	0.295	0.722	1.263
500 kHz	16.997	1.812	2.482	0.245	0.517	0.926
1 MHz	16.208	1.750	2.665	0.232	0.374	0.945
2 MHz	14.975	1.618	2.566	0.202	0.275	0.866

As expected, the incipient short circuit fault generates PD pulses with larger magnitude. Besides, making a comparison between the different frequencies, it is clear than in the lower frequencies, in the order of hundreds of kHz, the magnitudes of the pulses are larger respect to those in higher frequencies, in the order of the MHz. This is due to the transfer function of the power line (Equation 3.20), in which the magnitude of the pulses decreases in function of the distance d and the propagation constant γ of the line. As seen in the Chapter 3, the propagation constant has two propagation constant which are frequency dependant. Therefore, with the increase of the frequency, the magnitude of the PD pulses decreases. The simulations are accurate because they are in line with the expectations.

Besides, the pulses are zoomed in, as in Figure 6.21, where it is possible to make a comparison between the pulses at 100 kHz and at 2 MHz. With lower frequencies, the waveform is cleaner, while in the higher frequencies the waveforms have more oscillations and the signal seems to be more dirty, showing a difference in the quality of the signal.

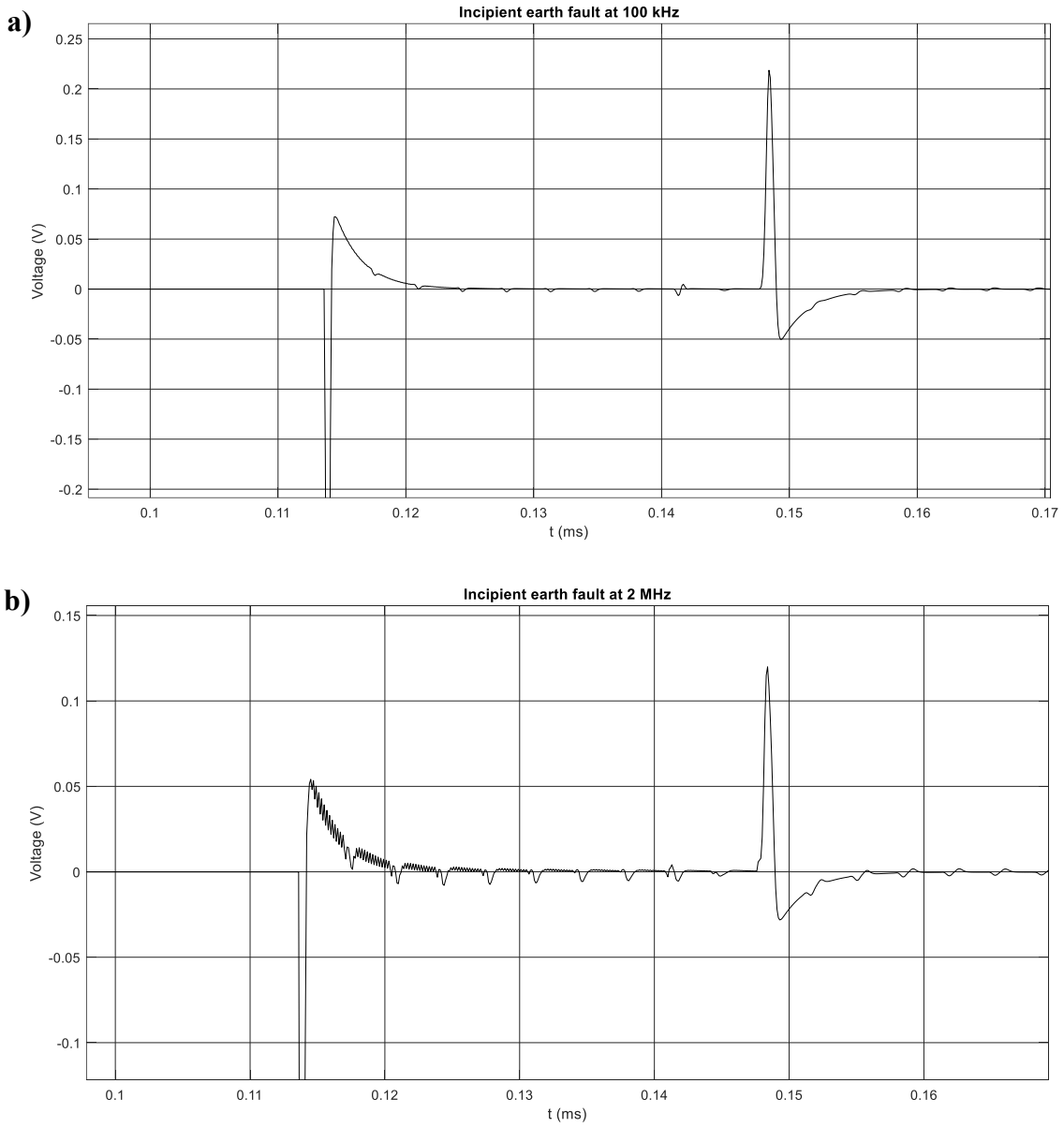

Figure 6.21 *Zoom of PD pulses at 100 kHz* **a)** *and at 2 MHz* **b)***, after an incipient earth fault.*

6.5 Neutral grounding variation in the line

The last thing to do is the study of the neutral grounding in a covered conductor high voltage power line. The aim of these simulations is to check if the partial discharges change in magnitude or, in general, in propagation, along the line, after their generation, with different kind of management of the neutral conductor.

The configurations of the neutral grounding are:

- With the isolated neutral: the neutral conductor is not grounding and the return for the fault capacitive currents are through the capacities of the sane phases of the line;

- Directly with a short circuit between the neutral conductor and the ground;
- With a large and a small resistance: the neutral conductor is grounded using initially a small resistance (Ω) and then replacing it with a large one (MΩ).
- With a tuned inductance: using a Petersen coil to limiting the fault current circulation from the line and self-extinguishing the fault arc.

All the previous simulations are conducted modifying the neutral grounding, using the configuration just listed. The results, however, are not different with the variation of the neutral grounding. In fact, the simulations simulate the real condition that happens when a tree falls on a covered conductor line: the distortion of the magnetic field, due to the contact of the tree with the covered line, produces partial discharges signals with small pulses of current. Incipient tree fault is generated, but it cannot be considered a traditional fault with the arc formation and the fault current circulation. So the different types of neutral grounding do not influence the generation of the partial discharge, neither their propagation along the line nor the magnitudes measured at the end line in the sensors. As expected, the results confirm this.

Conclusions

As conclusion of this thesis, I can make some reflections about my work in simulating the incipient fault conditions, after the falling of a tree on the covered conductor line. The aim of the EMTP work is to create a model of the covered conductor line to utilize in the study of the partial discharges phenomena. After some simplifications, the model created can be considered a good beginning in the study of this new type of overhead power line, since the results respect the expectations. Certainly, it can be improved by adding all those elements of the network that have been neglected since they are irrelevant for these specific simulations, as the wooden tower or the elements of the substation, as the surge arresters and so on. Therefore, the simulation can be repeated with the completed network, adding other lines and with a line longer. My model line is only a simple experiment in order to verify the operation of the model in the computing environment.

Moreover, in the simulations, the variation of the environmental conditions is not considered. As seen in the second chapter they influence a lot the partial discharge formation and its magnitude. However, the latter can be modified by varying the resistance of the tree in contact to the line. The aim of my simulations was not the study the environmental conditions variation, but the propagation of the partial discharges along the line and the correct measurement of them by means of the sensors.

In the case of relative short line, the propagation attenuation is not appreciable, so the simulation should be repeated with longer trial line, considering that the maximum length detectable from a single PD sensor was estimated of 30 km from the field tests. An important conclusions is that the sensors are able to perfectly detect the PD pulses and the time needed to travel along the line according to the lattice diagram. Moreover, in my opinion, the most important point, is the coupling between the phases and the difference in magnitude between the earth incipient fault and the short circuit one: in fact, thanks to the coupling between the phases, it is possible to use only one sensor in one on the phases to monitor all the three of them. This could lead to a decreasing in the cost of the monitoring system, without leave out the accuracy, though the three phase sensors have the benefit of the redundancy in case of some sensors out of order. Moreover, with the magnitude difference between the earth and the short circuit ITF, the pulses system of analysis could easily distinguish between the two kinds of fault.

Finally, as far as I'm concerned, I think covered conductors could be a valid alternative to the traditional overhead high voltage line, if they are used in specific zones, where no very long pieces are required: for example, in the forest areas, where the wheatear conditions could lead the falling of a tree or a branch over the line, or in the urban zone where a small electromagnetic field is required. They are a good environmental choice, probably well accepted from the public opinion. It is task of the electric network operators to evaluate if in a specific area it is more convenient the use of the traditional overhead line, with its possible risk and drawback, or the installation of a new covered conductor overhead line, with the advantage to be able to detect the point in which the fault takes place. Sure, covered conductors are a possible alternative to take in consideration in the project of a new part of the line or in the rebuilding of an old one.

Bibliography

[1] J. B. Wareing, A. Hinkkury, "NEW DEVELOPMENTS IN THE USE OF COVERED CONDUCTOR LINES UP TO 132 KV", Paper present at Lines and Cables Conference Preston, 9 – 11 September 1997.

[2] J. Ojala, T. Leskinen, M. Lahtinen, A. Hinkkury, "110 kV OVERHEAD TRANSMISSION LINE WITH COVERED CONDUCTORS", *Cigre'* 1998.

[3] J. Ojala, T. Leskinen, M. Lahtinen, A. Hinkkury, "USING OVERHEAD COVERD CONDUCTORS AT HIGH VOLTAGES" *Modern power systems*, July 1998.

[4] A. Hinkkury, "THE STRUCTURE AND TESTING OF HIGH VOLTAGE CC", Covered Conductors Conference, Capenhurst U.K. 1999.

[5] A. Hinkkury, "VIBRATION – THE FINNISH EXPERIENCE", Covered Conductors Conference, Capenhurst U.K. 1999.

[6] R. M. Doone, A.Atkins, "LIGHTNING PROTECTION FOR HIGHVOLTAGE COVERED CONDUCTORS", 1999.

[7] V. Weiss, "20 kV TRANSMISSION LINES WITH COVERED CONDUCTORS IN SLOVENIA", Maribore, Slovenia.

[8] J. B. Wareing, "UPGRADING 33 kV LINES TO 132 kV USING COVERED CONDUCTORS".

[9] T. Leskinen, "DESIGN OF MV AND HV COVERED CONDUCTOR OVERHEAD LINES", *Cired,* International Conference on Electricity Distribution Barcelona, 12-15 May 2003.

[10] T. Leskinen, V. Lovrenčić, "FINNISH AND SLOVENE EXPERIENCE OF COVERED CONDUCTOR OVERHEAD LINES", *Cigre'* 2004.

[11] J. B. Wareing, "COVERED CONDUCTOR SYSTEMS FOR DISTRIBUTION" Report, December 2005.

[12] P. Pakonen, "DETECTION OF INCIPIENT TREE FAULTS ON HIGH VOLTAGE COVERED CONDUCTOR LINES", Publication n.681 Tampere University of Technology, 16th November 2007.

[13] T. Leskinen, "VIBRATION STUDIES OF HVCC OHLS", *Eltel,* 2011.

[14] Ž. Voršič, “POLYURETHANE AS AN ISOLATION FOR COVERED CONDUCTORS”, 2012.

[15] M. Isa, “PARTIAL DISCHARGE LOCATION TECHNIQUE FOR COVERED-CONDUCTOR OVERHEAD DISTRIBUTION LINES”, Aalto University, 11th Jenuary 2013.

[16] Pirelli, *“*IMPROVE RELIA & SAFETY IN OVERHEAD LINES – SAX – LMF SAX COVERED CONDUCTORS SYSTEMS”, Brochure Tecniche,
- *Schede SAX-W;*
- *Presentazione “The Forest SAX Project”.*

[17] Pirelli, A. Hinkkury, “HV SAX LINE – OVERHEAD TRANSMISSION LINE WITH COVERED CONDUCTORS”, Brochure Tecniche.

[18] Pirelli, *“*TECHNICAL PAPER*”.*

[19] Westernpower, “HENDRIX COVERED CONDUCTOR MANUAL”, 2010.

[20] Christina, A. J., et al. "PARTIAL DISCHARGE MODELING WITH INCREASING APPLIED VOLTAGES ACROSS DIFFERENT VOID SIZES.", *2017 4th International Conference on Advances in Electrical Engineering (ICAEE)*. IEEE, 2017.

[21] Zhang, Wei, et al. "AN IMPROVED TECHNIQUE FOR ONLINE PD DETECTION ON COVERED CONDUCTOR LINES.", *IEEE transactions on power delivery* 29.2 (2014): 972-973.

[22] Hashmi, G. Murtaza, M. Lehtonen, and Abdelsalam ELHAFFAR. "MODELING OF ROGOWSKI COIL FOR ON-LINE PD MONITORING IN COVERED-CONDUCTOR OVERHEAD DISTRIBUTION NETWORKS.", *Pulse* 1 (2007): P2.

[23] Nafar, Mehdi. "SIMULATION OF PARTIAL DISCHARGE MECHANISM USING EMTP." *International Conference on Innovations in Electrical and Electronics Engineering, Dubai, UAE*. 2012.

[24] P. Pakonen, et al. "ON-LINE PARTIAL DISCHARGE MONITORING OF 110 KV AND 20 KV COVERED CONDUCTOR LINES." *Cigré* (2004).

[25] P. Pakonen, "CHARACTERISTICS OF PARTIAL DISCHARGES CAUSED BY TREES IN CONTACT WITH COVERED CONDUCTOR LINES." *IEEE Transactions on Dielectrics and Electrical Insulation* 15.6 (2008): 1626-1633.

[26] Hashmi, G. Murtaza, M. Lehtonen, and M. Nordman. "MODELING AND EXPERIMENTAL VERIFICATION OF ON-LINE PD DETECTION IN MV

COVERED-CONDUCTOR OVERHEAD NETWORKS." *IEEE Transactions on Dielectrics and Electrical Insulation* 17.1 (2010): 167-180.

[27] Hashmi, G. M., M. Isa, and M. Lehtonen. "MODELING ON-LINE THREE-PHASE PD MONITORING SYSTEM FOR MV OVERHEAD COVERED-CONDUCTORS." *International Conference on Power Systems Transients (IPST2009)*. 2009.

[28] Omidiora, M. A., M. Lehtonen, and R. J. Millar. "EMTP SIMULATION OF LIGHTNING OVERVOLTAGE DISCHARGE TO MEDIUM VOLTAGE OVERHEAD LINES WITH COVERED CONDUCTORS." *Proc. 20th International Conference on Electricity Distribution*. 2009.

[29] Fekete, Kresimir, et al. "SIMULATION OF LIGHTNING TRANSIENTS ON 110 KV OVERHEAD-CABLE TRANSMISSION LINE USING ATP-EMTP." *MELECON 2010-2010 15th IEEE Mediterranean Electrotechnical Conference*. IEEE, 2010.

[30] Hashmi, G. Murtaza, and M. Lehtonen. "COVERED-CONDUCTOR OVERHEAD DISTRIBUTION LINE MODELING AND EXPERIMENTAL VERIFICATION FOR DETERMINING ITS LINE CHARACTERISTICS." *2007 IEEE Power Engineering Society Conference and Exposition in Africa-PowerAfrica*. IEEE, 2007.

[31] P. Pakonen, M. Björkqvist, and V. Latva-Pukkila. "ARRANGEMENT AND METHOD FOR DEFINING THE LOCATION OF SOURCE OF PARTIAL DISCHARGES." (2002).

[32] P. Pakonen, M. Björkqvist, and V. Latva-Pukkila. "METHOD AND SYSTEM FOR IDENTIFYING CAUSE OF PARTIAL DISCHARGES." (2002).

[33] J. Mahseredjian, C. Dewhurst, “EMTP RV USER MANUAL VERSION 4.0”, 30th July 2018.

[34] EMTP-EMTPWorks, “CONDUCTOR DATA IN CABLE DATA DEVICE”, 20th October 2013.

[35] EMTP-EMTPWorks, “FREQUENCY DEPENDENT Q MATRIX: FDQ M-PHASE”, 25th November 2003.

[36] EMTP-EMTPWorks, “MODEL DATA OPTIONS IN CABLE DATA DEVICE”, 20th October 2013.

[37] Unificazione ENEL, “LINEA A 132-150 KV. CONDUTTORI E CORDE DI GUARDIA”, February 1971.

[38] Unificazione ENEL, “CORDA DI GUARDIA DI ACCIAIO Ø10,5”, Genuary 1995.

[39] Unificazione ENEL, “CORDA DI GUARDIA DI ACCIAIO RIVESTITA DI ALLUMINIO Ø 11,5”, Genuary 1995.